

# For Reference

---

NOT TO BE TAKEN FROM THIS ROOM



For Reference

---

NOT TO BE TAKEN FROM THIS ROOM

EX LIBRIS  
UNIVERSITATIS  
ALBERTAENSIS







Digitized by the Internet Archive  
in 2019 with funding from  
University of Alberta Libraries

<https://archive.org/details/Milton1962>









Thesis  
1962 (F)  
# 8 D.

THE UNIVERSITY OF ALBERTA  
A SPECTROSCOPIC STUDY OF THE EMISSIONS PRODUCED BY  
ACTIVE NITROGEN WITH BROMINE, HYDROGEN BROMIDE,  
AMMONIUM BROMIDE, AND AMMONIA

by

Earl Richard Vincent Milton, M.Sc.

A THESIS  
SUBMITTED TO THE FACULTY OF GRADUATE STUDIES  
IN PARTIAL FULFILMENT OF THE REQUIREMENTS FOR THE DEGREE  
OF  
DOCTOR OF PHILOSOPHY

DEPARTMENT OF CHEMISTRY

EDMONTON, ALBERTA

September 24th, 1962





## DEDICATION

This work is dedicated  
to my Mother and to the memory of my late Father.

Their loyalty and devotion  
provided the means by which the work began  
and the impetus needed for its successful completion.  
Such dedication is made in partial thanks for their sacrifices.





## ABSTRACT

When bromine, hydrogen bromide, or ammonium bromide are reacted with active nitrogen, complete quenching of the yellow Lewis-Rayleigh nitrogen afterglow is noted at the point of mixing. In place of the yellow afterglow, a reddish-orange wall emission has been noted. From the isotopic shift provided by the almost equally abundant bromine isotopes ( $^{79}\text{Br}$  and  $^{81}\text{Br}$ ), the wall emission has been attributed to the diatomic molecule  $\text{NBr}$ , nitrogen monobromide. Formed from ground state nitrogen and bromine atoms, the excited state producing the observed emission has been postulated to arise from a radiationless transition of an excited state of  $\text{NBr}$  which correlates with the ground state atoms, into a  $^1\Sigma^+$  state. Transition has been observed from the  $^1\Sigma^+$  upper state to one form ( $F_1$ ) of the  $^3\Sigma^-$  ground state of the  $\text{NBr}$  molecule. The transition is allowed and can probably be designated as  $^1\Sigma^+ \rightarrow 0^+$ , indicating that  $\text{NBr}$  exhibits an appreciable amount of case "c" coupling behavior. The absence of transition to the two other forms of the  $^3\Sigma^-$  ground state (which form a "1" or  $\Pi$  type state in case "c") can not be explained. The dissociation energy of  $\text{NBr}$  has been estimated to be  $67 \pm 5$  kcal. The spectrum has provided accurate measurement of the energy of the minimum of the excited  $^1\Sigma^+$  state ( $T_e$ ) and of the vibrational constants  $\omega_e$  and  $\omega_e x_e$  for the two states involved in the transition. Accurate determination of the rotational constant  $B_e$  has been made for the upper state and estimates have been obtained for the values of  $B_e$  and the splitting constants ( $\lambda$  and  $\gamma$ ) for the lower state.

Study has also been made of the blue afterglow noted when the flow of bromine or hydrogen bromide into active nitrogen is discontinued. The emission seems to be due to members of the





bands of nitric oxide. The source of the nitric oxide has been postulated to be from oxygen or water vapour occluded upon the walls with the wall poison. The vibrational distribution of the  $\beta$  bands of nitric oxide during the bromine blue afterglow differs markedly from that distribution normally obtained in active nitrogen in the presence of nitric oxide and the absence of bromine. Also, in the absence of bromine excitation of the  $\gamma$  and  $\delta$  bands of nitric oxide is observed. These bands are not present in the bromine blue afterglow.

A pink discharge, which consistently appeared to pass from the condensed discharge through the reaction vessel to the pumps was investigated. Bands from the second positive and first negative systems of nitrogen were detected. It was concluded that this pink discharge might be the condensed discharge counterpart of the short-lived pink afterglow noted in active nitrogen generated with a microwave exciter. The bands may be excited by electron impact provided by the mild pink discharge through the flowing nitrogen.

Ammonia was shown to partially quench the Lewis-Rayleigh afterglow when added to active nitrogen. When the ammonia was frozen out in the stream of active nitrogen (by cooling to  $-196^{\circ}\text{C}$ ) a brilliant blue glow was obtained at the cold point. The spectrum of this glow proved to be a continuum with short wavelength edge at about  $3150 \text{ \AA}$ .



## ACKNOWLEDGEMENTS

It is indeed a privilege to acknowledge with thanks the excellent direction and friendly council offered by Dr. H. B. Dunford, research supervisor for this study. In addition, I would like to express my appreciation to all those persons at the University of Alberta who influenced my years on the campus.

The co-operation given by the Molecular Spectroscopy group at the National Research Council, Ottawa was of immeasurable help in obtaining and interpreting the high resolution spectrograms required for this study; we are very appreciative of this co-operation.

I am indebted for the financial assistance provided by The Canadian Industries Limited, in the form of two Graduate Fellowships, and by the Province of Alberta, who provided a Queen Elizabeth Graduate Scholarship. These awards allowed the work to be completed more quickly than otherwise would have been possible.





## TABLE OF CONTENTS

## INTRODUCTION

On the Chemical Nature of Active Nitrogen	1
The Nitrogen Afterglow	10
The Present Problem	15

## THE EXPERIMENTAL PART

Introduction of Materials	16
The Apparatus	19
Experimental Procedure	29
Analysis of the Spectra	31

## RESULTS

The Reaction of Active Nitrogen with Bromine	34
The Reaction of Active Nitrogen with HBr and $\text{NH}_4\text{Br}$	73
The Reaction of Active Nitrogen with Ammonia	79
The Optical Spectrum of Active Nitrogen	81

## DISCUSSION

On the Nature of NBr	90
The Correlation of NBr with the HBr Kinetics	104
The Ammonium Bromide Reaction	107
The Blue Bromine Afterglow	109
The Ammonia Trap Reaction	113
On the Active Nitrogen Emissions	115
Conclusions	124
Suggestions for Further Work	126

## BIBLIOGRAPHY 128

## APPENDICES

I-Calibration of Flow Jets	134
II-Output of the Power Supply	137
III-Analysis of the Spectrum	139
IV-The 8 $\mu$ -6 $\mu$ Band	146



## Index to Tables

1-Deslandres Table for N <sup>79</sup> Br Band Heads	39
2-Deslandres Table for N <sup>81</sup> Br Band Heads	40
3-Summary of Vibrational Constants for NBr	41
4-Vibrational Isotope Shift for NBr (Cm <sup>-1</sup> )	42
5-Vacuum Wavenumbers in Cm <sup>-1</sup> for N <sup>79</sup> Br Bands	49-52
6-Vacuum Wavenumbers in Cm <sup>-1</sup> for N <sup>81</sup> Br Bands	53-56
7- $\Delta v(J)$ and $\Delta^2 v(J)$ for P Branch NBr 8-6	57
8- $\Delta v(J)$ and $\Delta^2 v(J)$ for R Branch NBr 8-6	58
9-Upper State Combination Differences and Rotational Constants (in Cm <sup>-1</sup> ) for N <sup>79</sup> Br	62-3
10-Independent Evaluation of $\Delta_2 F''(J)$ Values for Low J Levels from 9'-7" Band Data for N <sup>79</sup> Br	66
11-Lower State Combination Differences in Cm <sup>-1</sup> $\Delta_2 F''(J)$ Values for N <sup>79</sup> Br	67
12-Observed and Calculated $\Delta_2 F(J)$ Values Lower State of NBr	70
13-Nitric Oxide $\beta$ Bands in Active Nitrogen in the Presence of Bromine	75
14-First Positive Bands in Active Nitrogen	82
15-Second Positive Bands in Active Nitrogen	85
16-First Negative Bands in Active Nitrogen	85
17-Nitric Oxide $\beta$ Bands Excited in Active Nitrogen	87
18-Nitric Oxide $\gamma$ Bands Excited in Active Nitrogen	88
19-Nitric Oxide $\delta$ Bands Excited in Active Nitrogen	88
20-Cyanogen Violet System in Active Nitrogen	89





21-Rate of Evacuation of Nitrogen Flow Jet	134
22-Flow Rates Through Reactant Flow Jets	134
23-Bromine--Active Nitrogen Flow Jet Combinations	135
24-Analysis of the Reference Spectrum for NBr 8'-6"	139
25-Calculation of the Correction Graph	140
26-Analysis of the NBr Spectrum	142-3
27-Calculation of NBr Wavelengths	144-5
28-F <sub>1</sub> Lines of NBr 8-6 Band (Manual Comparator)	146-7
29-Listing of Faint Unassigned Lines in 8-6 Band	147-8



## Index to Figures

1-Partial Energy Diagram for Nitrogen	3
2-Trap for Bromine Introduction	17
3-The Nitrogen Introduction System	20
4-Reactant Storage and Introduction System	22
5-The Discharge Tube and Power Supply	24
6-Preliminary Reaction Vessels	26
7-Reaction System for High Resolution Work	28
8-Correction for Deviation from Average Linear Dispersion	33
9-A Diatomic Molecule as a Non-Rigid Rotor	43
10-Convergence of P and R Parabolas	46
11-Square Method of Determining Self-Consistent J Values	47
12-Convergence of Intersecting Q and S Parabolas	59
13-Determination of Upper State Combination Differences	60
14-Absolute J Numbering--Upper State N <sup>81</sup> Br	61
15-Determination of Lower State Combination Differences	64
16-Absolute J Numbering--Lower State N <sup>81</sup> Br	65
17-Coupling Diagrams for $\Sigma$ States	68
18-Calculation of Splitting-NBr Lower State	71
19-Formation of NBr from Ground State Atoms	92
20-Hund's "b" and "c" Coupling Cases	93





21- $1\Sigma^+ \rightarrow 3\Sigma^-$ Transition	94
22-Transition from Case "b" to Case "c" Coupling	95
23-Morse Potential Energy Curves for NBr	98
24-Partial Potential Curves for Nitrogen	118
25-Nitric Oxide Energy Level Diagram	122
26-Rate of Flow Through Flow Jets	136
27-Oscillogram of the Discharge	138
28-Output of the Power Supply	138
29-The Vacuum Correction for Wavelengths in Air	141



## Index to Plates

1-Active Nitrogen--Bromine Reaction Flame	35
2-NBr $8^1-6''$ Band Under High Dispersion	37
3-Spectrum During the Emission of the Bromine Blue Afterglow	74
4-Active Nitrogen--Hydrogen Bromide Emission	76
5-Ammonia Continuum Excited in Active Nitrogen (Red Sensitive)	80
6-Ammonia Continuum Excited in Active Nitrogen (Blue Sensitive)	80
7-Nitrogen Bands in Active Nitrogen	83
8-Nitric Oxide Bands Excited in Active Nitrogen	86
9-Break-off of the NBr Bands at $v^1 = 10$	100





A SPECTROSCOPIC STUDY OF THE EMISSIONS  
PRODUCED BY ACTIVE NITROGEN WITH  
BROMINE, HYDROGEN BROMIDE,  
AMMONIUM BROMIDE, AND AMMONIA

INTRODUCTION

Past studies of active nitrogen and its reactions have been, in general, confined to either a spectroscopic study of the emissions accompanying a reaction, or to a chemical kinetic study of the active nitrogen system. A primary object in the present study of the reactions of active nitrogen with bromine, hydrogen bromide, ammonium bromide, and ammonia has been to try to establish some rapport between the spectroscopic evidence and the most recent kinetic findings about the systems.<sup>1-6</sup>

ON THE NATURE OF ACTIVE NITROGEN

It was noted by Lewis,<sup>7</sup> in 1900, that an intense yellow afterglow was produced when nitrogen gas was subjected to a condensed electrode discharge. Because the glowing nitrogen gas showed enhanced chemical activity, it was named active nitrogen by Strutt.<sup>8</sup> Active nitrogen has been produced, in subsequent investigations, using a high voltage glow discharge,<sup>9</sup> and in an electrodeless discharge activated by a microwave exciter<sup>10</sup> and, more recently, activated by a radio-frequency generator.<sup>11</sup>

In order to explain the enhanced chemical activity of active nitrogen the physical nature of the component species that might be present must be examined.



The component species can be divided into two classes; nitrogen atoms and nitrogen molecules.\* Three low-lying atomic states of nitrogen exist; the ground state ( $2p^3\ ^4S$ ) and two metastable excited states, ( $2p^3\ ^2D$  and  $2p^3\ ^2P$ ) lying 2.383 and 3.574 e.v. above the ground state. A great many molecular states of nitrogen are known; most of them can be grouped into two main types, those of singlet multiplicity and those which are triplets (Figure 1).

Many of the singlet states are of very high energy, lying more than 12 e.v. above the ground state. Nevertheless, a few low-lying singlet states are known. The ground state of the nitrogen molecule has been identified as  $X\ ^1\Sigma_g^+$ . Three excited singlets having energies between 8 and 9 e.v. above the ground state are known, the  $a\ ^1\Pi_g$  from which the Lyman-Birge-Hopfield bands ( $a\ ^1\Pi_g \rightarrow X\ ^1\Sigma_g^+$ ) arise in the vacuum ultraviolet region, the  $a'\ ^1\Sigma_u^-$ , and the  $w\ ^1\Delta_u$  states.<sup>14</sup>

The  $X\ ^1\Sigma_g^+$  ground state of nitrogen has been correlated with the recombination of two ground state atoms. A Birge-Sponer extrapolation on the ground state (from the 26th vibrational level, with energy 6.33 e.v. above  $v = 0$ ) has led to a dissociation energy for the state of 9.8 e.v.

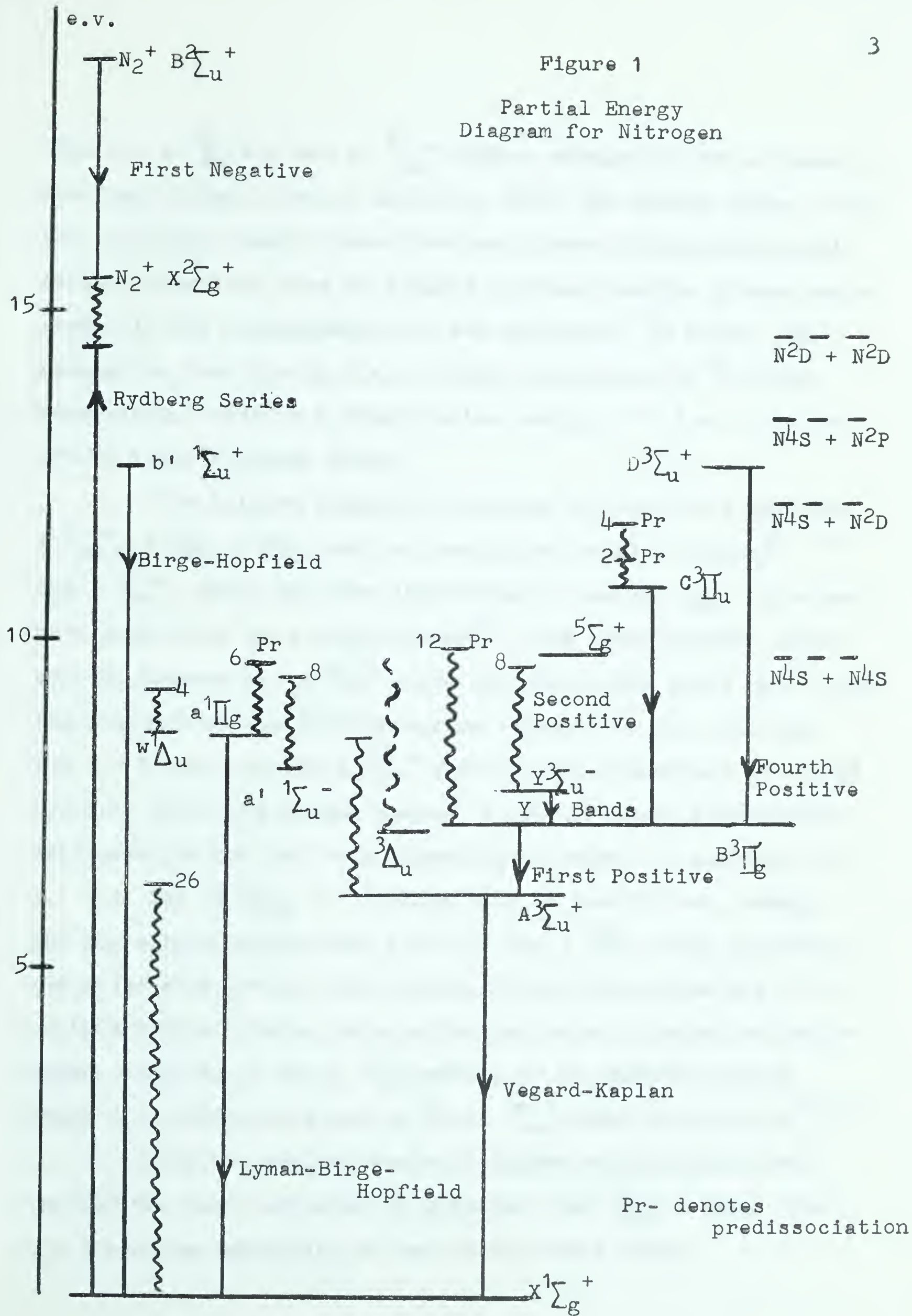
\* The discussion of states and their energies of atomic and molecular nitrogen has been taken largely from the discussion of these topics by Herzberg<sup>12</sup> (p.448f) and by Gaydon<sup>13</sup> (p.152f). Other references have been specifically indicated.





Figure 1

# Partial Energy Diagram for Nitrogen





Both the  $a\ ^1\Pi_g$  and the  $a'\ ^1\Sigma_u^-$  states extrapolate to a dissociation limit lying close to 14.5 e.v. above the ground state. From the low-lying atomic states the next lowest dissociation limit capable of giving rise to singlet systems (besides ground state atoms) is the recombination of two metastable  $^2D$  atoms. The assumption that the 14.5 e.v. limit corresponds to  $^2D$  atoms recombining leads to a dissociation energy of 9.8 e.v. for two ground state nitrogen atoms.

The triplet states of nitrogen include the long-known  $A\ ^3\Sigma_u^+$ ,  $B\ ^3\Pi_g$ ,  $C\ ^3\Pi_u$ , and two postulated triplet states,<sup>14, 15</sup> the  $Y\ ^3\Sigma_u^-$ , which has been identified,<sup>16</sup> and the  $3\Delta_u$ , which may have been found in a recent study<sup>17</sup>. The Vegard-Kaplan bands arising between the  $A\ ^3\Sigma_u^+$  state and the ground state have fixed the position of the triplet system relative to the singlets. The  $v = 0$  level of the  $A\ ^3\Sigma_u^+$  state has been assigned an energy 6.2 e.v. above the ground state. A nearly linear Birge-Sponer extrapolation has led to a dissociation energy of approximately 3.7 e.v. for  $A\ ^3\Sigma_u^+$ . Adding this to the 6.2 e.v. energy for the zeroth vibrational level of the  $A\ ^3\Sigma_u^+$  state correlates the state with ground state atoms. Transitions from all of the excited triplet states noted above can arise allowing radiation either directly to the  $A\ ^3\Sigma_u^+$  state, or to another triplet state from which radiation to the  $A\ ^3\Sigma_u^+$  state is possible.<sup>14, 18</sup>

Only one excited state of higher multiplicity than triplet has been indicated in nitrogen, the  $^5\Sigma_g^+$  arising from the direct recombination of two ground state atoms.





For many years the value for the dissociation energy of nitrogen was in doubt due to evidence presented by several known predissociations amongst the excited states of nitrogen. Two values for the dissociation energy were deemed to be most probable. For ground state atoms arising from the dissociation of the molecular ground state, the values of 7.373 e.v.<sup>12</sup> and 9.756 e.v.<sup>13</sup> were predicted.

The levels  $v = 1, 2, 3,$  and  $4$  of the  $C \ ^3\Pi_u$  state have been observed to predissociate, leading to a dissociation limit 12.139 e.v. above the ground state.<sup>19</sup> Kaplan<sup>20</sup> studied the behavior of a second predissociation appearing at  $v = 12$  level of the  $B \ ^3\Pi_g$  state. A third predissociation had been noted in the  $a \ ^1\Pi_g$  state and was identified with the  $v = 6$  level.<sup>21</sup> Several other predissociations are suspected in the highly excited states of nitrogen, notably above  $v = 0$  of the  $D \ ^3\Sigma_u^+$  state since nothing but the  $v' = 0$  progression has been observed from bands arising from this state.

Van der Zeil<sup>22</sup> originally concluded that the  $B \ ^3\Pi_g$  state must predissociate into a  $^3\Delta_g$  state. This conclusion required the  $^3\Delta_g$  state to arise from a dissociation energy below 9.8 e.v. An alternative explanation was that the  $B \ ^3\Pi_g$  state predissociated into a  $^5\Sigma_g^+$  state, arising from ground state atoms.<sup>23</sup> This explanation was later verified by Douglas and Herzberg.<sup>21</sup> Assignment of the predissociation from  $B \ ^3\Pi_g$  into  $^5\Sigma_g^+$  leads to the most probable dissociation energy for nitrogen to be 9.756 e.v.



It has long been agreed that the presence of atomic nitrogen could explain most of the chemical reactivity of active nitrogen. The Wrede gauge<sup>24</sup> has detected the presence of a considerable quantity of atoms in a stream of active nitrogen. Mass spectrometric studies have shown an enhanced 14/28 mass ratio in active nitrogen<sup>25</sup> and nitrogen atoms in the cold-trap condensate.<sup>26</sup> Paramagnetic resonance spectra have indicated that these atoms are predominantly in the ground state.<sup>27</sup> Ground state atoms have also been detected by a strong absorption line at 1200 Å in the vacuum ultraviolet.<sup>28</sup>

Under conditions where about one percent nitrogen atoms were produced in electrodeless discharges, active nitrogen was obtained from which the only detectable constituent was nitrogen atoms.<sup>10,11</sup> Using a glow discharge only ground state nitrogen atoms were detected when a low-energy input was used to produce one percent atom concentrations.<sup>9</sup> A high energy condensed discharge through nitrogen is thought to produce other reactive species besides ground state atoms.<sup>6</sup>

From the nature of the reaction of active nitrogen with ammonia and its derivatives, it has been concluded that active nitrogen contains a second reactive species in addition to atoms.<sup>1,29</sup> Ammonia shows a quenching effect, somewhat greater than that of mere dilution, upon the nitrogen afterglow. When ammonia is added to a stream of glowing active nitrogen, produced by an electrodeless discharge, the mass spectrum shows no diminution of the nitrogen atom concentration as the addition occurs.<sup>2</sup> An earlier study had shown ammonia to undergo only slight decomposition during the quenching of the afterglow.<sup>30</sup>





The reactions of active nitrogen with the saturated hydrocarbons methane and ethane have been described as being characterized by an initial induction period preceding the main reaction, which shows only slight decomposition of the parent hydrocarbon by the active nitrogen.<sup>31</sup> The addition of ammonia to active nitrogen prior to reaction with these saturated hydrocarbons has indicated that the reaction is inhibited almost completely by the ammonia.<sup>32</sup> The postulate has been forwarded that the second reactive species in active nitrogen is required to initiate the reaction with these saturated hydrocarbon molecules, and thus the addition of ammonia, which removes the initiating species, inhibits all reaction requiring the second reactive species, leaving only slight decomposition from reaction directly with nitrogen atoms. In contrast, ammonia has been shown not to inhibit, nor to diminish the extensive amount of reaction which occurs between active nitrogen and unsaturated molecules like ethylene and nitric oxide.<sup>33,34</sup> Both ethylene and nitric oxide are known to involve nitrogen atoms in at least a part of their reaction with active nitrogen since both react extensively in active nitrogen containing only atoms.<sup>33</sup>

It has been noted that ammonia is only destroyed in appreciable amounts when mixed with active nitrogen produced in a condensed discharge.<sup>34</sup> Also, an increase in the power dissipated by the condensed discharge, in the production of the active nitrogen, produces a corresponding increase in the amount of ammonia decomposed by the active nitrogen.<sup>35,36</sup>





Thus the evidence presented by the reactions of ammonia in active nitrogen leads to the conclusion that the second reactive species in active nitrogen is, in all probability, a molecular species. Mass spectrometric studies of active nitrogen produced in a condensed discharge has demonstrated the existence of a highly excited molecular species.<sup>25</sup> Several excited states of molecular nitrogen have been detected in active nitrogen,<sup>6,9,34,36-43</sup> some of which might possess sufficient lifetimes to allow them to exhibit appreciable chemical reactivity. Recently, the half-life of the  $A\ ^3\Sigma_u^+$  state has been estimated to be about 0.08 sec. using two different methods.<sup>6,34</sup> The  $a\ ^1\Pi_g$  state has been shown to have a lifetime of about  $1.7 \times 10^{-4}$  sec. utilizing a molecular beam as the mode of measurement.<sup>18</sup> In addition, the lifetime of the  $^3\Delta_u$  state may be as long as 1 or 2 sec.<sup>17</sup> It has been suggested that the quenching action of ammonia upon the active nitrogen afterglow is due to reaction of ammonia with the  $^5\Sigma_g^+$  molecular precursor of the afterglow.<sup>41</sup>

The presence of excited atoms in active nitrogen has been detected by the emission of metastable nitrogen  $^2P$  atoms in transition to the ground state at 3466 Å.<sup>44,45</sup> Absorption spectra have shown the presence of both  $^2D$  and  $^2P$  metastable nitrogen atoms (at 1493 and 1743 Å) but from the intensities of these transitions relative to that shown by ground state absorption, at 1200 Å, the concentration of excited atomic species must be several orders of magnitude lower than that of ground state atoms.<sup>45</sup> Such a low concentration of metastable atoms in active nitrogen has been borne out by the complete absence





of these species in the mass spectrum of active nitrogen produced in a glow discharge;<sup>9</sup> while their presence in small quantities has been postulated from the mass spectrum of active nitrogen from a condensed discharge.<sup>25</sup> The paramagnetic resonance spectrum of active nitrogen has shown no positive evidence of metastable atoms, but concentrations up to one percent would have gone undetected by the method used.<sup>27</sup>

From the presence of approximately one electron per  $10^6$  active particles in active nitrogen it has been concluded that ionic species in the reaction region do exist, but do not contribute as a major source of chemical reactivity.<sup>25,46</sup>

When a microwave exciter is used to produce active nitrogen, vibrationally excited ground state nitrogen molecules have been indicated to exist from the liberation of considerable amounts of heat when nitrous oxide is added to the afterglow stream.<sup>47</sup> Two other independent investigations using condensed discharges to produce the active nitrogen have detected no heating when nitrous oxide or carbon dioxide is added to the active nitrogen stream.<sup>32,48</sup> The absorption spectrum arising from the excitation of the Lyman-Birge-Hopfield bands, using a microwave exciter, has shown that about one in ten absorbing molecules has  $v'' = 1$ .<sup>49</sup> Vibrational relaxation times for ground state nitrogen have indicated a lifetime for vibrational excitation to be of the order of 50 milliseconds,<sup>50,51</sup> from which it has been concluded that in active nitrogen one in three molecules in the ground state will have one quantum of vibrational excitation. Such vibrationally excited nitrogen molecules could contribute to the reactivity of active nitrogen by collisional activation.





## THE NITROGEN AFTERGLOW

When active nitrogen is produced by an electrical discharge through flowing nitrogen gas its production is accompanied by an intense, long-lived afterglow which streams out of the discharge region. Much work has been done on the afterglow so emitted during the decay of active nitrogen.

The spectroscopic nature of the visible afterglow was studied originally by Lewis<sup>7,52</sup> and Strutt (later Lord Rayleigh)<sup>53</sup> it was later named the Lewis-Rayleigh afterglow in recognition of their pioneer studies. Until very recently the most prominent feature of this visible afterglow had been thought to be due to selected bands belonging to the first positive system of nitrogen ( $B \ ^3\Pi_g \longrightarrow A \ ^3\Sigma_u^+$ ). These bands were historically denoted as the  $\alpha$  bands of active nitrogen. A weaker, but nonetheless distinguishing, feature of the afterglow spectrum has been the appearance of the  $v' = 0$  progression of the fourth positive system of nitrogen ( $D \ ^3\Sigma_u^+ \longrightarrow B \ ^3\Pi_g$ ) lying about 12.5 e.v. above the ground state;<sup>38,54</sup> thought to have been necessary for the production of stoms from a condensed discharge.<sup>55</sup> Also the selective enhancement of certain members of the second positive system of nitrogen ( $C \ ^3\Pi_u \longrightarrow B \ ^3\Pi_g$ ) lying 11 e.v. above the ground state has been observed, through the specific enhancement of vibrational levels belonging to the  $C \ ^3\Pi_u$  state which gives rise to the system.<sup>38,54</sup>

In addition to the nitrogen band systems, the  $\beta$  and  $\gamma$  bands of nitric oxide were discovered to be prominent features of the active nitrogen spectrum. These bands were originally characterized as the  $\beta$  and  $\gamma$  bands of active nitrogen;



the  $\gamma$  bands were even ascribed to be the third positive system of nitrogen. Both the  $\beta$  and the  $\gamma$  systems of nitric oxide appear in the violet and ultraviolet regions and have since been ascribed to two different excited states of nitric oxide,<sup>56</sup> the B  $^2\Pi$  and A  $^2\Sigma^+$ , in transition to the X  $^2\Pi$  ground state.

Kaplan has demonstrated that the spectrum characteristic of a condensed electrode discharge, as investigated by Fowler and Strutt,<sup>54</sup> could be duplicated by passing a mild uncondensed electric discharge through glowing active nitrogen.<sup>57</sup> Such a discharge has been shown to lose energy to the active nitrogen and to partially quench the Lewis-Rayleigh afterglow.<sup>58</sup>

A recent look at the vacuum ultraviolet region has revealed that weak emission bands belonging to the Lyman-Birge-Hopfield bands of nitrogen are being excited in active nitrogen.<sup>28</sup> Only levels below the well known nitrogen predissociation at  $v' = 6$ , of the a  $^1\Pi_g$  state, have been shown to be present. This, associated with the fact that the first positive bands observed in active nitrogen also break-off at another well known predissociation, with almost the same energy as the former, has led Kistiakowsky and co-workers<sup>9</sup> to conclude that both emission band systems in active nitrogen share a common origin, which has been associated by Gaydon<sup>23</sup> with a  $^5\Sigma_g^+$  state of nitrogen arising directly from the recombination of two ground state atoms. Another study<sup>39</sup> also revealed that certain of the weaker bands, in the photographic infrared region (at 6934, 7823, and 8949 Å), thought to be members of the first positive system were in actuality members of a previously unobserved band system of





nitrogen. The upper state giving rise to the new system was designated Y, later identified as  $^3\Sigma_u^-$ ; <sup>16</sup> the band system was extended in a following study.<sup>39</sup>

Bayes and Kistiakowsky<sup>41</sup> have carefully studied the mechanism giving rise to the Lewis-Rayleigh afterglow. Their conclusion verified the one made in the earlier study that a shallow  $^5\Sigma_g^+$  state of nitrogen arising from and in equilibrium with ground state nitrogen atoms was the ultimate molecular precursor of the nitrogen afterglow. They concluded that besides the cross-overs into the  $a\ ^1\Pi_g$  state giving rise to the Lyman-Birge-Hopfield bands, into the B  $^3\Pi_g$  state, emitting the first positive bands, and into the Y  $^3\Sigma_u^-$  state from which arises the newly observed Y bands; that cross-over was also induced into another new, unobserved state of nitrogen,  $^3\Delta_u$ . The existence of this  $^3\Delta_u$  state has since been indicated by experiments independent of active nitrogen!<sup>17</sup> Thus, the afterglow mechanism is now believed to be due to several radiationless cross-overs, induced by collision with a third body, between the  $^5\Sigma_g^+$  and the upper states giving rise to the various afterglow emissions. In early works, Rayleigh<sup>59</sup> and McLennan<sup>60</sup> showed that the addition of foreign gases to active nitrogen altered the observed distribution of the afterglow spectrum. Bayes and Kistiakowsky<sup>41</sup> have shown recently that various molecular gases alter the vibrational distribution of the upper levels of the first positive bands (ammonia enhances  $v' = 12$ , carbon dioxide  $v' = 11$ , and hydrogen  $v' = 10$  and 6). The atomic gases seem to enhance the production of the Y bands relative to the first positive bands, explaining the reddening of the after-





glow noted by Rayleigh and McLennan when argon and neon were added to active nitrogen. In general, most of the distributional effects shown by the first positive bands in the afterglow, in the presence of an excess of foreign gas, have been attributed to the effects of the foreign gases on the various states being populated from the  $5\Sigma_g^+$  state.<sup>41</sup>

From quantitative measurements taken of the intensity of the Lewis-Rayleigh afterglow and the rate of recombination of nitrogen atoms on a platinum probe it has been concluded that of twenty nitrogen molecules forming, from the three-body recombination process occurring in the gas phase, only one molecule emits a photon in the first positive bands.<sup>61</sup> It has long been known and recently verified that the afterglow shows a negative temperature coefficient<sup>9,53,55</sup> and that the intensity of the afterglow is proportional to the square of the nitrogen atom concentration present.<sup>9,61,62</sup> The effect of the wall conditions and pressure upon the intensity of the afterglow has been studied. With the walls un-poisoned against wall recombination of nitrogen atoms, pressures above 0.3 mm. were required to obtain reproducible amounts of gas phase recombination of the nitrogen atoms;<sup>61</sup> while with poisoned walls the afterglow intensity has been observed to persist for several hours in a static system containing low pressures of active nitrogen.<sup>53</sup>

The afterglow has been shown to contain a small concentration of free electrons (some with energies in excess of 20 e.v.), the presence of which has been used to explain the weak emission of the first negative bands of nitrogen ( $N_2^+ B \rightarrow X^2\Sigma_g^+$ ) in the afterglow spectrum.<sup>63-65</sup> Studies of the electrical conductivity of the afterglow have indicated that ionized





species present are incidental to the production of the Lewis-Rayleigh afterglow,<sup>53,66,67</sup> yet appear quite strongly in a strong, short-lived flash preceeding the Lewis-Rayleigh afterglow.<sup>68</sup>

The presence of traces of oxygen impurity in the nitrogen has been demonstrated to affect markedly the electron density emanating from a microwave discharge producing active nitrogen.<sup>69,70</sup>

Optimum condition for electron production has been shown to occur when approximately 0.1 percent oxygen is present, with which the electron density reaches a maximum about 0.1 sec. after the discharge is begun. Studies of the shortlived afterglow produced by these electrons have established the colour to be pink and that it possesses two inter-dependent intensity maxima.<sup>71,72</sup>

The intensity distribution of the pink afterglow was found to be closer to that of the discharge than to that exhibited by the Lewis-Rayleigh afterglow.<sup>71</sup> The most recent study of this pink

afterglow has shown the presence of metastable nitrogen atoms (both  $^2D$  and  $^2P$ ) from very prominent transitions in the vacuum ultraviolet spectrum (to the  $3s\ ^2P$  level 10.6 e.v. above the atomic ground state).<sup>73</sup> In addition one weak set of bands from the Birge-Hopfield system ( $b'\ ^1\Sigma_u^+ \rightarrow X\ ^1\Sigma_g^+$ ) has been noted arising from levels below  $v' = 2$ ; these bands also appearing in the vacuum ultraviolet. Both maxima of the pink afterglow were shown to be partially quenched in the region of metal foil electrodes, wrapped around the outside of the decay tube, when a radio frequency field was applied to the electrodes. The pink afterglow was never completely quenched by the radio frequency field and could not be quenched at all by focused radiation from a microwave exciter. The study attributed the major part of the energy of the pink afterglow to be stored in ground state atoms





of nitrogen present with some admixture of metastable atoms. The radio frequency quenching has been attributed to an increase in electron temperature, while the absence of microwave quenching has been interpreted as implying that positive ions (most probably  $N_3^+$  and  $N_4^+$ <sup>74</sup>) provide the crucial parameter required to release the energy stored in the high concentration of nitrogen atoms present.

### THE PRESENT PROBLEM

In the course of his early studies with active nitrogen, Strutt observed that when bromine was admitted into the afterglow stream the yellow afterglow was replaced by a feeble orange luminosity.<sup>75</sup> A spectroscopic investigation of the orange emission was made by Elliott,<sup>76</sup> who attributed the emissions to the diatomic molecule NBr (nitrogen monobromide). No reaction product was noted in another study of the reaction of bromine with active nitrogen;<sup>77</sup> a reddish light in the region of mixing of the two reactant molecules was the only observable feature of the reaction.

A reaction flame very similar to that produced by bromine in active nitrogen has been noted when active nitrogen is admitted into a reaction vessel with hydrogen bromide or ammonium bromide.<sup>3</sup> The orange flame produced when hydrogen bromide is mixed with active nitrogen was attributed to the emission of a "modified" nitrogen afterglow.<sup>78</sup>

The present study has involved the investigations of the similarity between these three orange emissions. An investigation of a blue trap-glow observed when ammonia is mixed with active nitrogen at low temperatures<sup>5</sup> was made because of the presence of a blue glow during the course of an earlier hydrogen bromide investigation.<sup>3</sup> The latter part of the study has investigated the nature of nitrogen monobromide and has attempted a correlation of its spectroscopic existence with the observed chemical processes in the systems.



## THE EXPERIMENTAL PART

### INTRODUCTION OF MATERIALS

Nitrogen: Nitrogen (purified grade, The Canadian Liquid Air Co. Ltd.) was introduced directly into the apparatus through n-butyl phthalate bubbler, which acted as a pressure regulator. For some of the experiments, the nitrogen was passed through a 500°C. copper-filled furnace to remove any traces of oxygen which might have been present. At such times, a cold trap of either ice-water or liquid nitrogen was used after the furnace to remove condensable products formed during the purification in the furnace. In general the use of pre-purified nitrogen made such extra purification unnecessary, since with pre-purified nitrogen no condensable products were obtained either with or without the furnace in use.

Bromine: Liquid bromine (analytical reagent, Baker and Adamson) was introduced into a removable trap which could be attached to the vacuum system by means of a 15/30 ground glass joint (Figure 2). No initial purification steps were performed. The bromine sample was frozen using liquid nitrogen, attached to the apparatus, evacuated, and degassed by the usual methods.\* In all cases, the bromine sample was used immediately upon introduction, and all excess bromine was removed from the vacuum system immediately after the experiment was completed.

\* A comprehensive review of general vacuum techniques is to be found in the work by Sanderson.<sup>79</sup>







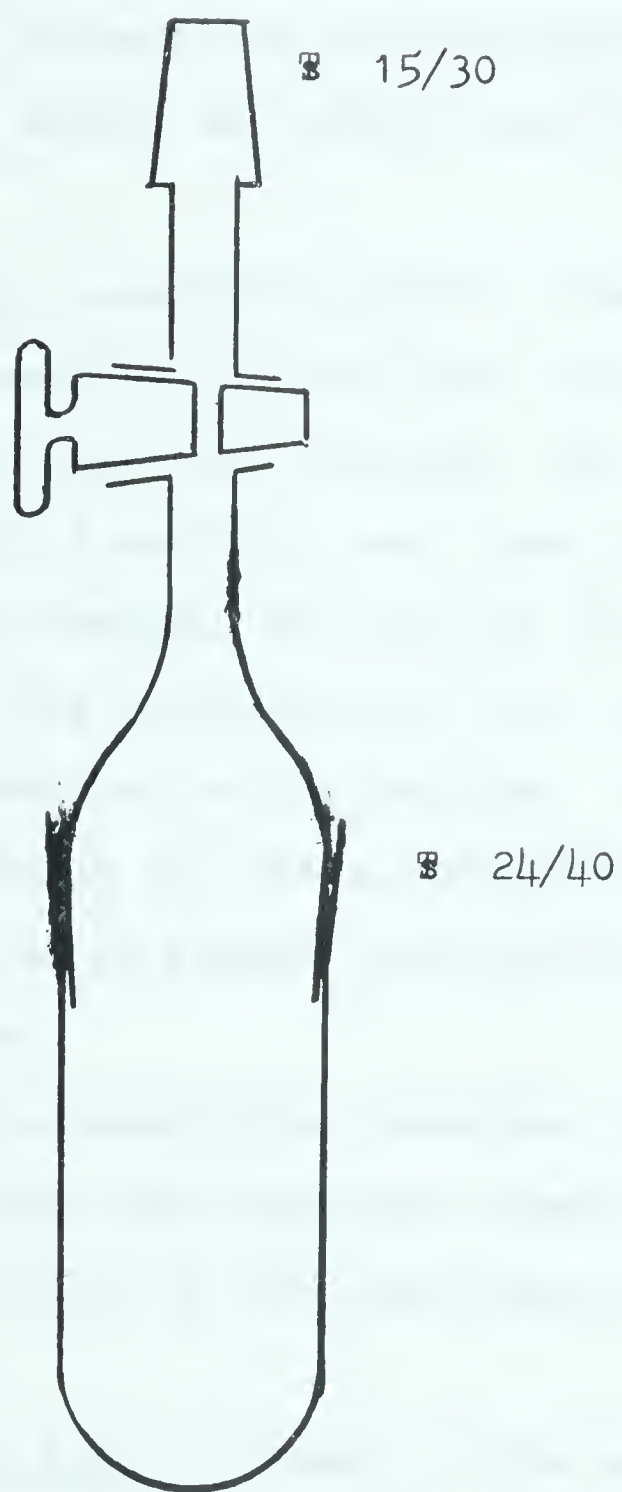


Figure 2

Trap for Bromine Introduction



Hydrogen Bromide: Hydrogen bromide (anhydrous, The Matheson Co. Ltd.) was introduced into the apparatus directly from the cylinder and condensed into a cold-trap. A routine fractional distillation was performed upon the frozen sample from which a ten percent forerun and residue were discarded. The remainder of the gas sample was stored under vacuum for later use.

Ammonium Bromide: Ammonium bromide (Fisher Certified Reagent) was used as a reactant in some later experiments. The reagent was dissolved in water and introduced into the apparatus as a solution. A coating of solution was rinsed onto the walls of the reaction vessel by drawing the solution into the apparatus using an aspirator. The solution was then allowed to drain out of the apparatus by removal of the suction. Several rinsings were made each time a coating of reactant was required. Solution strengths varying from 5 to 40 percent were used during the course of the experiments.

Ammonia: Ammonia (anhydrous, Canadian Industries Limited) was introduced into the apparatus directly from the cylinder, purified, and stored in the same manner as was the hydrogen bromide.

Ortho-Phosphoric Acid: In many of the experiments it was deemed desirable to "poison" the walls of the reaction system against recombination of nitrogen atoms. To accomplish this, solutions of ortho-phosphoric acid (Fisher Certified Reagent) were used. In most of the "poisoned" experiments a 5 percent solution was employed; however, solutions ranging from 1 to 10 percent were also used. The wall poison was introduced in a similar manner to that used for the ammonium bromide solutions.





## THE APPARATUS

The Nitrogen Introduction System: Active nitrogen was prepared by passing pre-purified nitrogen into the vacuum apparatus (Figure 3) through a pressure bubbler which contained n-butyl phthalate. The use of such a bubbler enabled a constant pressure head of nitrogen to be maintained independent of fluctuations in atmospheric pressure. From the bubbler the nitrogen gas passed upwards through a liquid trap, designed to catch any n-butyl phthalate which might have been splashed upwards with the nitrogen stream in the bubbler. The nitrogen was then passed through a wide tube containing copper turnings. This tube was surrounded with a mantle of asbestos containing an imbedded coil of Nichrome wire which could be heated by means of an electrical current (controlled from a Variac) to  $500^{\circ}\text{C}$ . or more. When it was desirable to be sure that absolutely no residual traces of oxygen remained in the nitrogen, the furnace was activated by setting the Variac to 50 volts. Otherwise, the nitrogen was allowed to flow through the copper at room temperature into a removable trap, where any condensable materials could be frozen-out of the nitrogen stream by immersing the trap in a bath containing either an ice-water mixture or liquid nitrogen. When it was desirable to introduce traces of moisture into the nitrogen stream a water-saturated wad of cotton and glass wool was inserted into this removable trap.

The nitrogen was then allowed to fill a known ballast volume ( $V_N$ ) before being admitted into a flow meter ( $F_N$ ), in which a capillary orifice was used to regulate the amount of nitrogen gas "leaking" into the vacuum system. Interchangeable capillary jets could be inserted into the flow meter to give

# THE HISTORY OF THE

... of the ...

... of the ...

... of the ...

... of the ...

... of the ...

... of the ...

... of the ...

... of the ...

... of the ...

... of the ...

... of the ...

... of the ...

... of the ...

... of the ...

... of the ...

... of the ...

... of the ...

... of the ...

... of the ...

... of the ...

... of the ...

... of the ...

... of the ...

... of the ...

... of the ...

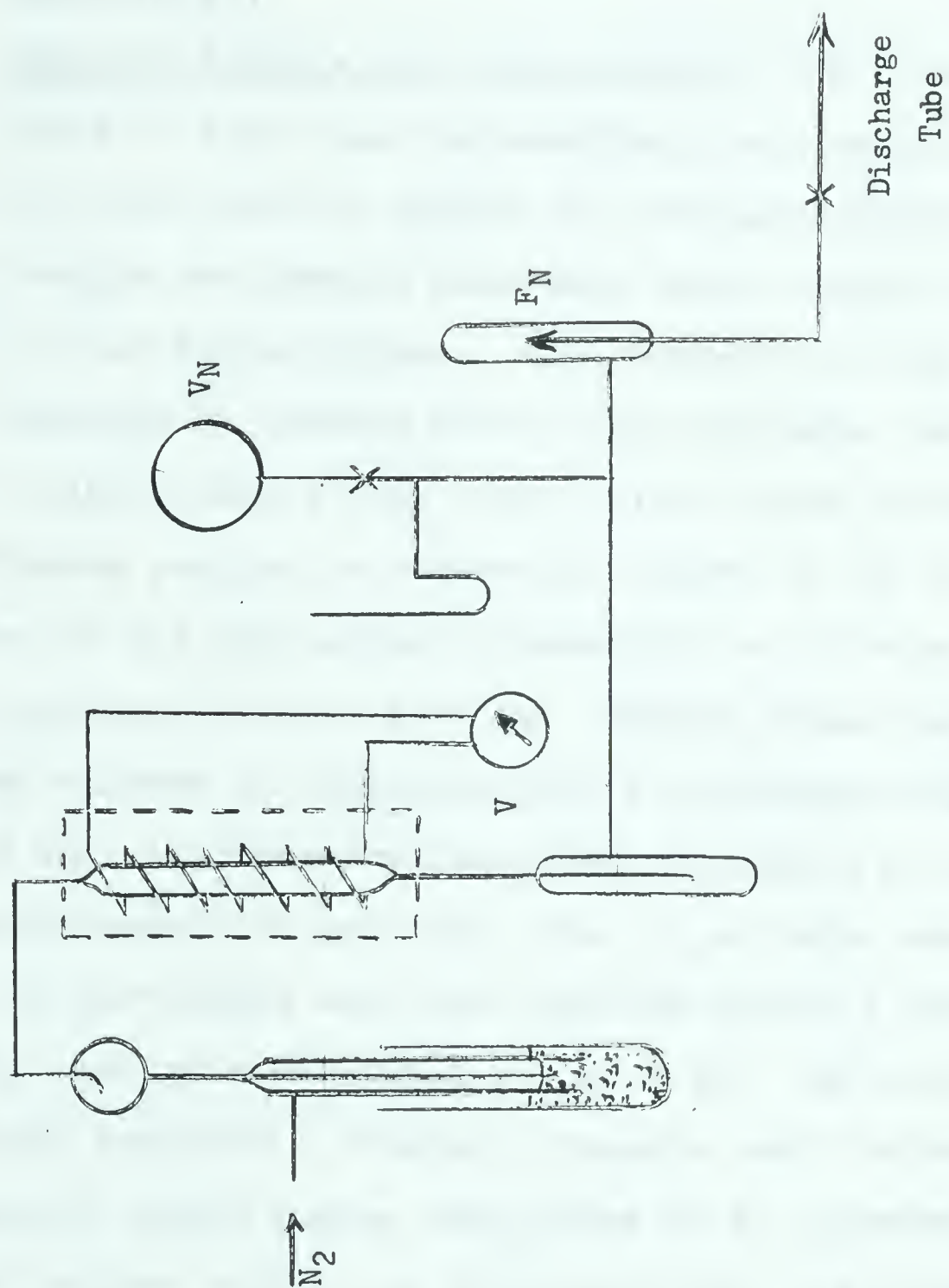


Figure 3  
The Nitrogen Introduction System





differing rates of introduction into and resultant pressures of nitrogen in the vacuum system. The flow meter was calibrated for each jet by measuring the rate of evacuation of the known ballast volume (Appendix I).

Reactant Storage and Introduction: All reactants were handled, prior to their use for reaction, in a vacuum system separate from that used to handle the nitrogen (Figure 4). Both hydrogen bromide and ammonia were kept under vacuum in a storage bulb ( $V_S$ ) of two litres volume. When desired for use the stored gas was condensed by cooling with liquid nitrogen; and then allowed to distil into a trap cooled with liquid nitrogen ( $T_2$ ) with continuous pumping to remove any traces of air which may have accumulated in the gas during introduction or storage. The gas was then re-distilled back into the storage volume and a small portion was allowed to vapourize into a calibrated volume ( $V_C$ ). The use of this calibrated volume when securing a gas sample allowed measurements of gas flow rates to be taken when required.

The gas sample was then admitted directly into a ballast volume ( $V_R$ ) through a scratched stopcock (S). By manipulation of the scratched stopcock a constant pressure could be maintained in the ballast volume during the course of an experiment. The gas in the ballast volume was introduced into the reaction system through a flow meter ( $F_R$ ) in a similar manner to the nitrogen.

Bromine was introduced into the apparatus at the  $\text{N} 15/30$  ground glass joint (A) and distilled directly, with pumping, into the removable trap ( $T_1$ ) from which it was re-distilled into a second removable trap ( $T_2$ ) adjacent to the ballast volume. Because of the corrosive action of bromine upon mercury, all mercury measuring devices had to be separable from those parts



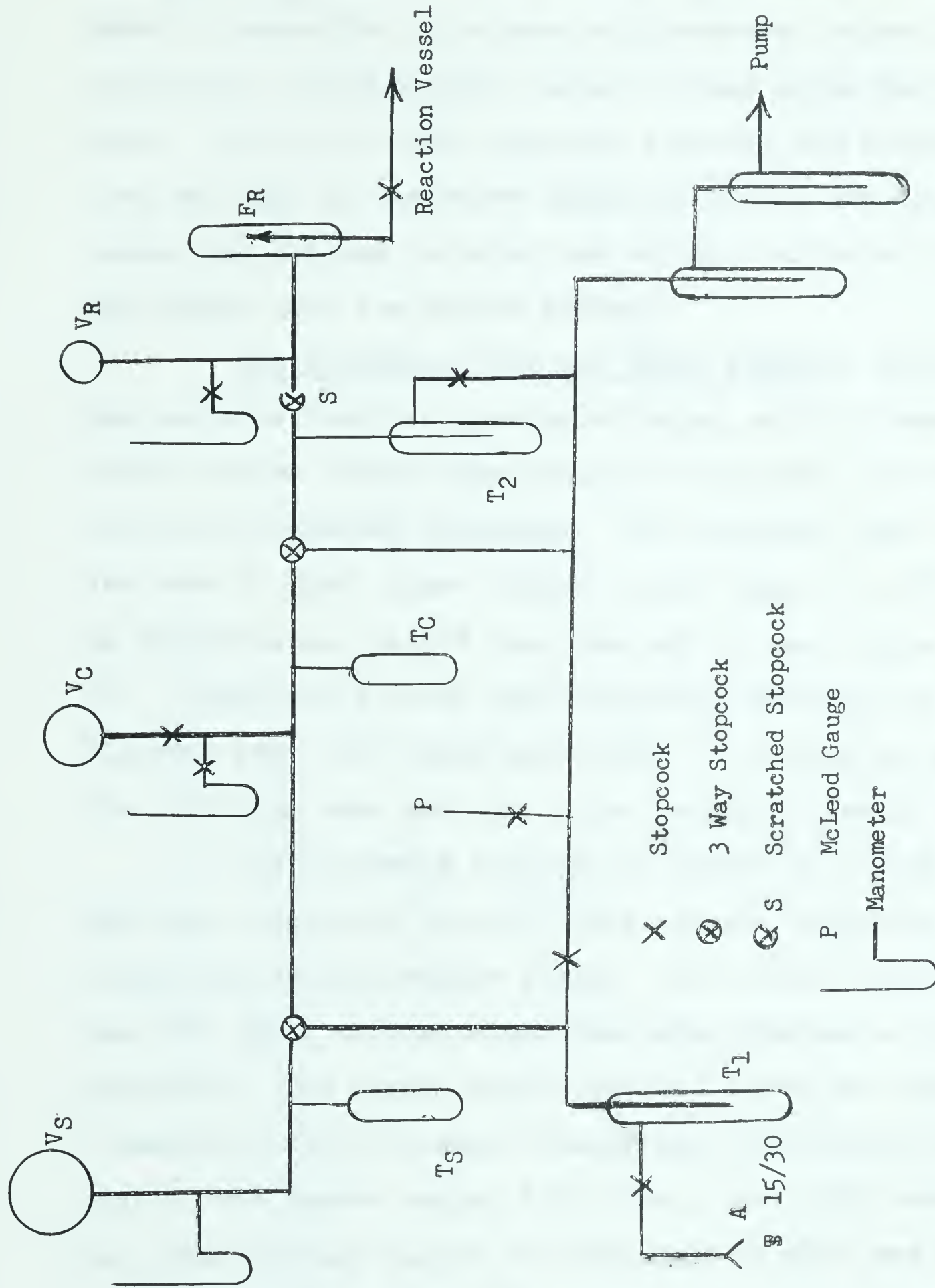


Figure 4  
Reactant Storage and Introduction System





of the system in which the bromine was handled. Such separation made it impossible to attempt any pressure control between the calibrated volume and the ballast volume using the scratched stop-cock. In lieu of other pressure control, the bromine containing trap was kept at ice-water temperature; and the equilibrium vapour was allowed to enter the ballast volume and flow meter, and thence into the vacuum system.

The Discharge Tube and Power Supply: Active nitrogen was prepared from the gaseous nitrogen, which flowed into the vacuum system through the nitrogen flow meter, by means of an electrode condensed discharge. The discharge tube (Figure 5) was made of 25mm. glass tubing in the shape of a "Y". An aluminum electrode was sealed into the end of each upper arm of the "Y". Immediately below each electrode there was an inlet for the nitrogen gas. The third arm of the "Y" served as an outlet from the discharge tube and led to the reaction vessel.

The discharge tube was activated by a high voltage, half-wave rectifier circuit. The circuit consisted of two parallel 866A mercury-vapour diodes. The output load of each tube was 5000 ohms, through which the tubes charged a 4 micro-farad capacitor. The heater supply for the diodes was obtained from a Hammond 1123x60 filament transformer, each diode utilizing one side of the center tapped 5.0 r.m.s., a.c. volt secondary. The a.c. high voltage supply for the plate circuit was accomplished by energizing a Hammond 793 step-up transformer, using a Variac. The output of the variac was connected to the "Hi" and "Com" terminals of the primary through a small open-core inductance (6.3 millihenries) which served to minimize transient currents in the 8 ampere Variac fuse circuit. Both 2410 terminals of the



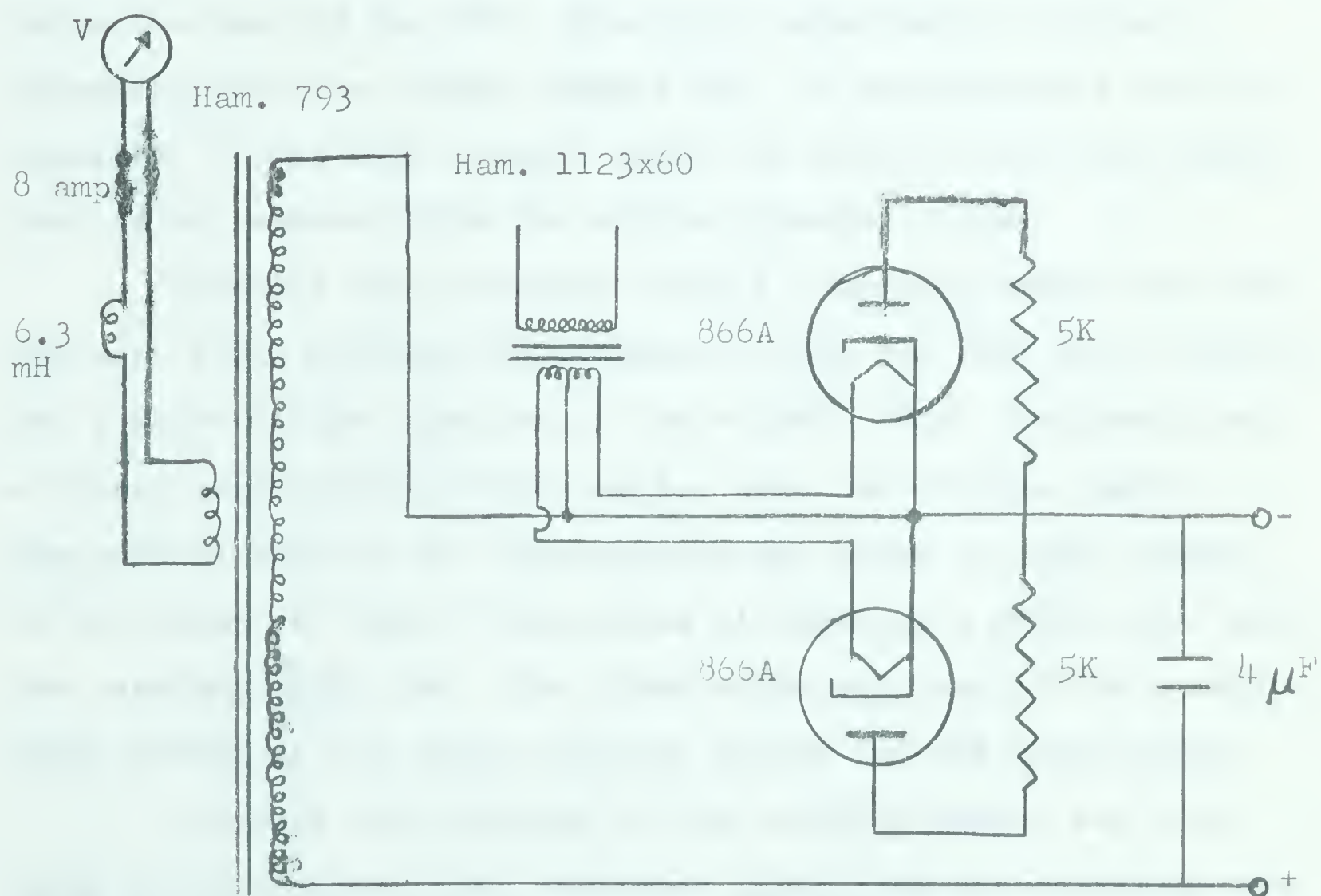
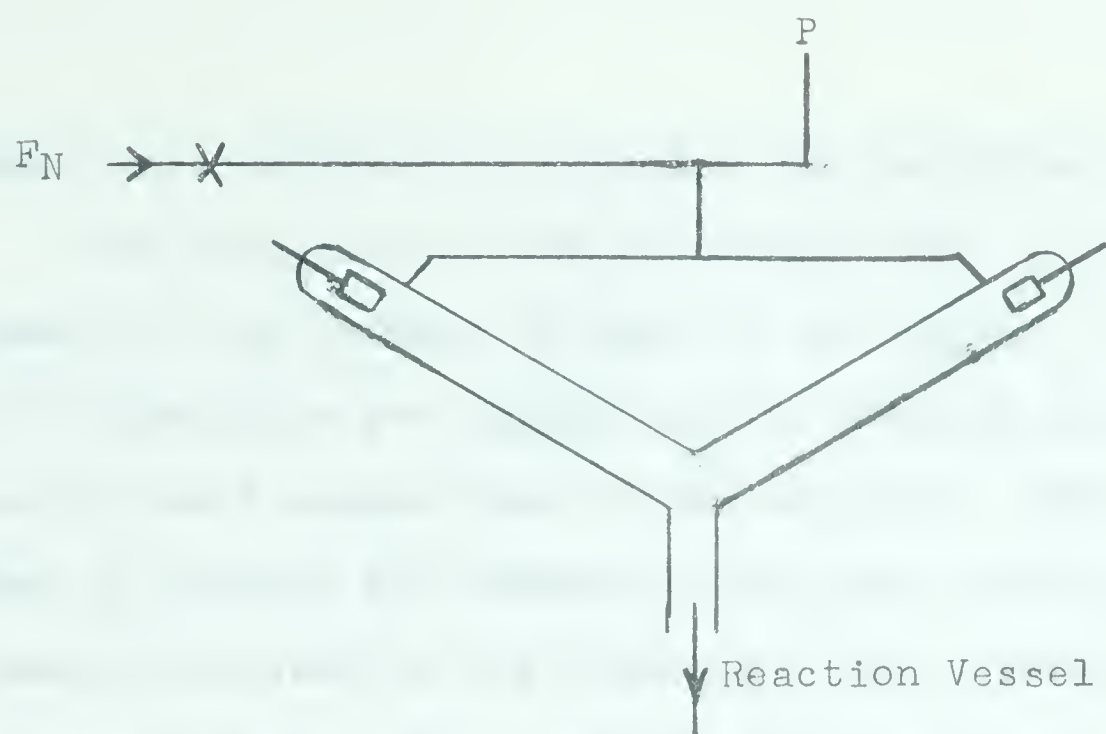


Figure 5

The Discharge Tube and Power Supply





secondary were utilized to energize the rectifier tubes.

The frequency of the discharge could be controlled by adjustment of the primary voltage on the Variac. A frequency of about 15 discharges per second was the maximum that could be handled by the 8 ampere fuse in the circuit. The Variac setting required to produce the maximum flash rate varied with the total gas pressure present in the discharge tube; higher pressures required more voltage. Most experimental work was done with a frequency approaching the upper limit of flash rate.\*

The Reaction System for Preliminary Work: The reaction vessel was fitted to the outlet of the discharge tube about 80mm. below the apex of the "Y". The first experiments utilized a spherical reaction vessel (Figure 6a), of approximately 300 ml. capacity, fitted with a small inlet jet near the neck for introduction of reactant into the active nitrogen stream.

Spectra were obtained using a converted Bausch and Lomb, 250 mm., f/4.4 grating monochrometer, with the exit slits removed and a plate holder inserted at the outlet. This instrument gave a linear dispersion of 0.015 mm/Å. over the visible region. The optical axis of the spectrograph was aimed at right angles to the plane of flow of the active nitrogen at a point just below the reactant inlet jet. The fixed condenser lens of the spectrograph served as the entire optical system for the experiments.

Because the position of the reaction vessel was just below the discharge tube, reflected light from the discharge was

\* The electrical output of the power supply is discussed further in Appendix II.



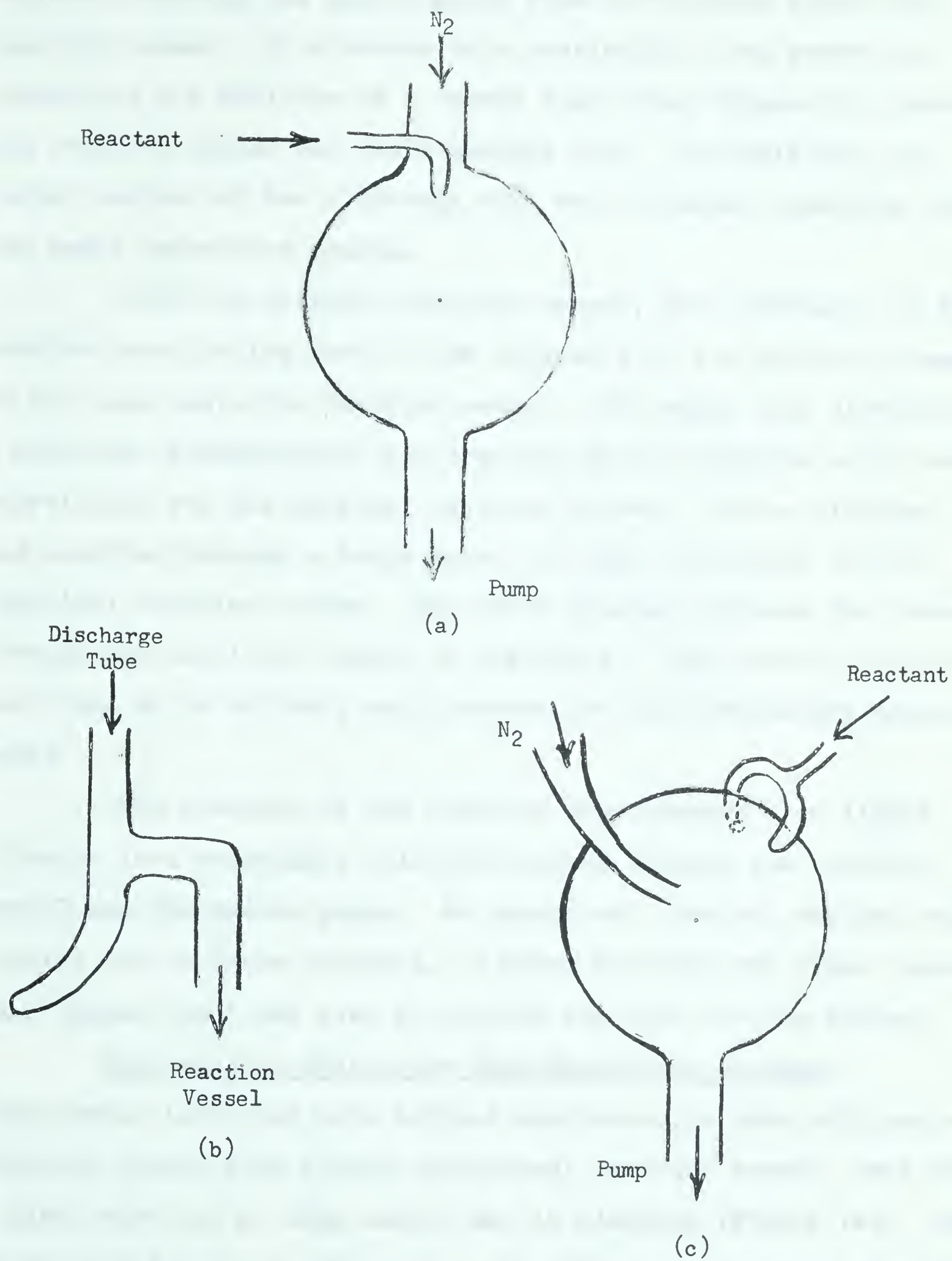


Figure 6

Preliminary Reaction Vessels





believed entering the spectrograph from reflections inside the reaction vessel. To minimize this possibility, the system was refined by the addition of a curved light trap (Figure 6b) between the reaction vessel and the discharge tube. In addition, the outer surface of the discharge tube was blackened excepting for two small inspection spaces.

With the original reaction vessel, back diffusion of the reactant was placing most of the intensity of the reaction flame in the neck above the reaction vessel. To combat this difficulty, a modified "stirred-flow" low pressure reactor (Figure 6c)<sup>10</sup> was substituted for the original reaction vessel. Active nitrogen was admitted through a large inlet jet near the center of the spherical reaction volume. The other reactant entered the vessel through two capillary inlets on the walls. This reaction vessel was found to be entirely satisfactory for the preliminary experiments.

The products of the reaction were trapped over liquid nitrogen in a detachable cold-trap placed between the reaction vessel and the vacuum pumps. No subsequent chemical analysis was carried out on these products. A Welch Duo-Seal, two stage vacuum pump (Model 1402) was used to provide the flow for the system.

#### The Reaction System for High-Resolution Spectra:

Experiments involving more refined spectroscopic work utilized a reaction system with a long cylindrical reaction vessel, made from a glass tube 1.5 m. long and 20 mm. in diameter (Figure 7a). Quartz windows were sealed across each end of the reaction tube with pitch. Active nitrogen was admitted through a small inlet tube, at the wall, close to the upper end of the reaction tube. The reactant



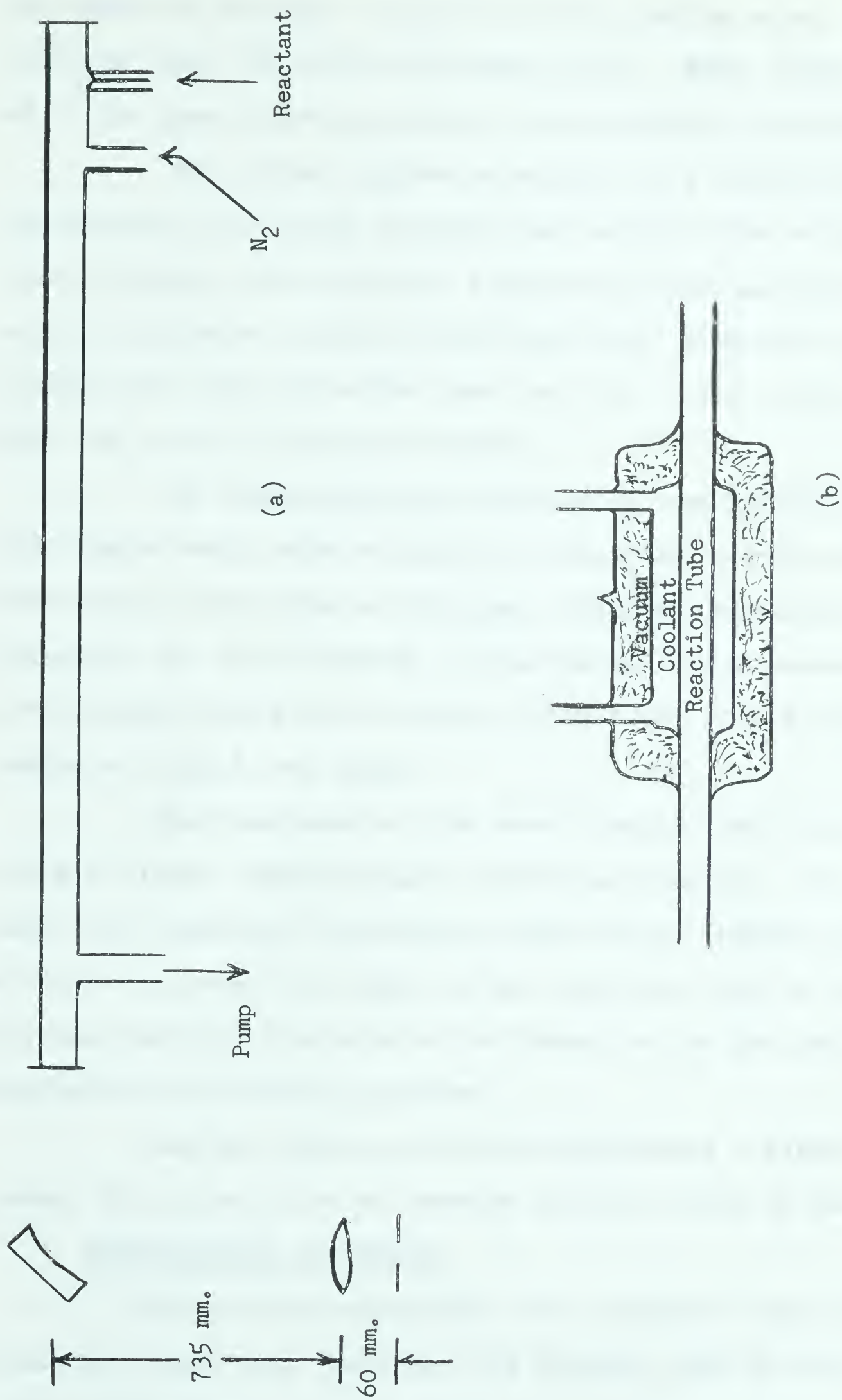


Figure 7  
Reaction System for High Resolution Work





was admitted through a capillary wall opening about 50 mm. further upstream than the active nitrogen inlet. Both inlets were connected to the same sources used in the preliminary experiments.

The optical system consisted of a concave mirror and a condensing lens placed between the reaction-tube window and the spectrograph; quartz optical components were used throughout. The use of a mirrored system facilitated easy alignment of the optics so that the light from the reaction tube could be focused directly upon the slit of the spectrograph.

The high-resolution spectra of the bromine-active nitrogen orange bands were obtained in the Molecular Spectroscopy Laboratory, Pure Physics Division, National Research Council, Ottawa by Dr. H.B. Dunford. A ten metre, f/100 concave grating spectrograph which gave a linear dispersion of  $1.4 \text{ mm}/\text{\AA}$ . in the region of  $6000 \text{ \AA}$  was used.

The remainder of the spectroscopic work was performed using a Hilger, Medium Quartz prism spectrograph. In the experiment with ammonia a horizontal Dewar flask (Figure 7b) was inserted half-way down the length of the reaction tube to allow the glowing reaction products to be frozen out of the gas stream in the path of the optical system.

For all high-resolution experiments a Kinney vacuum pump (Model KC-15) was used to provide fast gas flow in the apparatus.

#### EXPERIMENTAL PROCEDURE

For a given experiment (or series of experiments) the reaction vessel was "poisoned" by washing with an ortho-phosphoric acid solution or cleaned of wall poison by several rinsings with distilled water. After treatment the reaction vessel was drained



and then dried under vacuum. In almost all of the experiments the discharge tube and inlet connection to the reaction vessel were "poisoned", regardless of how the reaction vessel was treated, to prevent undue wall recombination of the active nitrogen before it entered the reaction vessel.

Once the apparatus had been dried, nitrogen was introduced into the flow meter, at a pressure close to 700 mm. and allowed to leak into the flow system. The condensed discharge was started by activating the Variac. The active nitrogen produced by the discharge emitted a sufficiently intense, yellow afterglow to be visible throughout the entire reaction system, from discharge tube to cold-trap. After a minute or two had elapsed, the active nitrogen flow was assumed to have become stabilized; and minute traces of impurities, on the walls of the reaction vessel, were assumed to have been flushed out of the apparatus. The particular reactant (excepting ammonium bromide) was then introduced into the active nitrogen stream.

The shutter of the spectrograph was opened to allow the plate to be exposed. The reactant and active nitrogen flow were then maintained uninterrupted for the duration of the exposure. Kodak glass spectroscopic plates were used throughout the experiments. Exposure times and slit apertures were determined by trial. Generally, times in the range 10 min. to 10 hrs. with slit widths of  $200\mu$  or less, were required to expose type 103a emulsions. Upon completion of the exposure, the shutter was closed and the reactant flow, discharge, and nitrogen flow were discontinued.







A reference spectrum was then exposed on the plate immediately adjacent to the reaction spectrum. Both a mercury lamp and an iron hollow-cathode arc, with neon filler gas, were used as references in the course of the experiments. Reference exposures were of the order of a few seconds with a slit width of  $10\mu$  or less.

#### ANALYSIS OF THE SPECTRA

A three power, travelling-microscope manual comparator (Hilger and Watts) was used to measure the positions of the spectral lines appearing on the spectroscopic plates. The plate was secured on the viewing stage of the comparator, approximately parallel to the direction of travel of the comparator stage. The plate was illuminated with a light (preferably bluish in colour) of moderate intensity. All motion of the viewing stage was carried out in one direction, moving at a slow rate, in order to minimize errors from stage inertia and screw friction. When a particular spectral line was centered in the cross-hairs of the microscope the position of the stage was read to 0.001 mm. using the micrometer dial. Whenever possible, the line was identified and a rough estimate of its intensity was made. When the positions of all the lines under investigation had been read, several reference lines on either side of the spectrum were also recorded. The stage was then re-set at the starting point and the spectroscopic plate was moved on the viewing stage such that a new setting for the first line was obtained exactly one-half turn of the screw away from the previous setting. The position of each line was then re-read.





By averaging the two sets of readings, of the positions of the spectral lines, errors in the pitch of the winding screw were eliminated from the readings. The vacuum wavelengths of the observed reference lines were obtained from wave-length table.<sup>80</sup> The two extreme reference lines were then used to calculate an average linear dispersion ( $\delta$ , in mm/ $\text{\AA}$ ) for the spectrum over the region under investigation. The displacement ( $\Delta s$ ) of all other reference lines from one of these extreme reference lines ( $\lambda_0$ ) and the average linear dispersion was then used to calculate an "observed" wavelength for each reference line.

$$\Delta s \times \frac{1}{\delta} = \Delta \lambda \quad . . . . (1)$$

$$\Delta \lambda + \lambda_0 = \lambda_{\text{obs}} \quad . . . . (2)$$

The difference between the observed and vacuum wavelengths for each reference line was then calculated.\* These differences were then plotted versus the observed wavelengths across the entire region (Figure 8). This graph was used to correct the observed wavelengths of the reaction spectrum, for deviations from average linear dispersion.

The observed wavelength for each line in the reaction spectrum was then calculated using the displacement of the line from  $\lambda_0$  and the average linear dispersion. Using the correction graph, the observed wavelengths were then converted to vacuum wavelengths. Reciprocals were taken of all wavelengths to convert them to wavenumbers ( $\nu \text{ cm}^{-1}$ ).

\* Sample calculations and raw comparator data, for both the reference lines and the actual reaction spectrum are included in Appendix III.

The following is a list of the names of the persons who have been

admitted to the office of the Secretary of the State of New York

for the purpose of receiving the same, and who have been

admitted to the office of the Secretary of the State of New York

for the purpose of receiving the same, and who have been

admitted to the office of the Secretary of the State of New York

for the purpose of receiving the same, and who have been

admitted to the office of the Secretary of the State of New York

for the purpose of receiving the same, and who have been

admitted to the office of the Secretary of the State of New York

for the purpose of receiving the same, and who have been

admitted to the office of the Secretary of the State of New York

for the purpose of receiving the same, and who have been

admitted to the office of the Secretary of the State of New York

for the purpose of receiving the same, and who have been

admitted to the office of the Secretary of the State of New York

for the purpose of receiving the same, and who have been

admitted to the office of the Secretary of the State of New York

for the purpose of receiving the same, and who have been

admitted to the office of the Secretary of the State of New York

for the purpose of receiving the same, and who have been

admitted to the office of the Secretary of the State of New York

for the purpose of receiving the same, and who have been

admitted to the office of the Secretary of the State of New York

for the purpose of receiving the same, and who have been

admitted to the office of the Secretary of the State of New York



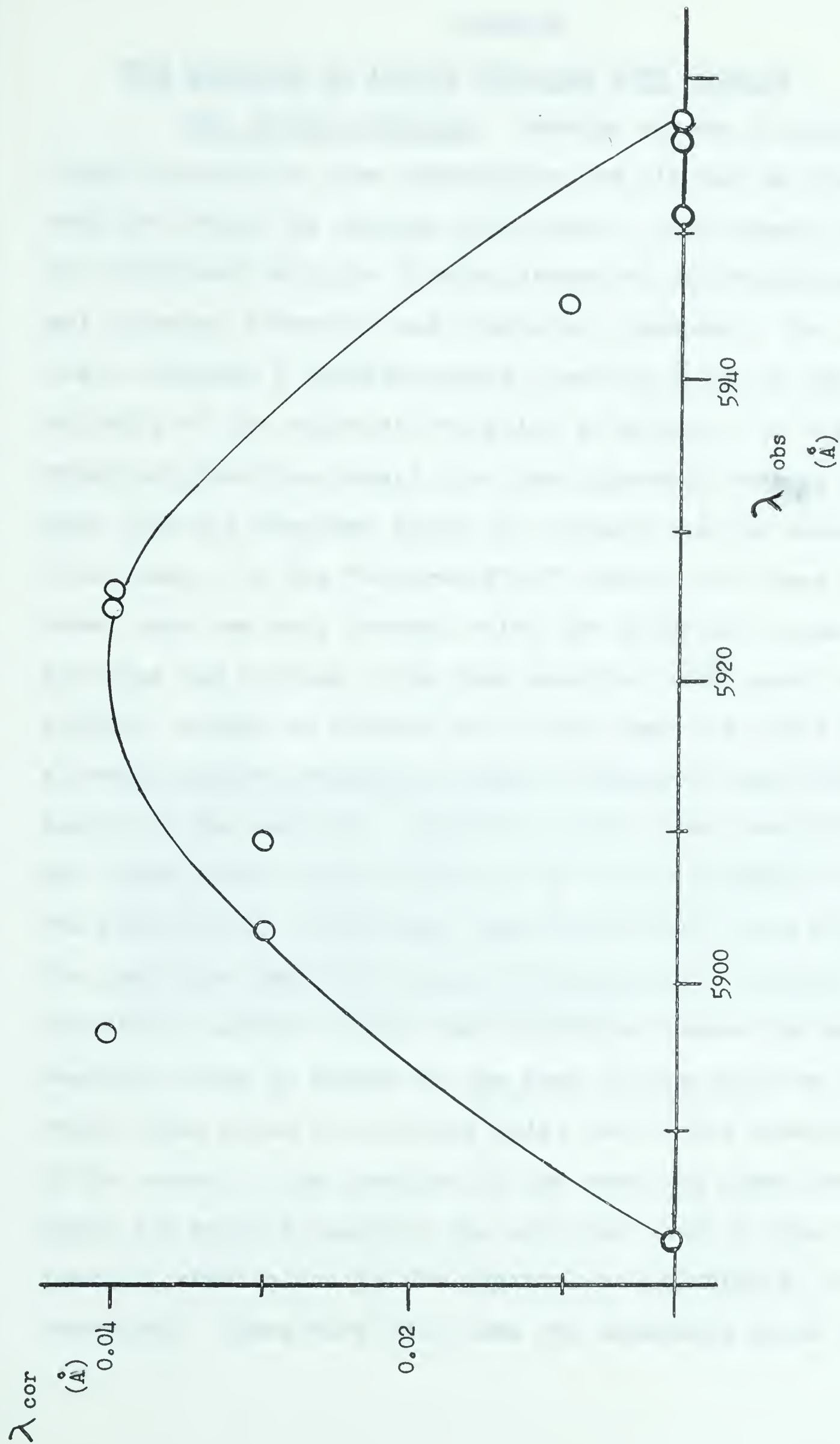


Figure 8

Correction for Deviation from Average Linear Dispersion

1000

1000



## RESULTS

THE REACTION OF ACTIVE NITROGEN WITH BROMINE

The Orange Emission: Bromine vapour in equilibrium with liquid bromine at room temperature was allowed to flow into the reaction vessel at varying flow rates. When bromine vapour was so introduced into the flowing stream of active nitrogen the normal nitrogen afterglow was completely quenched. In its place there appeared a reddish-orange reaction flame in the immediate vicinity of the walls at the point of mixing. In the original spherical reaction vessel the flame appeared tenuous and streamed away from the reactant inlet jet through the gas phase in all directions. In the "stirred-flow" reactor the flame was concentrated upon the wall towards which the entering stream of active nitrogen was flowing. The long reaction tube, used in later studies, showed an intense wall flame near the inlet openings, although fainter emissions could be observed down most of the length of the reactor. However, in all three reactors the maximum flame intensity was noted to be in the immediate vicinity of the glass walls. Only weak flame intensities were observed in the gas phase near the centre of the reaction vessels. In the spherical reaction vessel back diffusion caused the most intense reaction flame to appear in the neck of the reaction vessel rather than below the bromine inlet jet in the spherical portion of the vessel. The location of the reaction flame above the inlet jet greatly hampered the efficient use of this vessel for spectral studies due to the physical positioning of the components used. Since more wall area was available above the reactant





inlet jet than below it in the original reaction vessel the greater relative intensity of the back-diffused emissions to those below the inlet jet can be explained. Neither the "stirred-flow" reactor nor the tubular reaction vessel presented any back diffusion problems.

Investigations were made of the spectrum of the reaction flame in the red and orange regions of the spectrum using all three spectrographs. Preliminary surveys with the Bausch and Lomb instrument confirmed the bands observed by Elliott (Plate 1).<sup>76</sup>

$\Delta v = 1$	$\Delta v = 2$	$\Delta v = 3$
→ 7-6	→ 9-7	→ 8-5



5799.7 Å || 5769.6 Å

Plate 1

Active Nitrogen—Bromine Reaction Flame

Bausch and Lomb f/4.4 grating spectrograph  
 Kodak Type 103-F(3) Spectroscopic Plates  
 Slit Width 250μ Exposure Time 4 hours



Since the dispersion with the Bausch and Lomb instrument (66 Å/mm) was approximately half of that obtained in the study by Elliott, poorer resolution of the bands were obtained than was reported previously by Elliott. However, in these preliminary studies specific conditions were obtained for the production of a reaction flame with maximum intensity. It was found that a fast active nitrogen flow at low pressure with a very low bromine flow rate facilitated the most intense wall reaction. When the bromine was introduced through a pin-hole leak the orange emissions were observed to be brightest with the molecular nitrogen flow rates normally employed ( $6.7 \times 10^{-6}$  moles/sec).<sup>\*</sup> These reaction conditions were utilized in the 10 m. grating study from which the fine structure of the most intense bands were ultimately obtained. Kodak spectroscopic plates, type 103a-F, were used with 7 to 10 hour exposure times and a slit width of  $60\mu$  to photograph the reaction flame under high dispersion using the 10 m. grating. Comparison spectra of active nitrogen were obtained on the same instrument with 4 to 6 hour exposure times. Reference spectra utilized the iron hollow-cathode, neon-filled arc.

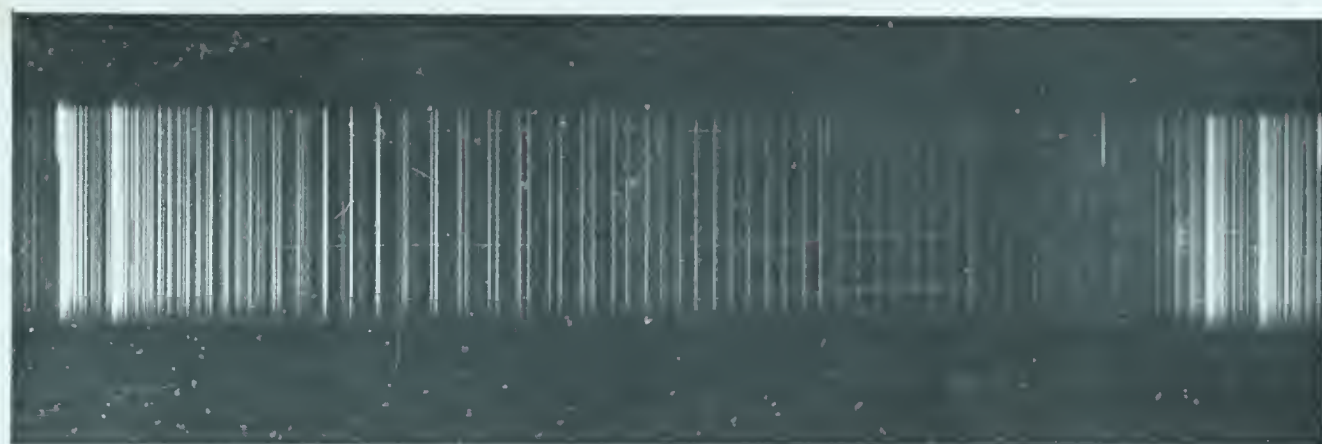
Excellent fine structure of the band system was obtained from the flame photographed under high resolution (Plate 2). The  $\Delta v = 2$  sequence was obtained essentially free of active nitrogen bands. Bands from the  $\Delta v = 1$  and  $\Delta v = 3$  sequences were overlapped to a considerable extent by the active nitrogen bands. The  $\Delta v = 0$  sequence was too weak to photograph under high dispersion.

\* Appendix I









8-6  
N<sup>81</sup>Br N<sup>79</sup>Br

Plate 2

9-7  
N<sup>81</sup>Br N<sup>79</sup>Br

NBr 8'-6'' Band Under High Dispersion

N.R.C. 10 m. f/100 grating spectrograph  
Kodak Type 103a-F Spectroscopic Plates  
Slit Width 60 $\mu$  Exposure Time 10 hours

The orange band system consists of a number of double headed bands degraded to the violet. Elliott has ascribed the double heads to the equally abundant isotopic molecules N<sup>79</sup>Br and N<sup>81</sup>Br.

The frequency of a vibrating molecule is slightly affected by a change in isotopic mass.<sup>12\*</sup>

$$\nu_{\text{osc}} (\text{sec}^{-1}) = 1/2\pi \sqrt{k/\mu} \quad \dots (1)$$

The force constant (k) of the molecule is only affected by the electronic motion, however, the reduced mass of the molecule ( $\mu$ ) changes with change of isotope. Thus we obtain different frequencies of oscillation for the two isotopic molecules.

$$\nu^i/\nu = \sqrt{\mu/\mu^i} = \rho \quad \dots (2)$$

where  $\nu^i (\text{sec}^{-1})$  is the frequency of oscillation of the heavier molecule. The constant  $\rho$  can be utilized to obtain the shift in

\*

All theory pertaining to diatomic molecules will be taken from this source unless otherwise stated.



frequency (in  $\text{cm}^{-1}$ ) of the observed vibrational spectrum shown by the two isotopic molecules. The net effect of the difference in isotopes is that the band system of the heavier molecule is contracted compared to that of the lighter by almost a constant factor  $\rho$ .\*

The wave numbers of each band head were recorded and the vibrational assignment given by Elliott was verified from the following relationships. The vibrational levels of an anharmonic oscillator can be obtained from the power series

$$G(v) (\text{cm}^{-1}) = \omega_e(v+\frac{1}{2}) - \omega_e x_e(v+\frac{1}{2})^2 + \omega_e y_e(v+\frac{1}{2})^3 + \dots \quad (3)$$

where  $v$  is the vibrational quantum number having only integer values, and where the coefficients of the individual terms have values such that  $\omega_e \gg \omega_e x_e \gg |\omega_e y_e|$ .

The vibrational structure of a molecular system can be arrived at from the relationship

$$\nu (\text{cm}^{-1}) = \nu_e + \nu_v \quad \dots \dots (4)$$

for which in any given transition

$$\nu_e = T_e' - T_e'' \quad \text{is a constant,} \quad \dots \dots (5)$$

where the  $T_e$  values are the energies of the minima of the two electronic states involved in the observed transition, and where

$$\nu_v = G'(v) - G''(v) \quad \dots \dots (6)$$

\* Reference 12, page 162ff.





TABLE 1

Deslandres Table for N<sup>79</sup>Br Band Heads

	v'	3	4	5	6	7	8	9
2	v''	15,783.08						
3			15,870.23	741.91 16,612.14				
4				654.91				
5				15,958.23	733.06 16,691.29			
6						16,771.14 715.61 17,486.85		
7						535.23 635.12 707.05		
						16,135.91 715.81 16,851.73		17,558.78
							625.54 625.52	
							16,226.19 16,933.26	
							707.07	



TABLE 2

Deslandres Table For N<sup>81</sup>Br Band Heads

$\nu'$	3	4	5	6	7	8	9
$\nu''$							
2	15,781.25						
3		15,868.23	16,608.88				
		740.65					
4			652.97				
			15,955.91	16,687.92			
5				732.01			
					16,767.65	17,482.14	
					634.14	634.04	705.89
6					16,133.51	16,848.10	17,553.99
					714.59	624.47	624.48
7						16,223.63	16,929.51
						705.88	





from which, using equation 3, we obtain

$$\begin{aligned} \nu_v = & \omega_e'(v'+\frac{1}{2}) - \omega_e'x_e'(v'+\frac{1}{2})^2 + \dots \\ & - [\omega_e''(v''+\frac{1}{2}) - \omega_e''x_e''(v''+\frac{1}{2})^2 + \dots] \end{aligned} \quad \dots \dots (7)$$

This relationship represents all possible transitions between the different vibrational levels of the two transitioning states.

These equations lead to the Deslandres vibrational analysis for the NBr bands shown in Tables 1 and 2. The vibrational constants from NBr, as derived from the above Deslandres tables, are given in in Table 3.

TABLE 3

Summary of Vibrational Constants for NBr

	$T_e' - T_e'' = 14,787.3 \text{ cm}^{-1}$	
	$N^{79}\text{Br}$	$N^{81}\text{Br}$
$\omega_e'$	$785.5 \text{ cm}^{-1}$	$784.0 \text{ cm}^{-1}$
$\omega_e'x_e'$	$4.363$	$4.344$
$\omega_e''$	$691.75$	$690.45$
$\omega_e''x_e''$	$4.720$	$4.702$

Thus for the observed NBr transitions we can write the following equations (using equations 4-7).

$$\begin{aligned} \nu_{\text{head}}^{79} (\text{cm}^{-1}) = & 14,787.3 + 785.5(v'+\frac{1}{2}) - 4.363(v'+\frac{1}{2})^2 \\ & - 691.75(v''+\frac{1}{2}) + 4.720(v''+\frac{1}{2})^2 \end{aligned} \quad \dots \dots (8)$$

$$\begin{aligned} \nu_{\text{head}}^{81} (\text{cm}^{-1}) = & 14,787.3 + 784.0(v'+\frac{1}{2}) - 4.344(v'+\frac{1}{2})^2 \\ & - 690.45(v''+\frac{1}{2}) + 4.702(v''+\frac{1}{2})^2 \end{aligned} \quad \dots \dots (9)$$

From the vibrational constants for  $N^{79}\text{Br}$  predictions were made of the values for  $N^{81}\text{Br}$  using the approximate formula for isotopic shift derived from equation 4 using equation 2

$$\nu^i (\text{cm}^{-1}) = \nu_e + \rho \nu_v \quad \dots \dots (10)$$



The values obtained agree remarkably well with the observed differences in wavenumbers of the double heads (Table 4). The agreement provides good evidence that the emitting species are in fact the two isotopic molecules of NBr.

TABLE 4

Vibrational Isotope Shift for NBr ( $\text{cm}^{-1}$ )

$v' - v''$	Calculated $\rho$	Observed from Band Heads
9 - 6	4.786	4.78
8 - 5	4.687	4.68
9 - 7	3.754	3.75
8 - 6	3.622	3.61
7 - 5	3.492	3.49
6 - 4	3.367	3.34
5 - 3	3.245	3.25
8 - 7	2.592	2.58
7 - 6	2.427	2.41
5 - 4	2.105	2.10
4 - 3	1.951	1.95

The Rotational Structure of the NBr Bands: Two sets of spectroscopic plates showing the NBr bands were obtained with sufficient detail of the fine structure to allow rotational analysis to be carried out.

For a rotating molecule we must modify the relationship applying to a non-rotating vibrator (equation 1) to account for rotation. The rotating vibrator will have a slightly different force constant ( $k$ ) from that of the simple oscillator. The resultant effect will be a slight change in frequency (in  $\text{sec}^{-1}$ ) of the





oscillator, which will alter the observed spectral frequency (in  $\text{cm}^{-1}$ ). This alteration appears as an additional term, to account for rotational transitions, in the equation giving the frequency of transitions (equation 4)

$$\nu(\text{cm}^{-1}) = \nu_e + \nu_v + \nu_r \quad . . . . (11)$$

For any specific vibrational transition

$$\nu_0 = \nu_e + \nu_v \text{ is a constant} \quad . . . . (12)$$

The rotational contribution is given by

$$\nu_r = F'(J) - F''(J) \quad . . . . (13)$$

where  $J$  is the rotational quantum number, having only integer values. The  $J$  quantum number represents the total angular momentum of the rotating molecule.

A rotating diatomic molecule can be considered as a non-rigid rotor (Figure 9).

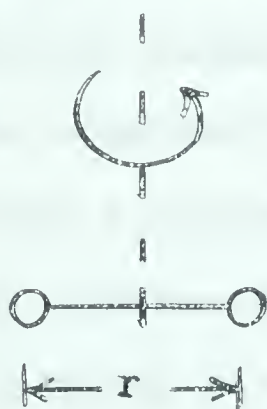


Figure 9

#### A diatomic Molecule as a Non-Rigid Rotor

For such a rotating system we have

$$F_v(J) = B_v(J)(J+1) - D_v(J)^2(J+1)^2 \quad . . . . (14)$$

representing the rotational term for any vibrational level.



The first rotational constant  $(B_v)'$ , for any vibrational level  $v$ , is given by

$$B_v = \frac{h}{8\pi^2\mu c} \left( \overline{\frac{1}{r}} \right)^2 \quad \dots (15)$$

where  $h$ ,  $\pi$ ,  $c$ , and  $\mu$  have their usual meanings, and where  $\left[ \overline{\frac{1}{r}} \right]^2$  is the mean value of  $1/r^2$  during the vibration. The value of  $B_v$  will be somewhat smaller than that of the first rotational constant  $B_e$  [which is related to the equilibrium separation of the atoms in the molecule ( $r_e$ )] due to anharmonicity of vibration. The two rotational constants are related by

$$B_v = B_e - \alpha_e \left( v + \frac{1}{2} \right) + \dots \quad \dots (16)$$

The constant  $\alpha_e$  will be small compared to  $B_e$  since the difference in inter-nuclear distance due to vibration will be small compared to the inter-nuclear distance itself. The second rotational constant  $D_v$  represents the influence of centrifugal force on the rotating molecule and can be corrected for vibration to an equilibrium  $D_e$  value in a similar manner to  $B$ . However since  $B_e \gg D_e$  we shall not consider the constant  $D_e$  at all in our analysis.

Strictly speaking a diatomic molecule is not a non-rigid rotor but a symmetric top (where the electrons have a very slight angular moment of inertia about the internuclear axis). The treatment of the two models will lead to the same rotational energies if we choose the energy value of the lowest rotational level ( $J$ ) appropriately. We therefore require that all rotational levels are measured from the level  $J = 0$ .





One additional rotational relationship which relates  $B_e$  to the moment of inertia ( $I$ ) of the rotor will be found useful.

$$B_e = \frac{h}{8\pi^2 c} \left( \frac{1}{I_e} \right) \quad \dots (17)$$

$$\text{where } I_e = \mu r_e^2. \quad \dots (18)$$

We therefore have for the rotational structure

$$\nu(\text{cm}^{-1}) = \nu_0 + B_v' (J')(J'+1) - B_v'' (J'')(J''+1) \quad \dots (19)$$

Inspection of the NBr spectrum showed two branches (one head and one tail branch). If the transition is assumed to be  $1\Sigma - 1\Sigma$  then we would have a single P and an R branch. A "P" branch is one in which  $J' - J'' = -1$ , while an "R" branch has  $J' - J'' = +1$ . Such branches can be described as follows

$$R(J) = \nu_0 + F_v'(J''+1) - F_v''(J'') \quad \dots (20)$$

$$P(J) = \nu_0 + F_v'(J''-1) - F_v''(J'') \quad \dots (21)$$

Substituting equation 19 into the above branch equations we obtain

$$R(J) = \nu_0 + 2B_v' + (3B_v' - B_v'')J + (B_v' - B_v'')J^2 \quad \dots (22)$$

$$P(J) = \nu_0 - (B_v' + B_v'')J + (B_v' - B_v'')J^2 \quad \dots (23)$$

Further, these two branches can be represented by a single equation

$$\nu(\text{cm}^{-1}) = \nu_0 + (B_v' + B_v'')M + (B_v' - B_v'')M^2 \quad \dots (24)$$

where  $M = -J$  for the P branch and  $M = J+1$  for the R branch.  $M$  can take all positive and negative integer values. Both series of  $M$  values form points on a single parabola. The two corresponding P and R branches must therefore converge into one another at the band origin (Figure 10).

The first part of the proof is to show that the function  $f$  is continuous at  $a$ . Let  $\epsilon > 0$  be given. We need to find  $\delta > 0$  such that if  $|x - a| < \delta$ , then  $|f(x) - f(a)| < \epsilon$ .

$$|f(x) - f(a)| = \left| \frac{1}{x} - \frac{1}{a} \right| = \left| \frac{a - x}{ax} \right| = \frac{|x - a|}{|ax|}$$

We want to make this less than  $\epsilon$ . Since  $|x - a| < \delta$ , we have  $|x| > |a| - \delta$ . If we choose  $\delta < |a|$ , then  $|x| > |a|/2$ . So  $|ax| > |a|^2/2$ .

$$\frac{|x - a|}{|ax|} < \frac{\delta}{|a|^2/2} = \frac{2\delta}{|a|^2}$$

We want  $\frac{2\delta}{|a|^2} < \epsilon$ , so we choose  $\delta < \frac{\epsilon |a|^2}{2}$ . Also, we need  $\delta < |a|$  to ensure  $|x| > |a|/2$ . So we take  $\delta = \min\left\{\frac{\epsilon |a|^2}{2}, |a|\right\}$ . Then if  $|x - a| < \delta$ , we have  $|f(x) - f(a)| < \epsilon$ .

$$f(x) = \frac{1}{x} \text{ is continuous at } a \text{ for any } a \neq 0.$$

The second part of the proof is to show that  $f$  is differentiable at  $a$ . We need to find the limit  $\lim_{x \rightarrow a} \frac{f(x) - f(a)}{x - a}$ .

$$\frac{f(x) - f(a)}{x - a} = \frac{\frac{1}{x} - \frac{1}{a}}{x - a} = \frac{\frac{a - x}{ax}}{x - a} = -\frac{1}{ax}$$

$$\lim_{x \rightarrow a} \frac{f(x) - f(a)}{x - a} = \lim_{x \rightarrow a} -\frac{1}{ax} = -\frac{1}{a^2}$$

$$\lim_{x \rightarrow a} \frac{f(x) - f(a)}{x - a} = -\frac{1}{a^2} \text{ for } a \neq 0.$$

$$f'(a) = -\frac{1}{a^2} \text{ for } a \neq 0.$$

This shows that the function  $f(x) = 1/x$  is differentiable at  $a$  for any  $a \neq 0$ , and its derivative is  $f'(a) = -1/a^2$ .

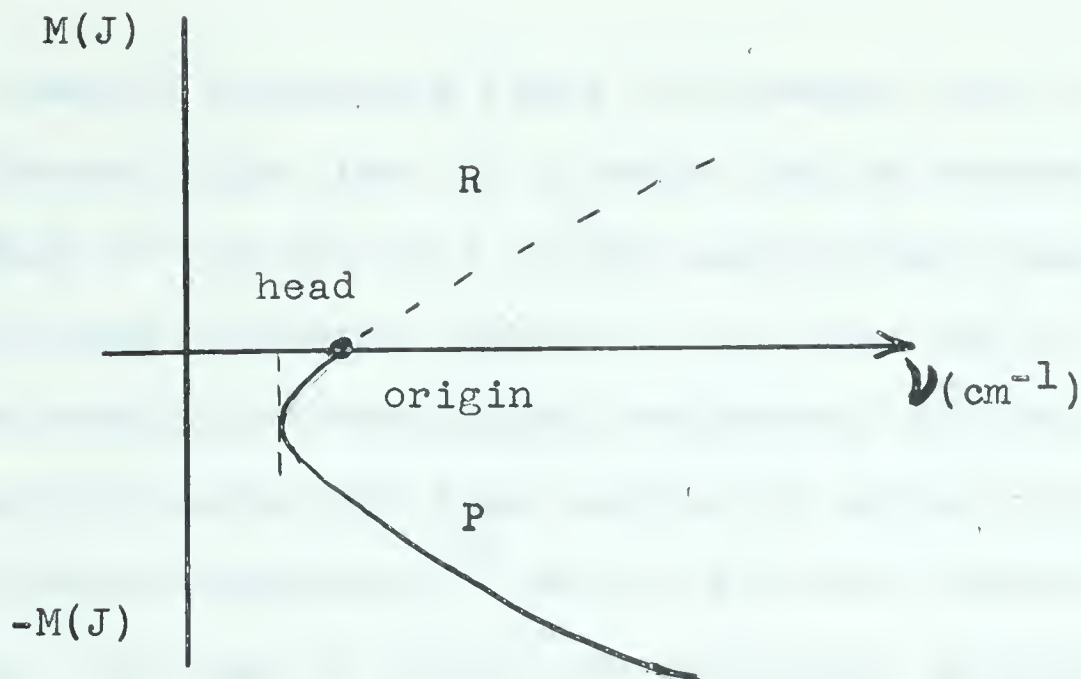


Figure 10

## Convergence of P and R Parabolas

Since the observed band is degraded to the violet (larger  $\nu_{\text{cm}^{-1}}$ ) we can conclude that  $I'$  is less than  $I''$ . Thus,  $B_e'$  is greater than  $B_e''$  and so both sets of coefficients in equation 24 will be positive. The P branch ( $M = -J$ ) will thus double back upon itself and form the band head since it contains one negative term which will be the larger of the two variable terms at low  $J$  values but will be overcome by the positive "square" term as  $J$  increases.

In order to assign  $J$  values to the rotational levels we must pick out the sequences of lines belonging to each branch of the band. The difference between successive branch members will be

$$\Delta \nu_M = \nu(M+1) - \nu(M) = 2B_V' + 2(B_V' - B_V'')M \quad \dots (25)$$

This value is known as the first difference and increases in a linear manner with increasing  $M$  (or  $J$ ) number. The amount of increment to the first difference is a constant second difference equal to the following

$$\Delta^2 \nu_M = \nu(M+1) - \nu(M) = 2(B_V' - B_V'') \quad \dots (26)$$





Using the linearly increasing first differences and the constant second difference, the lines of a branch can be determined.

Each of the two sets of NBr spectra were analyzed independently using different methods. The first set of plates were used to obtain the wavelength assignments of the rotational structure on all bands free from overlap by active nitrogen bands. A semi-electronic comparator,<sup>81</sup> at the National Research Council laboratories, was used to obtain the wavelength assignments. The second, and more intense, set of plates were analyzed on the manual comparator with a specific study being made on the  $8' - 6''$  band (the most intense non-overlapped band). The rotational assignments from the first (and most accurate set of data) were made using a square of four separate vibrational bands, utilizing the combinations of the four independent vibrational origins to arrive at a consistent rotational structure between the four levels (Figure 11).

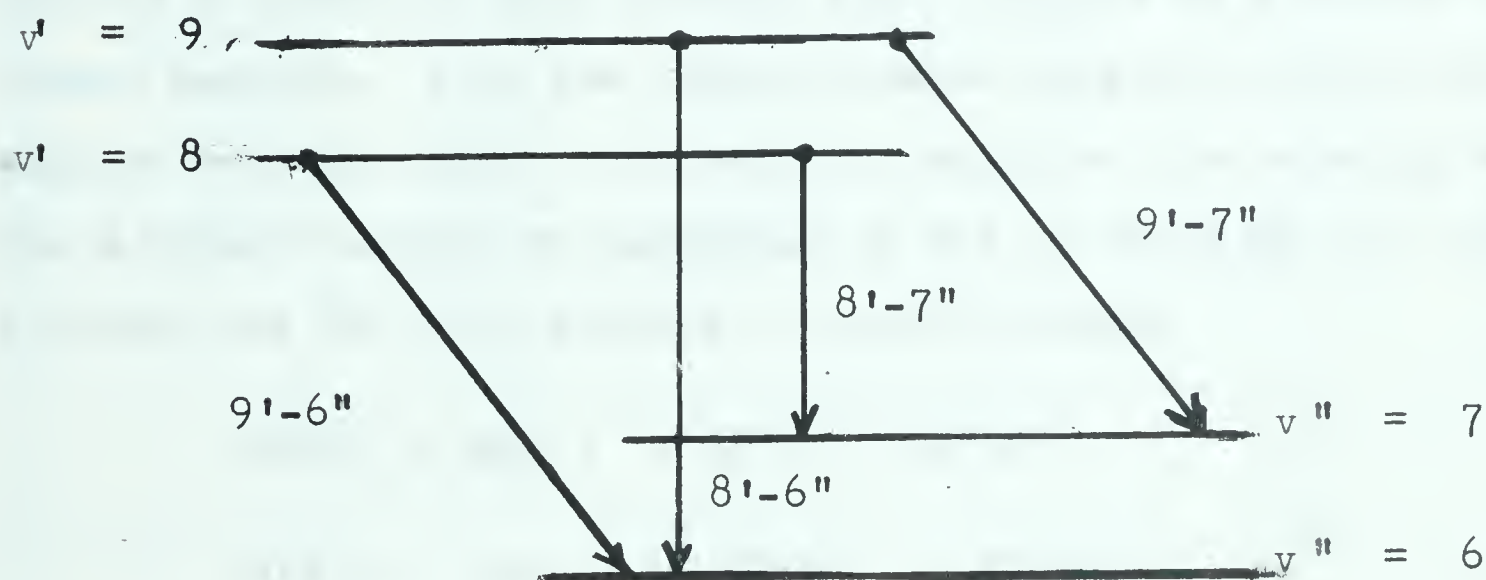


Figure 11

Square Method of Determining Self-Consistent J Values



The agreement by this square method was exact with the assignment obtained on the  $8' - 6''$  band by an internal method of analysis.

The wavelengths obtained for the branch members (with their J numbering) are listed in Tables 5 and 6. The first and second differences for the  $8' - 6''$  band are listed in Tables 7 and 8.

It was noted that the head and tail branches of the NBr bands did not converge into a single origin, yet both branches did show the same second differences. From these observations we can conclude that although both branches are part of the same band system, they can not be simple P and R branches. On the suggestion of Dr. G. Herzberg, analysis was continued assuming that the branches were possibly Q and S type branches. A "Q" branch is one in which  $J' - J'' = 0$ . An "S" branch is one in which  $J' - J'' = +2$ ; such a transition violates the selection rule  $\Delta J = 0, \pm 1$  and so is normally forbidden in optical spectra. To deal with an allowable optical S branch we must convert from J values to K values for the branch members. K is the quantum number related to the total angular momentum apart from electron spin for the rotating molecule. The Q branch can now be described as one in which  $\Delta K = 0$ , while the S branch has  $\Delta K = +2$ , leading to the following:

$$Q(K) = \nu_0 + F'(K'') - F''(K'') \quad . . . . (27)$$

$$S(K) = \nu_0 + F'(K''+2) - F''(K'') \quad . . . . (28)$$

If we are dealing with a  $\Sigma$  state, K can have any integer value from zero upwards. The branches will now be described by two intersecting parabolas with a common origin (Figure 12).







TABLE 5

Vacuum Wave Numbers in  $\text{cm}^{-1}$  for  $\text{N}^{79}\text{Br}$  Bands<sup>a, b</sup>

9' - 6"			8' - 5"		9' - 7"	
J"	R(J)	P(J)	R(J)	P(J)	R(J)	P(J)
0						
1						
2	17,565.19				16,939.35	
3	66.35				40.61	
4	67.75		17,496.03		41.95	
5	69.11		97.39		43.34	
6	70.48		98.76		44.81	
7	72.10		500.27		46.42	
8	73.66		1.85		48.09	
9	75.32		3.52		49.82	
10	77.06		5.27		51.65	16,933.26H
11	78.86		7.08		53.56	33.46
12	80.72	17,558.78H	8.93	17,486.85H	55.48	33.60
13	82.61	58.96	10.83	87.01	57.49	33.87
14	84.58	59.22	12.79	87.26	59.56	34.20
15	86.59	59.49	14.81	87.55	61.68	34.57
16	88.62	59.83	16.89	87.79	63.87	35.02
17	90.72	60.16	18.96	88.16	66.10	35.55
18	92.85	60.55	21.10	88.51	68.39	36.07
19	95.04	61.01	23.27	88.97	70.71	36.64
20	97.28	61.51	25.49	89.42	73.12	37.35
21	99.54	61.98	27.77	89.92	75.54	37.98
22	601.83	62.61	30.06	17,490.49	78.00	38.73
23	4.18	63.18	32.34		80.52	39.51
24	6.48	63.80	34.72		83.10	40.34
25	8.92	64.45	37.17		85.71	41.24
26	11.40	65.19	39.65		88.37	42.13
27	17,613.89	65.93	17,542.09		91.07	43.08
28		66.71			93.76	44.13
29		67.51			16,996.60	45.17
30		68.36				46.27
31		17,569.29				47.41
32						48.54
33						49.74
34						16,951.08

a - H = head. One asterisk indicates that the line is overlapped, two asterisks, badly overlapped.

b - 6 -5 band was not read because of extensive overlap by active nitrogen spectrum.



TABLE 5 (Page 2)

Vacuum Wave Numbers in  $\text{cm}^{-1}$  for  $\text{N}^{79}\text{Br}$  Bands

$J''$	8' - 6"		7' - 5"		6' - 4"	
	R(J)	P(J)	R(J)	P(J)	R(J)	P(J)
0						
1						
2	16,858.00		16,777.50			
3	59.22		78.73		16,698.97	
4	60.50		80.03		700.28*	
5	61.90		81.38		1.72	
6	63.42*		82.95		3.16**	
7	65.02		84.54**		4.82*	
8	66.61*		86.22*		6.84**	
9	68.44*		88.04*		8.27	
10	70.33		89.78		10.09	
11	72.14	16,851.73H	91.67	16,771.14H	11.99	16,691.29H
12	74.10	51.93*	93.63	71.29*	13.94	91.49*
13	76.10	52.25*	95.64	71.66	15.95	91.77
14	78.15	52.60*	97.72	71.97*	18.03	92.06*
15	80.30	52.99	99.85	72.29	20.17*	92.36
16	82.48	53.36*	802.03*	72.69*	22.37	92.77*
17	84.72	53.86	4.26	73.16	24.61*	93.24
18	87.00	54.40*	6.57	73.68	26.88	93.72
19	89.34	54.94*	8.89	74.23*	29.22	94.28*
20	91.71	55.60*	11.26	74.85	31.57	94.87
21	94.13	56.29*	13.66	75.49	34.00	95.53*
22	96.61	56.94*	16.14	76.23	36.50	96.15
23	99.11	57.75*	18.67	76.92*	39.00	96.90*
24	901.70	58.56*	21.21	77.76*	41.58	97.75*
25	4.28	59.44	23.87	78.58*	44.15	98.48
26	16,906.95	60.34	26.48	79.43*	46.83	99.37
27		61.32*	16,829.18	16,780.37	16,749.47	700.28*
28		16,862.24				16,701.19
29						
30						





TABLE 5 (Page 3)

Vacuum Wave Numbers in  $\text{cm}^{-1}$  for  $\text{N}^{79}\text{Br}$  Bands

5' - 3"			8' - 7"		7' - 6"	
J"	R(J)	P(J)	R(J)	P(J)	R(J)	P(J)
0						
1						
2						
3			16,233.22		16,143.24	
4			34.71		44.63*	
5	16,622.72		36.21		46.08	
6	24.20*		37.78		47.63	
7	25.90*		39.41		49.27	
8	27.49		41.15		51.03*	
9	29.25		42.96		52.85	16,135.91H
10	31.09		16,244.87*	16,226.19H	54.75	36.05*
<hr/>						
11	32.98			26.55*	56.73	36.28
12	34.93	16,612.14H		26.84	58.77	36.51*
13	36.96	12.52		27.20*	16,160.89*	36.88
14	39.05*	12.84*		27.64		37.28
15	41.18	13.15		28.08*		37.78*
16	43.38	13.55*		28.67		38.30
17	45.59*	13.98		29.28		38.91
18	47.90	14.46		29.95*		39.56*
19	50.19*	15.00*		30.38		40.27*
20	52.59	15.53*		16,231.10		40.96**
<hr/>						
21	55.02	16.18				41.79*
22	57.48	16.85				42.73
23	60.03	17.57*				43.64*
24	62.56	18.33				16,144.63*
25	16,665.17	19.12				
26		19.94*				
27		16,620.89				
28						
29						
30						



TABLE 5 (Page 4)

Vacuum Wave Numbers in  $\text{cm}^{-1}$  for  $\text{N}^{79}\text{Br}$  Bands

5' - 4"			4' - 3"		3' - 2"	
J"	R(J)	P(J)	R(J)	P(J)	R(J)	P(J)
0						
1						
2			15,876.42*			
3	15,965.53		77.81		15,790.91*	
4	66.91		79.19*		92.12*	
5	68.34**		80.64		93.64	
6	69.93		82.20		95.20	
7	71.60		83.93*		96.81*	
8	73.35*		85.68		98.63*	
9	75.18		87.38**		800.51*	
10	77.08		89.37**		2.30*	15,783.08H
11	79.04*15,958.03H		91.38*15,870.23H		4.40	83.22*
12	81.09*	58.45**	93.48*	70.64*	6.46	83.50
13	83.23*	58.81	95.64*	70.98**	15,808.58	83.78*
14	85.46*	59.22*	97.74*	71.44**		84.14
15	87.76*	59.54*	900.02*	71.75		84.55
16	89.90*	60.17	2.35	72.23		85.00*
17	92.53*	60.70**	4.70	72.81*		85.59*
18	94.84	61.39*	7.12*	73.48**		86.17
19	97.33	62.05*	9.60	74.08		86.83
20	99.82	62.77	12.15	74.65*		87.53
21	16,002.28**	63.55*	15,914.74*	75.58*		88.31
22	5.09	64.40		76.22		89.00**
23	7.74	65.29*		77.23*		89.99
24	16,010.53	66.22**		78.20*		90.91*
25		67.24*		79.19*		15,792.12*
26		68.34**		80.23*		
27		69.44*		81.29*		
28		70.51	15,882.44			
29		15,971.78*				
30						





TABLE 6

Vacuum Wave Numbers in  $\text{cm}^{-1}$  for  $\text{N}_2^{81}\text{Br}$  Bands

J"	9' -6"		8' -5"		9' -7"	
	R(J)	P(J)	R(J)	P(J)	R(J)	P(J)
0						
1						
2	17,560.36*				16,935.55*	
3	61.62*				36.83	
4	62.92		17,491.37*		38.18	
5	64.26		92.56*		39.51*	
6	65.71		94.00*		41.06	
7	67.25		95.40**		42.63	
8	68.82		97.10*		44.28*	
9	70.48*		98.76*		46.00*	
10	72.19*		500.51*		47.82	16,929.51H
11	73.99		2.31		49.74*	29.68**
12	75.85	17,553.99H	4.16	17,482.14H	51.65*	29.84**
13	77.74	54.18*	6.05	82.34*	53.63	30.14*
14	79.69	54.43*	8.08**	82.56*	55.70	30.46*
15	81.69	54.69*	10.03*	82.87**	57.83	30.82
16	83.74	55.05	12.06	83.09*	60.01*	31.29
17	85.83	55.38	14.15	83.44*	62.22	31.77
18	87.97	55.76	16.26*	83.82*	64.48	32.29
19	90.13	56.17*	18.45	84.24	66.82	32.88
20	92.33	56.69	20.65	84.69*	69.18	33.60**
21	94.61	57.20	22.89	85.17	71.60	34.20*
22	96.87	57.78	25.20	17,485.77*	74.10	35.02*
23	99.21	58.37	27.52		76.60	35.70*
24	601.57	58.96*	29.91		79.15	36.64*
25	3.98		32.34*		81.74	37.35*
26	6.48*	60.36*	34.72*		84.40	38.32
27	17,608.92*	61.01*	17,537.17*		87.09	39.35*
28		61.90			89.82	40.34*
29		62.61*			16,992.60	41.33*
30		63.51				42.46
31		17,564.45*				43.59
32						44.81*
33						46.00*
34						16,947.25



TABLE 6 (Page 2)

Vacuum Wave Numbers in  $\text{cm}^{-1}$  for  $\text{N}^{81}\text{Br}$  Bands

$J''$	$8' - 6''$		$7' - 5''$		$6' - 4''$	
	R(J)	P(J)	R(J)	P(J)	R(J)	P(J)
0						
1						
2	16,854.40*		16,773.95			
3	55.60*		75.20*		16,695.53*	
4	56.95*		76.49*		96.90*	
5	58.28		77.89*		98.34	
6	59.71		79.43*		99.80	
7	61.32		80.99		701.41	
8	62.99		82.67		3.16*	
9	64.73		84.45*		4.82*	
10	66.61*		86.20*		6.84**	
11	68.44*16,848.10H		88.04*16,767.65H		8.54*16,687.92H	
12	70.33*	48.30**	90.04	67.89*		88.17*
13	72.38	48.64*	92.06	68.15*	12.49	88.41*
14	74.40	48.98	94.11	68.46	14.55	88.66*
15	76.57	49.38*	96.24	68.77	16.69	89.00
16	78.74	49.77	98.41	69.19	18.86	89.37*
17	80.97	50.26	800.64	69.65*	21.09	89.84
18	83.24	50.76	2.92	70.18	23.36	90.33
19	85.57	51.30	5.25	70.71	25.69	90.87
20	87.95	51.93**	7.62	71.29*	28.06	91.49*
21	90.36	52.60*	10.05	71.97*	30.49	92.06*
22	92.82	53.36*	12.49	72.69*	32.93	92.77*
23	95.32	54.12	15.01	73.40	35.45	93.48
24	97.90	54.94	17.55	74.23*	38.00	94.28*
25	900.49	55.78	20.13	75.05	40.58	95.07
26	16,903.14	56.66	22.77	75.93	43.22	95.97
27		57.75*	16,825.44	16,776.84*	16,745.89	96.90*
28		16,858.56*				16,697.75*
29						
30						





TABLE 6 (Page 3)

Vacuum Wave Numbers in  $\text{cm}^{-1}$  for  $\text{N}^{81}\text{Br}$  Bands

$J''$	$5' - 3''$		$8' - 7''$		$7' - 6''$	
	R(J)	P(J)	R(J)	P(J)	R(J)	P(J)
0						
1						
2						
3			16,230.68*		16,140.96*	
4			32.11		42.19*	
5	16,619.41		33.60		43.64*	
6	20.89*		35.15		45.18	
7	22.54		36.74		46.81	
8	24.20*		38.50		48.54	
9	25.90*		40.33		50.35*	16,133.51H
10	27.75		16,242.24	16,223.63H	52.25*	33.63*
11	29.65			23.96*	54.34*	33.83*
12	31.62*	16,608.88H		24.25	56.26	34.12
13	33.62	9.27*		24.63	16,158.37	34.46
14	35.68	9.44		25.17*		34.87
15	37.82	9.88*		25.51		35.34*
16	40.00	10.27		26.19*		35.91**
17	42.23	10.71*		26.55*		36.51**
18	44.50	11.18*		27.20*		37.08*
19	46.82*	11.70*		27.74*		37.78*
20	49.22	12.14**		16,228.47		38.53*
21	51.62	12.84*				39.41*
22	54.07	13.55				40.27*
23	56.58	14.30				41.20*
24	59.12	15.00*				16,142.19*
25	16,661.71	15.82				
26		16.66*				
27		16,617.57				
28						
29						
30						



TABLE 6 (Page 4)

Vacuum Wave Numbers in  $\text{cm}^{-1}$  for  $\text{N}^{81}\text{Br}$  Bands

J"	5' -4"		4' -3"		3' -2"	
	R(J)	P(J)	R(J)	P(J)	R(J)	P(J)
0						
1						
2			15,874.42*			
3	15,963.45*		75.86		15,789.00**	
4	64.77		77.23*		90.35*	
5	66.22**		78.65*		91.82	
6	67.77		80.23*		93.36	
7	69.44*		81.79*		95.04	
8	71.20		83.63*		96.81*	
9			85.46		98.63	
10	74.88		87.38**		800.51*15,781.25H	
11	76.89	15,955.91H	89.37**15,868.23H		2.44*	81.44*
12	78.91*	56.36*	91.38*	68.60	4.56	81.69
13	81.09	56.69	93.48*	69.00	15,806.70	81.97
14	83.23*	57.11	95.86	69.35*		82.36
15	85.46*	57.54	97.96*	69.78		82.76
16	87.76*	58.03**	900.24			83.22*
17	90.12	58.45**	2.61	70.98*		83.78*
18	92.53*	59.22*	5.03	71.44*		84.35
19	95.04*	59.93*	7.38*	72.12		85.00*
20	97.55	60.70**	10.03*	72.81*		85.66*
21	16,000.17*	61.39*	12.62*	73.48*		86.49
22	2.77	62.32*	15,915.25	74.42		87.29
23	5.43*	63.16		75.28		88.13
24	16,008.23	64.09**		76.22		89.00**
25		65.11*		77.23*		15,790.35*
26		66.22**		78.20*		
27		67.24*		79.19*		
28		68.34**		15,880.42		
29		15,969.44*				
30						





TABLE 7

 $\Delta\nu(J)$  and  $\Delta^2\nu(J)$  for P Branch of NBr 8-6

$J''$	$N^{79}\text{Br}$	$\Delta\nu_J$	$\Delta^2\nu_J$	$N^{81}\text{Br}$	$\Delta\nu_J$	$\Delta^2\nu_J$	$\rho$
11	16,851.73			16,848.10			3.63
12	51.93*	0.20	0.18	48.30**	0.20	0.13	3.63
13	52.25*	0.38	0.03	48.64*	0.34	0.00	3.61
14	52.60*	0.35	0.04	48.98	0.34	0.06	3.62
15	52.99	0.39	0.02	49.38*	0.40	0.01	3.61
		0.37			0.39		
16	53.36*		0.13	49.77		0.10	3.59
17	53.86	0.50	0.04	50.26	0.49	0.01	3.60
18	54.40*	0.54	0.00	50.76	0.50	0.04	3.64
19	54.94*	0.54	0.12	51.30	0.54	0.09	3.64
20	55.60*	0.66	0.03	51.93**	0.63	0.04	3.67
		0.69			0.67		
21	56.29*		0.04	52.60*		0.09	3.69
22	56.94*	0.65	0.16	53.36*	0.76	0.00	3.58
23	57.75*	0.81	0.00	54.12	0.76	0.06	3.63
24	58.56*	0.81	0.07	54.44	0.82	0.02	3.62
25	59.44	0.88	0.02	55.78	0.84	0.04	3.60
		0.90			0.88		
26	60.34		0.08	56.66		0.01	3.68
27	61.32*	0.98	0.04	57.75*	0.89	0.08	3.57
28	16,862.24	0.92		16,858.56*	0.81		3.68
29							
30							

\* Overlapped line

\*\* Badly overlapped line



TABLE 8

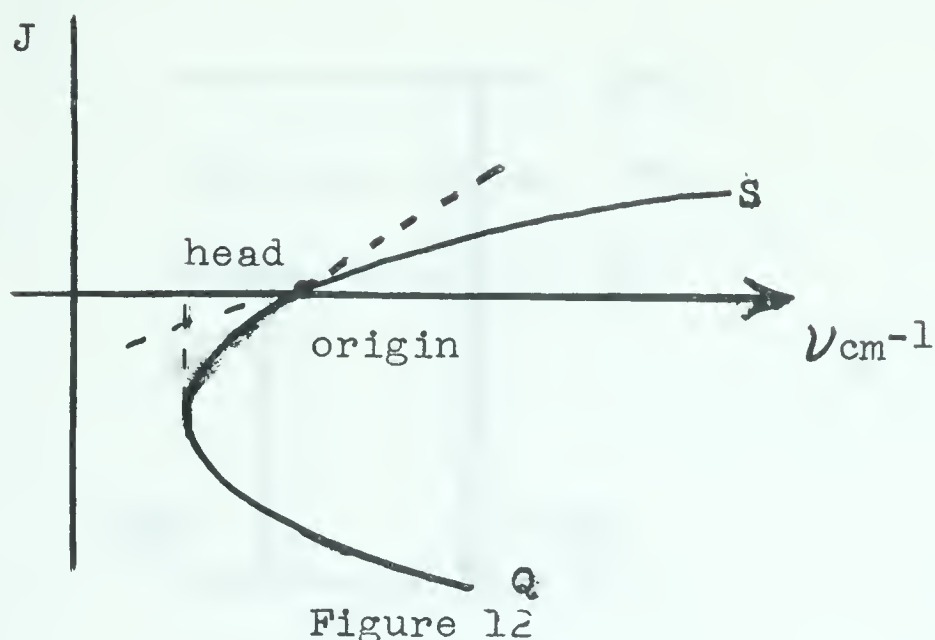
 $\Delta\nu_J$  and  $\Delta^2\nu_J$  for R Branch of NBr 8-6

$J''$	$N^{79}\text{Br}$	$\Delta\nu_J$	$\Delta^2\nu_J$	$N^{81}\text{Br}$	$\Delta\nu_J$	$\Delta^2\nu_J$	$\rho$
0							
1							
2	16,858.00	1.22		16,854.40*	1.20		3.60
3	59.22	1.28	0.06	55.60*	1.35	0.15	3.62
4	60.50	1.40	0.12	56.95*	1.33	0.02	3.55
5	61.90	1.52	0.12	58.28	1.43	0.10	3.62
6	63.42*						
7	65.02	1.60	0.08	59.71	1.61	0.18	3.71
8	66.61*	1.59	0.01	61.32	1.67	0.05	3.70
9	68.44*	1.83	0.24	62.99	1.74	0.07	3.62
10	70.33*	1.89	0.06	64.73	1.88	0.14	3.71
		1.81	0.08	66.61*	1.83	0.05	3.62
11	72.14						
12	74.10	1.96	0.15	68.44*	1.89	0.06	3.70
13	76.10	2.00	0.04	70.33*	2.05	0.16	3.77
14	78.15	2.05	0.05	72.38	2.02	0.03	3.72
15	80.30	2.15	0.10	74.40	2.17	0.15	3.75
		2.18	0.03	76.57	2.17	0.00	3.73
16	82.48						
17	84.72	2.24	0.06	78.74	2.23	0.06	3.74
18	87.00	2.28	0.04	80.47	2.27	0.04	3.75
19	89.34	2.34	0.06	83.24	2.33	0.06	3.76
20	91.71	2.37	0.03	85.57	2.38	0.05	3.77
		2.42	0.05	87.95	2.41	0.03	3.76
21	94.13						
22	96.61	2.48	0.06	90.36	2.46	0.05	3.77
23	99.11	2.50	0.02	92.82	2.50	0.04	3.79
24	901.70	2.59	0.09	95.32	2.58	0.08	3.79
25	4.28	2.59	0.01	97.90	2.59	0.01	3.80
		2.58	0.09	900.49	2.65	0.06	3.79
		2.67					
26	16,906.95			16,903.14			3.81

\* Overlapped line







### Convergence of Intersecting Q and S Parabolas

Provided that Q and S branches are allowable for the states of the NBr molecule producing the observed spectrum, then we can indeed account for the observed branches.

It was noted earlier that relative J numbering between the two branches can be determined by a "square" of four bands using the common levels in combination until a self-consistent system has been established. The same relative numbering can be obtained within any one particular band when it is remembered that each level of both the upper and lower states gives rise (in our spectrum) to one head line(Q) and one tail line (S).

Such an internal analysis was carried out upon the 8' - 6" band. The spacing of the upper state rotational levels was calculated using the fact that any two lines originating from a common level of the lower state will give the difference between two K (or J) levels of the upper state (Figure 13).



Figure 1: A graph of a function  $f(x)$  on the interval  $[-1, 1]$ .

The function  $f(x)$  is defined on the interval  $[-1, 1]$  and is continuous. It is a smooth curve that starts at  $(-1, 0)$ , reaches a maximum at  $(0, 1)$ , and ends at  $(1, 0)$ .

The function  $f(x)$  is a polynomial of degree 3. It is a smooth curve that starts at  $(-1, 0)$ , reaches a maximum at  $(0, 1)$ , and ends at  $(1, 0)$ .

The function  $f(x)$  is a polynomial of degree 3. It is a smooth curve that starts at  $(-1, 0)$ , reaches a maximum at  $(0, 1)$ , and ends at  $(1, 0)$ .

The function  $f(x)$  is a polynomial of degree 3. It is a smooth curve that starts at  $(-1, 0)$ , reaches a maximum at  $(0, 1)$ , and ends at  $(1, 0)$ .

The function  $f(x)$  is a polynomial of degree 3. It is a smooth curve that starts at  $(-1, 0)$ , reaches a maximum at  $(0, 1)$ , and ends at  $(1, 0)$ .

The function  $f(x)$  is a polynomial of degree 3. It is a smooth curve that starts at  $(-1, 0)$ , reaches a maximum at  $(0, 1)$ , and ends at  $(1, 0)$ .

The function  $f(x)$  is a polynomial of degree 3. It is a smooth curve that starts at  $(-1, 0)$ , reaches a maximum at  $(0, 1)$ , and ends at  $(1, 0)$ .

The function  $f(x)$  is a polynomial of degree 3. It is a smooth curve that starts at  $(-1, 0)$ , reaches a maximum at  $(0, 1)$ , and ends at  $(1, 0)$ .

The function  $f(x)$  is a polynomial of degree 3. It is a smooth curve that starts at  $(-1, 0)$ , reaches a maximum at  $(0, 1)$ , and ends at  $(1, 0)$ .

The function  $f(x)$  is a polynomial of degree 3. It is a smooth curve that starts at  $(-1, 0)$ , reaches a maximum at  $(0, 1)$ , and ends at  $(1, 0)$ .

The function  $f(x)$  is a polynomial of degree 3. It is a smooth curve that starts at  $(-1, 0)$ , reaches a maximum at  $(0, 1)$ , and ends at  $(1, 0)$ .

The function  $f(x)$  is a polynomial of degree 3. It is a smooth curve that starts at  $(-1, 0)$ , reaches a maximum at  $(0, 1)$ , and ends at  $(1, 0)$ .

The function  $f(x)$  is a polynomial of degree 3. It is a smooth curve that starts at  $(-1, 0)$ , reaches a maximum at  $(0, 1)$ , and ends at  $(1, 0)$ .

The function  $f(x)$  is a polynomial of degree 3. It is a smooth curve that starts at  $(-1, 0)$ , reaches a maximum at  $(0, 1)$ , and ends at  $(1, 0)$ .

The function  $f(x)$  is a polynomial of degree 3. It is a smooth curve that starts at  $(-1, 0)$ , reaches a maximum at  $(0, 1)$ , and ends at  $(1, 0)$ .

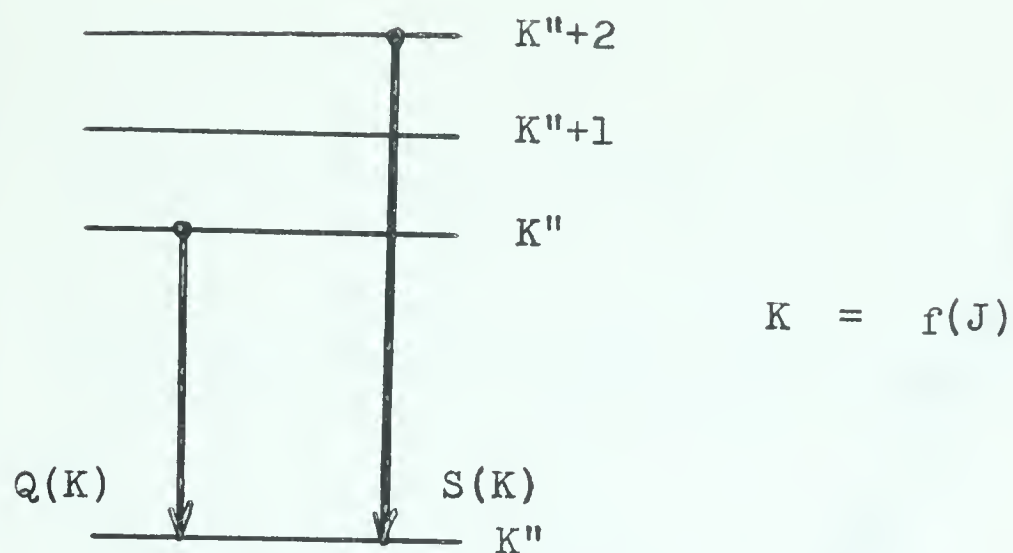


Figure 13

### Determination of Upper State Combination Differences

The difference between subsequent levels can be expressed mathematically by the following:

$$S(K) - Q(K) = \Delta_2 F(J) = 4B_v \left(J + \frac{1}{2}\right) \quad \dots (29)$$

The difference between  $J$  levels was plotted vs  $J$  number (Figure 14). A linear plot was obtained with zero intercept at minus one half. From the slope of the line the value of  $B_v$  was obtained equal to  $0.439 \text{ cm}^{-1}$  compared to  $0.4405$  by the "square" method (Table 9). For any singlet state, or for  $F_2$  (Form 2) of a  $^3\Sigma$  state, the plot of rotational level differences versus rotational level should only differ from linearity at high  $J$  values where  $D_v$  begins to have a measurable influence upon the rotational terms. Since the upper state plot is indeed linear we have good indication that we are dealing with a  $^1\Sigma$  or  $F_2$  of a  $^3\Sigma$  state.

The lower state rotational levels were determined by the same method as was used for the upper state. The differences for





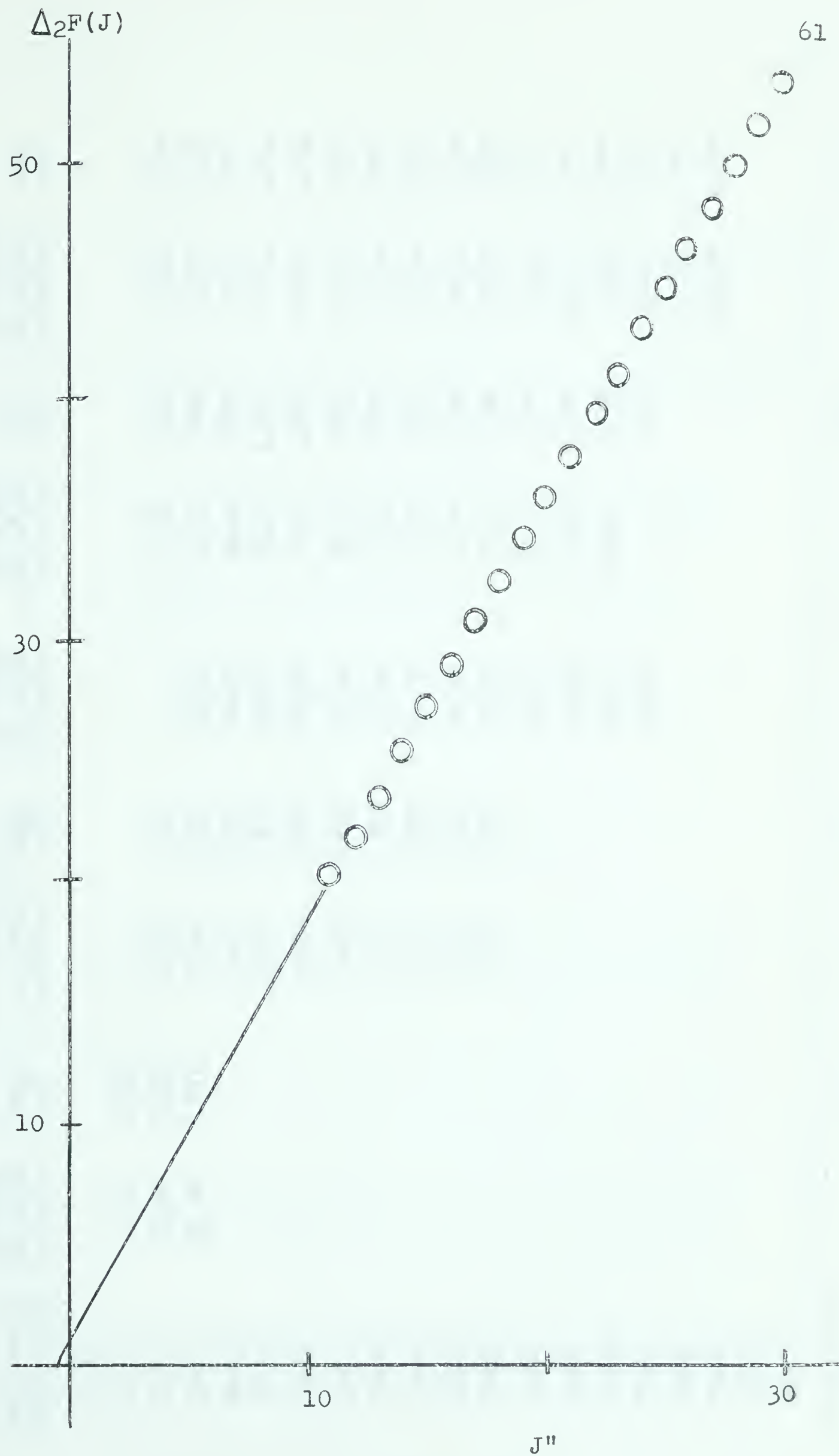


Figure 14

Absolute J Numbering - Upper State  $N^{81}\text{Br}$



TABLE 9

Upper State Combination Differences and Rotational Constants (in  $\text{cm}^{-1}$ ) -  $\text{N}^{79}\text{Br}$ 

$J''(S) - J''(Q)$	$\begin{array}{c} v' \\ (3'-2'')S= \\ (3'-2'')Q \end{array}$	$\begin{array}{c} 3 \\ 4B_3 \end{array}$	$\begin{array}{c} v' \\ (4'-3'')S \\ -(4'-3'')Q \end{array}$	$\begin{array}{c} 4 \\ 4B_4 \end{array}$	$\begin{array}{c} (5'-3'')S= \\ (5'-3'')Q \end{array}$	$\begin{array}{c} v' \\ (5'-4'')S \\ (5'-4'')Q \end{array}$	$\begin{array}{c} 5 \\ 4B_5 \end{array}$	$\begin{array}{c} v' \\ (6'-4'')S= \\ (6'-4'')Q \end{array}$	$\begin{array}{c} 6 \\ 4B_6 \end{array}$
10-10									
11-11	21.18	1.842							
12-12	22.96	1.837	22.86	1.827	22.64	22.45	1.811	22.45	1.796
13-13	24.80	1.837	24.66	1.827	24.44	24.18	1.810	24.18	1.791
14-14			26.30	1.814	26.21	25.97	1.808	25.97	1.791
15-15			28.27	1.824	28.03	27.81	1.814	27.81	1.794
16-16			30.12	1.825	29.83	29.60	1.805	29.60	1.794
17-17			31.89	1.822	31.61	31.37	1.813	31.37	1.793
18-18			33.66	1.818	33.44	33.16	1.808	33.16	1.792
19-19			35.52	1.822	35.19	34.96	1.807	34.96	1.792
20-20			37.50	1.829	37.06	36.70	1.808	36.70	1.790
21-21			39.16	1.821	38.84	38.67	1.804	38.67	1.789
22-22					40.63	40.35	1.808	40.35	1.793
23-23					42.46	42.10	1.807	42.10	1.791
24-24					44.23	43.83	1.807	43.83	1.789
25-25					46.05	45.67	1.806	45.67	1.791
26-26						47.46		47.46	1.791
27-27						49.19		49.19	1.789
28-28									
29-29									
Mean $4B_v$		1.838 <sub>7</sub>		1.822 <sub>9</sub>			1.808 <sub>3</sub>		1.791 <sub>6</sub>





TABLE 9 (Page 2)

Upper State Combination Differences and Rotational Constants (in  $\text{cm}^{-1}$ ) -  $\text{N}^{79}\text{Br}$ 

	$v'$	7	$v'$	8	$v'$	9
$J''(\text{S})-J''(\text{Q})$	$(7'-5'')\text{S}$ $-(7'-5'')\text{Q}$	$(7'-6'')\text{S}$ $-(7'-6'')\text{Q}$	$(8'-5'')\text{S}$ $-(8'-5'')\text{Q}$	$(8'-6'')\text{S}$ $-(8'-6'')\text{Q}$	$(9'-6'')\text{S}$ $-(9'-6'')\text{Q}$	$(9'-7'')\text{S}$ $-(9'-7'')\text{Q}$
10-10		18.70	1.781			20.10
11-11		20.45	1.778			21.88
12-12	22.34	22.26	1.784	22.17	1.774	23.62
13-13	23.98	24.01	1.778	23.85	1.766	25.36
14-14	25.75		1.776	25.55	1.761	27.11
15-15	27.56		1.778	27.31	1.760	28.85
16-16	29.34		1.778	29.12	1.764	30.55
17-17	31.10		1.777	30.86	1.762	32.32
18-18	32.89		1.778	32.60	1.762	34.07
19-19	34.66		1.777	34.40	1.762	35.77
20-20	36.41		1.776	36.11	1.760	37.56
21-21	38.17		1.775	37.84	1.760	39.27
22-22	39.91		1.774	39.67	1.761	41.01
23-23	41.75		1.776	41.36	1.760	42.76
24-24	43.45		1.773	43.14	1.761	44.47
25-25	45.29		1.776	44.84	1.758	46.24
26-26	47.05		1.775	46.61	1.759	47.99
27-27	48.81		1.775		47.96	49.63
28-28						51.43
29-29						
Mean $4B_v$			1.7769		1.7620	1.7459



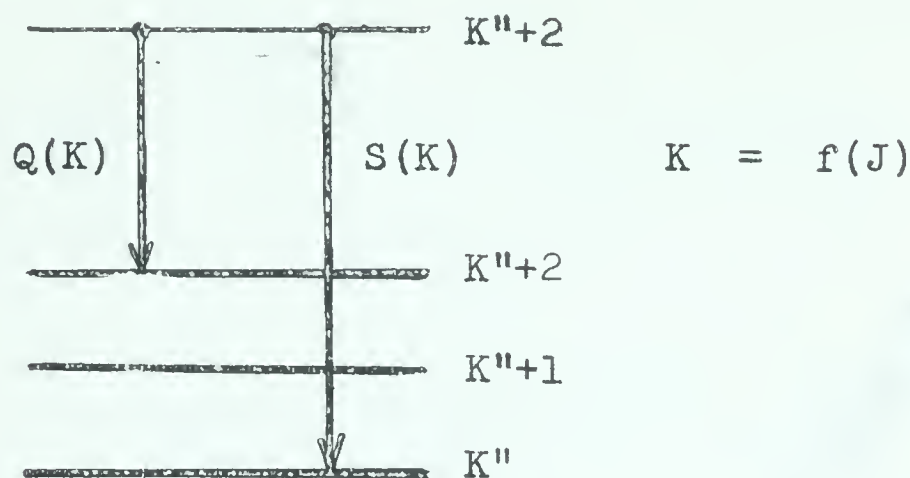


Figure 15

### Determination of Lower State Combination Differences

The mathematical expression for these differences is given by

$$S(K) - Q(K+2) \equiv \Delta_2 F(J) = 4B_v(J + \frac{1}{2}) \quad \dots (30)$$

When the lower state rotational level spacings were plotted the result showed marked positive deviation from linearity (Figure 16). The greatest deviation was shown at the lower  $J$  values. The exact amount of the deviation was difficult to ascertain due to the fact that lines of the head branch curved back upon themselves at relatively high  $J$  values ( $J = 12$ ) making combination differences below this  $J$  value impossible to obtain accurately. Using the upper state combination differences (which showed a linear relation and thus could be accurately extrapolated down to  $J = 1$ ) and the tail branch, which was observed directly down to low  $J$  values ( $J = 2$ ) lower state combination differences were indirectly determined down to  $J = 3$  (Table 10 and Table 11).

The curvature of the plot of lower state rotational levels for NBr seemed to behave much like the  $F_1$  branch of the  $^3\Sigma_g^-$  ground state of oxygen. It has been shown<sup>82</sup> that for multiplet  $\Sigma$  states, splitting occurs between the multiplet levels. A diatomic molecule in a  $^1\Sigma$  state is a simple rotor in which the nuclear rotation ( $\hat{N}$ )





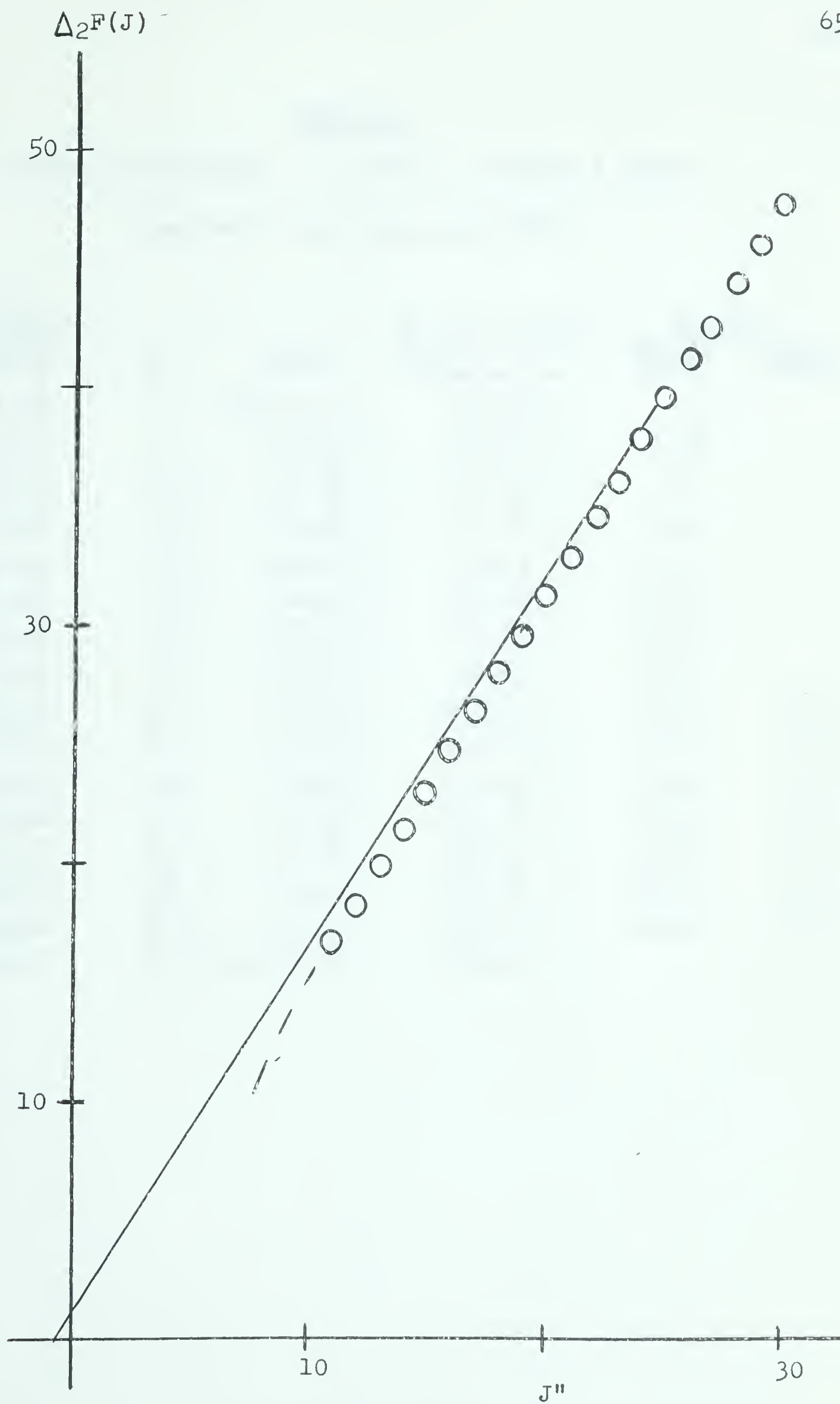


Figure 16

Absolute J Numbering - Lower State N<sup>81</sup>Br



TABLE 10

Indirect Evaluation of  $\Delta_2 F''(J)$  For Low J Levelsfrom 9<sup>1</sup>-7<sup>11</sup> Band Data for N<sup>79</sup>Rn

<u>J'</u>	<u><math>F'(J)</math></u> <u><math>0.4365 =</math></u> <u><math>J(J+1)</math></u>	<u>J''</u>	<u>S(J'')</u>	<u><math>F'(J)+17,000</math></u> <u><math>-S(J'')</math></u>	<u><math>\Delta_2 F''(J)</math></u>	
					<u>Calc.</u>	<u>Exptl.</u>
3	5.24	2	16,939.35	65.89		
4	8.73	3	40.61	68.12	5.25	
5	13.09	4	41.95	71.14	6.87	
6	13.33	5	43.34	74.99	8.49	
7	24.44	6	44.81	79.63	10.02	
8	31.43	7	46.42	85.01	11.56	
9	39.28	8	48.09	91.19	13.18	
10	48.01	9	49.82	98.19	14.77	
11	57.61	10	51.65	105.96	16.34	16.36
12	68.09	11	53.56	114.53	18.00	18.05
13	79.44	12	55.48	123.96	19.64	19.69
14	91.66	13	57.49	134.17	21.23	21.28
15	104.75	14	59.56	145.19	22.87	22.92
16	118.72	15	61.68	157.04	24.50	24.54
17	133.56	16	63.87	169.69	26.13	26.13
18	149.27	17	16,966.10	183.17		





TABLE 11

Lower State Combination Differences in  $\text{cm}^{-1}$  $\Delta_2 F''(J)$  Values for  $\text{N}^{79}\text{Br}$ 

$J''(S) - J''(Q)$	$v'' = 3$		$v'' = 7$	
	$5' - 3''$	$4' - 3''$	$9' - 7''$	$8' - 7''$
9-11			16.36	16.41
10-12		18.73	18.05	18.03
11-13	20.46	20.40	19.69	
12-14	22.09	22.04	21.28	
13-15	23.81	23.89	22.92	
14-16	25.50	25.51	24.54	
15-17	27.20	27.21	26.13	
16-18	28.92	28.87	27.80	
17-19	30.59	30.62	29.46	
18-20	32.37	32.47	31.04	
19-21	34.01	34.02	32.73	
20-22	35.74	35.93	34.39	
21-23	37.45	37.51	36.03	
22-24	39.15		37.66	
23-25	40.91		39.28	
24-26	42.62		40.97	
25-27	44.28		42.63	
26-28			44.24	
27-29			45.90	
28-30			47.49	
29-31			49.19	



forms the angular momentum figure axis for the molecule, directed at right angles to the inter-nuclear axis (Figure 17a). Multiplet  $\Sigma$  states have coupled to this nuclear rotation vector the electronic spin ( $\vec{S}$ ) forming a resultant total angular momentum ( $\vec{J}$ ), the figure axis, which is not necessarily at right angles to the inter-nuclear axis (Figure 17b).

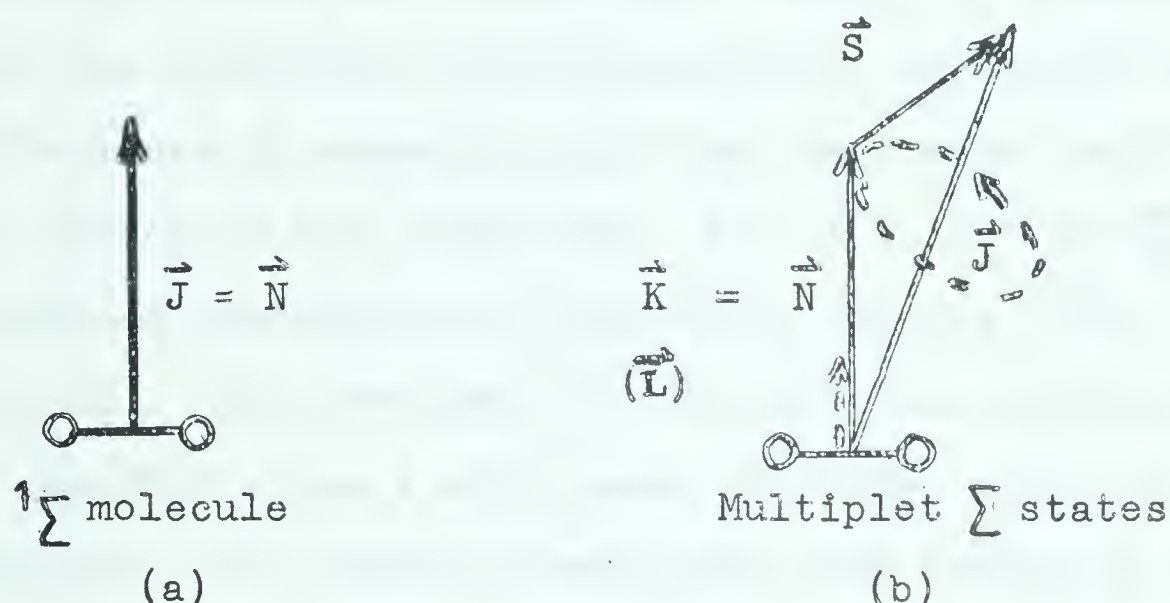


Figure 17

Coupling Diagrams for  $\Sigma$  States

In  $^2\Sigma$  states the splitting between multiplet levels has been attributed to magnetic moments along  $\vec{K}$  caused by nuclear motion, as well as to variable precession of  $\vec{L}$  (the orbital angular momentum of the electrons) due to rotational distortion.<sup>82</sup> This rotational distortion causes a non-zero average value for  $\vec{L}$  which is directed along  $\vec{K}$ , making  $\vec{K} = \vec{N} + \vec{L}_{\text{resultant}}$ . In addition, for  $^3\Sigma$  states we have spin interaction with the figure axis causing splitting, which is little dependent upon  $K$ .<sup>83</sup> Schlapp<sup>84</sup> has shown that these effects can be accounted for in the  $^3\Sigma_g^-$  ground state of oxygen by the following equations

$$F_1(K) = B_r(K)(K+1) + (2K+3)B_v - \lambda \\ - \sqrt{(2K+3)^2 B_v^2 + \lambda^2} - 2\lambda B_v + \gamma(K+1) \dots (31)$$





$$F_2(K) = B_v(K) - (K+1) \dots \dots (32)$$

$$F_3(K) = B_v(K) (K+1) - (2K-1) B_v - \lambda + \sqrt{(2K-1)^2 B_v^2 + \lambda^2} - 2\lambda B_v - \gamma K \dots \dots (33)$$

where  $\lambda$  and  $\gamma$  are the splitting constants (in  $\text{cm}^{-1}$ ). In order to see if the similarity between the lower state of NBr and the ground state of oxygen could be carried any further, an attempt was made to correct the deviations from linearity of the lower state combination differences by assuming splitting constants for  $F_1$ . By this empirical method it was found that  $\lambda = 8.7 \text{ cm}^{-1}$  and  $\gamma = -0.7 \text{ cm}^{-1}$  would produce a satisfactory linear plot for the lower state of NBr (Table 12). The certainty of the splitting constants chosen is quite doubtful since a wide range of values could be chosen which would duplicate the observed deviations from linearity when substituted in the  $F_1$  equation. However despite this uncertainty in the choice of splitting constants, the correct order of  $B_v$  could be ascertained from the equations since  $B_v$  is not strongly dependent upon the choice of  $\lambda$  and  $\gamma$ . The values of  $B_v$  were calculated for  $v'' = 3$  and  $v'' = 7$ . They were found to be  $B_3 = 0.430 \text{ cm}^{-1}$  and  $B_7 = 0.418 \text{ cm}^{-1}$ . All other lower state  $B_v$  values were calculated assuming a linear interpolation. The use of the chosen  $B_v$ ,  $\lambda$ , and  $\gamma$  values allowed the observed deviations from linearity of the lower state to be explained. Thus, it was concluded that Schlapps equations could be applied to the lower state of NBr. Calculations of the splitting of  $F_2$  and  $F_3$  from the observed  $F_1$  curve was attempted using equations 31-33. The results (Figure 18) showed that the magnitude of splitting of these two forms away from  $F_1$  was considerably greater than that observed in oxygen.



Table 12Observed and Calculated  $\Delta_2 F(J)$  Values

Lower State of NBr

J	Observed	Calculated
3	5.25	5.38
4	6.87	6.91
5	8.49	8.46
6	10.02	10.03
7	11.56	11.61
8	13.18	13.19
9	14.77	14.78
10	16.36	16.40
11	18.05	18.01
12	19.69	19.63
13	21.28	21.25
14	22.92	22.87
15	24.54	24.51
16	26.13	26.13
17	27.80	27.78
18	29.46	29.43

From the calculated splittings, attempts were made to resolve a number of unresolved faint lines observed within the 8' - 6" band (Appendix IV) into the possible transitions from the two other forms of a  $^3\Sigma$  state. Due to the faintness of the lines plus the uncertainties involved in reading the manual comparator, too great a scatter was introduced into the results to produce significant conclusions.

The Blue Emissions: It has been noted that when the flow of bromine is interrupted during the reaction with active nitrogen the orange emission is superseded by a brilliant blue glow which directly precedes the normal nitrogen afterglow as it flushes the orange emission zone through the apparatus towards the





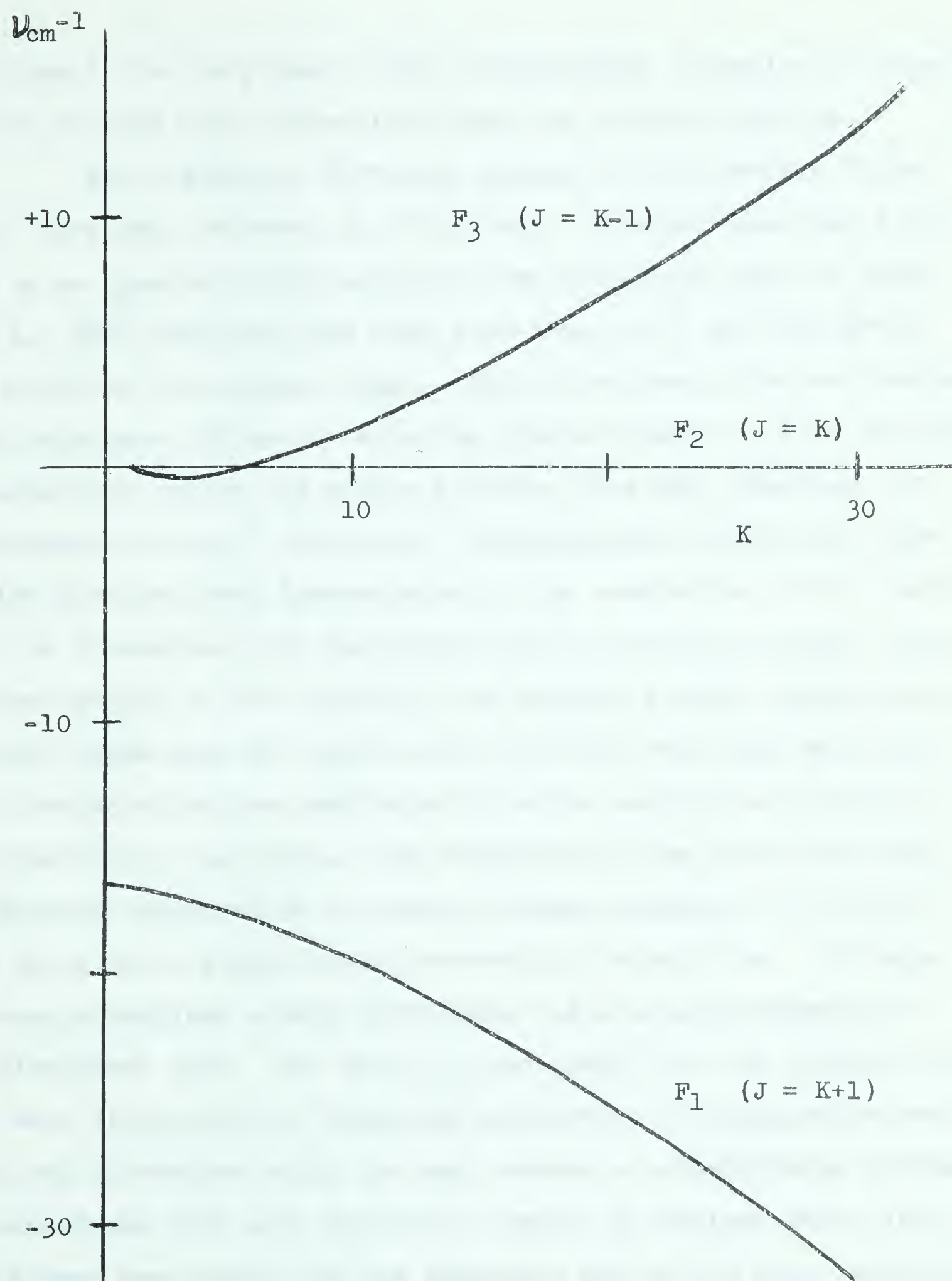


Figure 18

Calculated Splitting - NBr Lower State



cold trap.<sup>3</sup> In the present study considerable attention has been devoted to this blue "afterglow" from the bromine reaction.

Two distinctly different shades of blue bromine "afterglows" have been observed in this study. Dunford<sup>3</sup> reported a blue glow as an apparent continuum with long wavelength edge at about 5100 Å. This continuum has been associated with the blue-green glow noted in the present study. This blue-green glow was induced in the apparatus either by allowing bromine vapour to flow through the apparatus before the active nitrogen flow was commenced, or, as previously noted,<sup>3</sup> during the "flushing-out" period after the bromine flow had been discontinued at the completion of the reaction. No blue-green glow was noted when the yellow nitrogen afterglow was absent in the region of the apparatus under investigation. The glow began near the walls when the first very weak emissions of the nitrogen afterglow penetrated into the particular portion of the apparatus in question. The intensity of the blue-green glow was markedly enhanced as the weak nitrogen afterglow in contact with the glowing region became moderately intensified. Stronger nitrogen afterglows slowly diminished the area and intensity of the blue-green glow. The glow persisted for the longest periods when it occurred in "dead-end" portions of the apparatus away from, but in contact with, the main stream of afterglowing nitrogen. The blue-green glow also tended to persist in regions where stopcock grease was present in the apparatus and in the area immediately above the cold point in the cold trap. A slight enhancement in the intensity of the glow seemed to occur when the blue-green glowing regions were heated with a flame.





The second glow, blue-violet in colour, was more intense than the first and only appeared immediately following the passage of the blue-green glow which formed (near the walls of the apparatus) at the interface between the orange NBr emission and the yellow afterglow during the "flushing-out" period. The intensity of this blue-violet glow appeared to be enhanced by the presence of a very strong nitrogen afterglow. The presence of the glow in any particular region of the apparatus was short lived, the glow moving about as rapidly as the advancing yellow nitrogen afterglow. Whenever conditions allowed the blue-violet and blue-green glows to merge, the blue-violet glow disappeared and the blue-green was greatly intensified for a brief period.

The spectrum obtained from the blue emission was photographed using the Medium Hilger instrument, and is shown in Plate 3. Members of the second positive and first negative bands of nitrogen and the  $\beta$  bands of nitric oxide (Table 13) generally associated with active nitrogen were observed. (See also Tables 15 and 16 under Active Nitrogen.) No distinction between the two blue glows could be made from the spectrograms.

#### THE REACTION OF ACTIVE NITROGEN WITH HYDROGEN BROMIDE AND AMMONIUM BROMIDE

The Hydrogen Bromide—Active Nitrogen Spectrum: Hydrogen bromide, at room temperature, was allowed to flow through the flow meter at  $7 \times 10^{-7}$  moles/sec. into the reaction vessel. The effect upon active nitrogen was similar to that produced by bromine vapour. The normal nitrogen afterglow was completely quenched and in its place an orange emission appeared at the walls. Under low dispersion the spectrum of this emission appeared identical to that produced by bromine with active nitrogen (Plates 1 and 4).



NO *B*

4,18
3,17
2,14
5,18
4,17
3,16
2,15
1,14
0,13
2,14
1,13

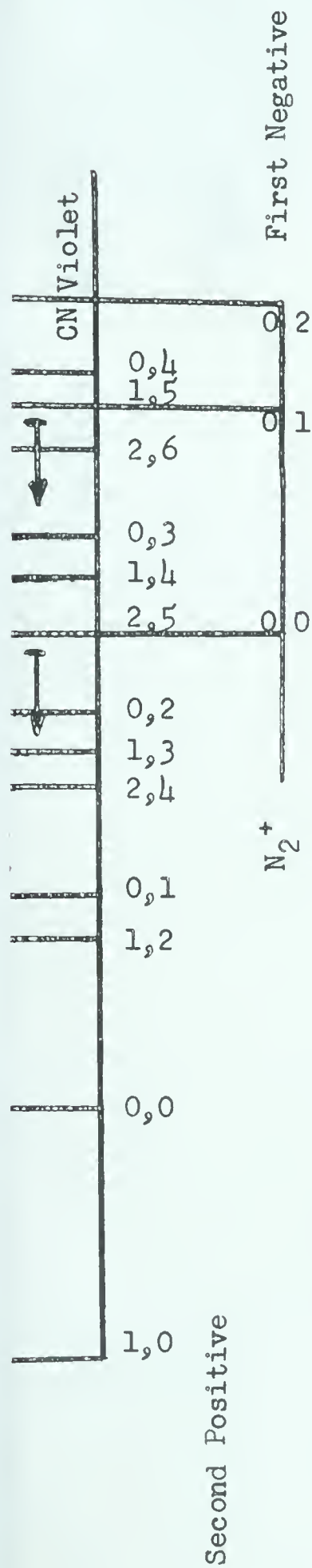


Plate 3

Spectrum During the Emission of the Bromine Blue Afterglow

Medium Hilger Prism Spectrograph

Kodak Type 103a-0 Spectroscopic Plates

Slit Width 90/4

Exposure Time 2 hours





TABLE 13

Nitric Oxide  $\beta$  Bands

Excited in Active Nitrogen in the Presence of Bromine

NO ( $B^2\Pi \rightarrow X^2\Pi$ )

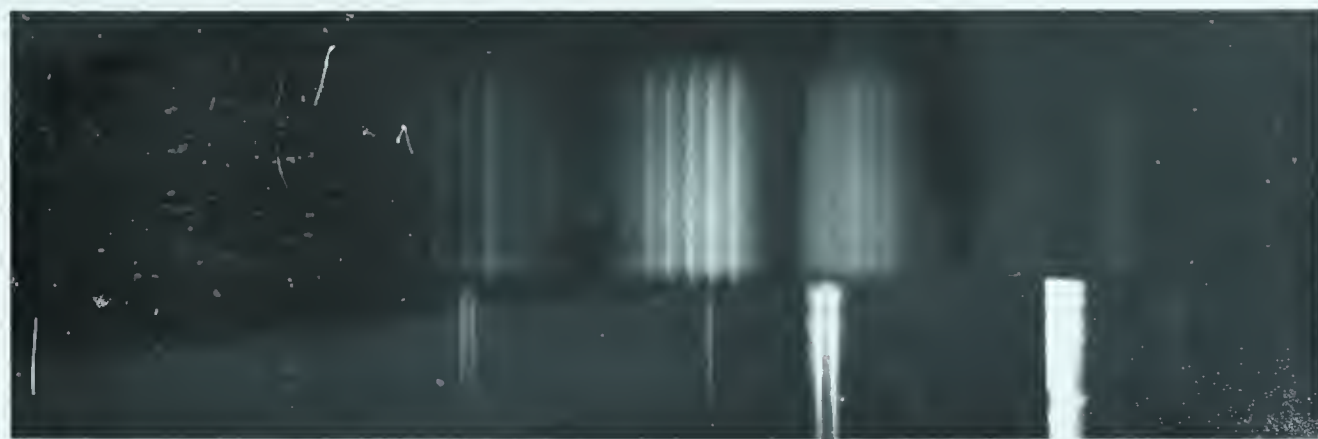
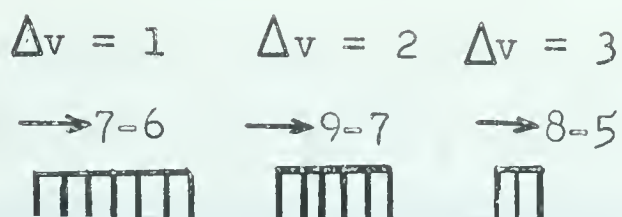
$v''$	12	13	14	15	16	17	18
$v'$							
0	*	23 203 23 290 m					
1		24 225 w 310	22 720 m 801				
2			23 724 w 806	22 241 ms 322	20 870 ms ---		
3				*	21 713 s 863	20 441 m ---	
4					*	21 419 s 380	20 016 mw ---
5						*	20 982 vw ---

Intensities: vw = very weak w = weak

ms = moderate to strong

s = strong \* = overlapped





5789.7 Å      5769.6 Å

#### Plate 4

Active Nitrogen—Hydrogen Bromide Reaction Emission

Bausch and Lomb f/4.4 grating spectrograph

Kodak Type III-F(3) Spectroscopic Plates

Slit Width 200  $\mu$       Exposure Time 6 hours

In a previous study the products of the reaction of hydrogen bromide with active nitrogen have been shown to be bromine, ammonium bromide, and hydrogen bromide.<sup>3</sup> It is quite likely that since bromine is generated by the reaction the observed emission is indeed the same in this reaction as the emission generated by bromine itself with active nitrogen.

It has been shown that the ammonium bromide which deposits itself upon the walls of the vessel during reaction can be reacted off with active nitrogen after the flow of hydrogen bromide has ceased.<sup>3</sup> In the present study, the accumulation of ammonium bromide deposits upon the reaction vessel walls were considerable during the course of a six hour spectroscopic experiment. In most cases, these deposits were removed from the walls by washing with water because of the time required to react away such quantities of salt using active nitrogen.





downstream from the reaction vessel near the cold trap. The glow seemed most intense and long-lived when the system had been left exposed to traces of the reaction products prior to the addition of the hydrogen bromide. This could be accomplished by allowing the products of a previous experiment to vapourize through the system, left standing under vacuum between experiments. Spectroscopic examination was made of this blue glow with the Medium Hilger instrument. The results obtained were identical to those with bromine.

The Reaction With Ammonium Bromide: A series of experiments were performed in which an ammonium bromide solution was sucked into the reaction vessel with a vacuum, allowed to drain out, and dried under vacuum to leave a coating of the salt on the walls of the reaction vessel. This salt when reacted with active nitrogen (in the absence of any additional reactant) produced an orange wall emission. In the tubular reaction vessel the salt was quite effective in quenching the yellow nitrogen afterglow. The quenching was such that the orange wall glow, produced by the reaction of the salt with the active nitrogen, would only be visible for a length of about 30 mm. along the reaction tube when a 40% ammonium bromide solution was used to coat the walls. The resultant orange emission was quite intense and no afterglow appeared in the gas phase of the reaction tube beyond the zone of wall reaction. The use of more dilute solutions of ammonium bromide (around 5%) gave a reaction zone close to 70 mm. in length and showed the same quenching effect upon the afterglow of active nitrogen. Although this reaction zone was longer than with the stronger solution of ammonium bromide, the orange emission produced was much fainter. Weaker solutions produced reaction zones up to 550 mm. long, albeit faintly after the first 100 mm. It was noted



that until the ammonium bromide upon the walls was completely dry, it would not quench the nitrogen afterglow and it was not until quenching was almost complete that the orange wall emission could be noted with any intensity. Completeness of quenching seemed to be a definite prerequisite for a wall emission of strong intensity. With all ammonium bromide solutions used, bromine could be trapped out downstream from the reaction zone in the horizontal Dewar.

During the course of an experiment the position of the wall reaction would move away from the nitrogen inlet towards the pumps as the active nitrogen reacted the ammonium bromide off the walls at the leading edge of the emission. The speed of this migration of the reaction flame down the tube was fastest with the dilute solutions. The reaction zone was shown to move about 500 mm/hr. with a 10% ammonium bromide solution whereas the 40% solution remained almost unmoved over a similar period of time. Experiments in this series were performed both with and without ortho-phosphoric acid wall poison on the walls below the ammonium bromide solutions. In the unpoisoned experiments, especially with low concentrations of ammonium bromide, intensity problems were encountered when the reaction zone progressed away from the active nitrogen inlet.

Using the Medium Hilger instrument, exposures ranging from 30 minutes to 5 hours with a slit width of 100 $\mu$  were required to expose successfully the reaction emission on Kodak Type I-F plates. No clearly defined spectra of the orange wall emission could be obtained free of serious overlapping by the active nitrogen afterglow, which was always present in the reaction tube prior to the reaction zone. The afterglow spectrum was much more intense on the plates than the orange wall emission (despite their







comparable intensities) due to the fact that more light from the gas phase was able to enter the slit of the spectrograph than light from the region of the wall. Members of both the first positive and second positive systems of nitrogen were obtained from the active nitrogen. Some nitric oxide bands were present in those spectra taken in the poisoned system.

In almost all of the experiments with ammonium bromide a very small boundary zone of blue appeared between the yellow nitrogen afterglow and the orange wall emission. However, this transition zone was not of sufficient size nor did it have sufficient intensity to be recorded upon any of the spectra taken.

#### THE REACTION OF ACTIVE NITROGEN WITH AMMONIA

Ammonia was introduced into a stream of active nitrogen by allowing a pressure head (of 600 mm. of mercury) to flow through a flow meter at  $5 \times 10^{-5}$  moles/sec. The only visible effect of the addition was that the intensity of the active nitrogen afterglow was quenched to about 1/10th of its normal value.

When the horizontal Dewar flask, located half-way down the reaction tube, was cooled with liquid nitrogen to  $-196^{\circ}\text{C}$ . a bright blue glow appeared along the walls of the Dewar for about 25 mm. past the cold point. This glow, previously noted by Zabolotny and Gesser,<sup>5</sup> was photographed using the Medium Hilger spectrograph. An exposure time of 2 hours with a 200 $\mu$  slit width was required to photograph the glow on Kodak Type 103a-0 and Type I-F spectroscopic plates. The glow was found to be a continuum between the limits of 3150 and 6800 Å (Plates 5 and 6). It exhibited an intensity maximum in the 3800 to 5500 Å range. The violet limit of the continuum is well within the useable limits of





Plate 5

Ammonia Continuum Excited in Active Nitrogen (Red Sensitive)

Medium Hilger Prism Spectrograph

Slit Width  $300\mu$

Kodak Type 103a-F Spectroscopic Plates

Exposure Time 1 hour



Plate 6

Ammonia Continuum Excited in Active Nitrogen (Blue Sensitive)

Medium Hilger Prism Spectrograph

Slit Width  $300\mu$

Kodak Type 103a-0 Spectroscopic Plates

Exposure Time 1 hour





the "O" type emulsion used, however the red end of the spectrum was limited by the sensitivity of the "F" emulsion.

In the presence of traces of air, oxygen, or mercury the blue glow showed a diminution of intensity. In oxygen or air the glow quickly changed in shade to a greenish-blue, while with mercury there was a black ring deposited upon the walls of the tube at the cold point. This black deposit could not be reacted off the wall with active nitrogen, but could easily be washed out of the tube with water or dilute acid solutions.

#### THE OPTICAL SPECTRUM OF ACTIVE NITROGEN

Various spectra of active nitrogen were taken for comparison purposes during the course of the different studies. The spectra were obtained with exposure times ranging from 10 minutes using the Bausch and Lomb grating instrument with a 100 $\mu$  slit width, to 6 hours using the N.R.C. 10 m. grating with a 60 $\mu$  slit width. The Medium Hilger was capable of photographing the nitrogen afterglow in 20 minutes with an 80 $\mu$  slit width. The type of spectroscopic plate used on the active nitrogen afterglow depended upon the region of the spectrum under investigation.

The Lewis-Rayleigh afterglow showed the sequences of the first positive bands of nitrogen long associated with the active nitrogen afterglow (Table 14, Plate 7).

Problems were consistently encountered during the experiments by the passage of a pink glow from the discharge tube into the reaction zone. This pink glow resembled closely the color of an uncondensed discharge through nitrogen gas, and often flickered in intensity just as a discharge does. Much effort was taken to eliminate the pink glow from the flowing stream of active nitrogen. An electrode probe, which could be maintained at any desired



TABLE 14

First Positive Bands in Active Nitrogen



Transition $v' - v''$	Relative Intensity	$\text{cm}^{-1}$
12 - 6	w	19,876
11 - 5	w	19,788
12 - 7	w	18,612
11 - 6	m	18,494
12 - 8	m	17,376
11 - 7	s	17,229
10 - 6	m	17,081
9 - 5 <sup>a</sup>	w	16,932
8 - 4	w	16,781
7 - 3	w	16,629
6 - 2	w	16,475
12 - 9, 4 - 0	m	16,168
11 - 8 <sup>b</sup>	s	15,993
10 - 7	m	15,816
9 - 6	w	15,638
8 - 5	w	15,460
7 - 4	w	15,279
6 - 3 <sup>c</sup>	m	15,098
5 - 2	w	14,915
,4 - 1, 11 - 9 <sup>d</sup>	w	14,731

Bands Overlapped by  $\text{N}_2 (\text{Y} \rightarrow \text{B}^3\Pi_g)^{41}$

a) 7'-0" b) 8'-1" c) 6'-0" d) 7'-1"

Intensity: w - weak m - moderate s - strong





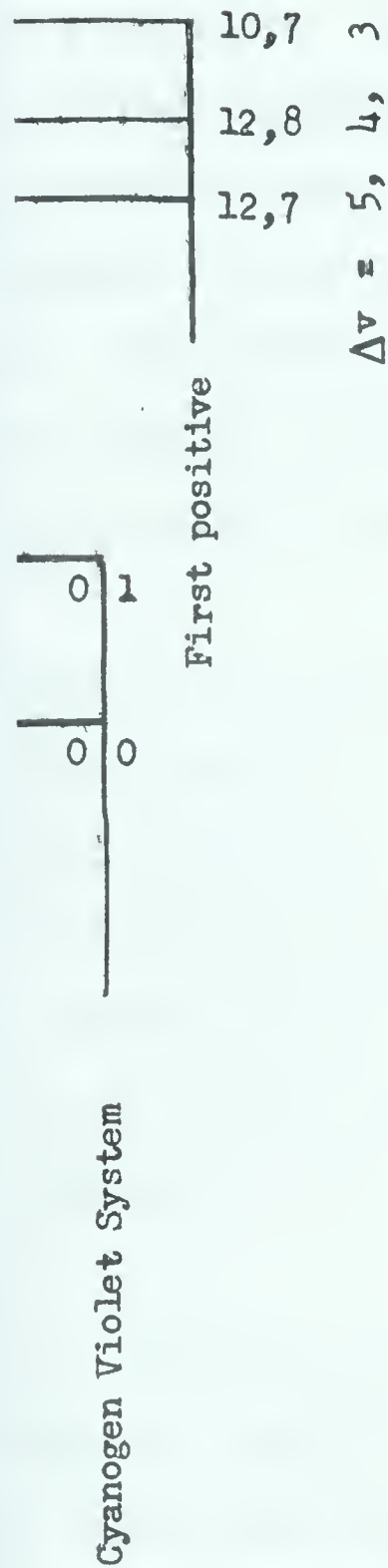
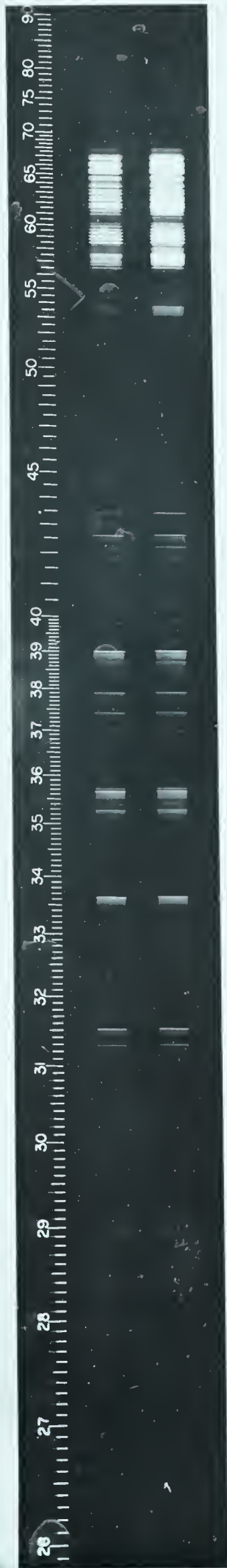
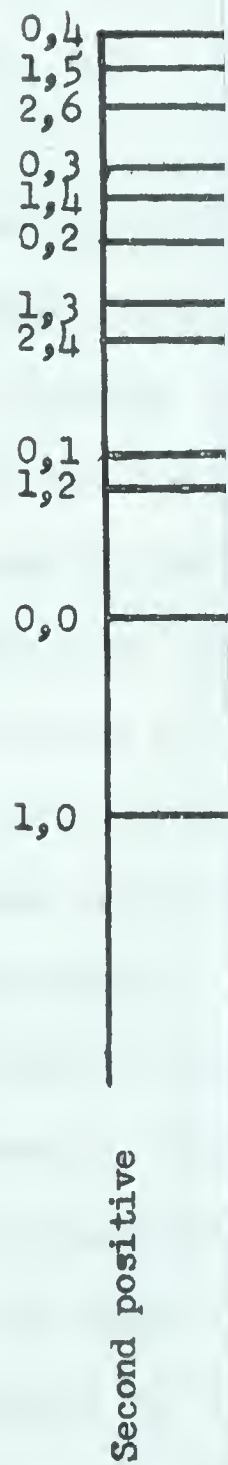


Plate 7

Nitrogen Bands in Active Nitrogen  
 Medium Hilger Prism Spectrograph  
 Kodak Type 103a-F Spectroscopic Plates  
 Slit Width  $60\mu$   
 Exposure Times 10 and 15 minutes



potential, was placed between the reaction vessel and the discharge tube in an effort to eliminate the glow. The net effect of the probe was to quench much of the yellow nitrogen afterglow with little alteration in the intensity of the pink glow. Small magnetic fields were placed between the outlet of the discharge and the reaction vessel but these seemed to have no effect upon the pink glow. Finally, a grounded layer of aluminum foil was wrapped around the outlet tube from the discharge. The effect was to eliminate a small portion of the pink glow before it reached the reaction zone, but at no time could the pink glow be completely eliminated.

The spectrum of the pink glow showed the presence of several fainter heads belonging to the second positive band system of nitrogen (listed in Table 15) and of bands from the  $v' = 0$  progression of the first negative bands of nitrogen (arising from  $N_2^+$  and listed in Table 16). From its spectrum it was concluded that the pink glow was either identical to, or quite similar to, the "pink short-lived afterglow of nitrogen" observed by Beale and Broida.<sup>71</sup>

When ortho-phosphoric acid wall poison was used to poison the reaction vessel, several bands belonging to the  $\beta$ ,  $\gamma$ , and  $\delta$  systems of nitric oxide appeared prominently in the violet and ultraviolet regions of the spectrum (Plate 8). The  $\beta$  bands (Table 17) were fairly extensive and showed bands from all levels below  $v' = 6$ , albeit some of them rather faintly. The  $\gamma$  bands (Table 18) were the most intense of the three nitric oxide systems; only the  $v' = 0$  progression was observed. The  $v' = 0$  progression of the  $\delta$  bands (Table 19) was observed to extend up to the limit of sensitivity





TABLE 15

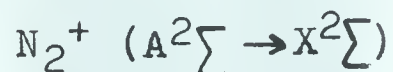
Second Positive Bands in Active Nitrogen



Transition $v' - v''$	Relative Intensity	$\nu_{\text{cm}^{-1}}$	Transition $v' - v''$	Relative Intensity	$\nu_{\text{cm}^{-1}}$
0 - 0	m	29,662	1 - 0	w	31,653
0 - 1	m	27,957			
0 - 2	s	26,282	1 - 2	w	28,275
0 - 3	w	24,634	1 - 3	w	26,628
			1 - 4	w	25,010
Transition $v' - v''$	Relative Intensity	$\nu_{\text{cm}^{-1}}$			
2 - 4	w	26,951			
2 - 5	w	25,361			
2 - 6	m	23,807			

TABLE 16

First Negative Bands in Active Nitrogen



Transition $v' - v''$	Relative Intensity	$\nu_{\text{cm}^{-1}}$
0 - 0	s	25,547
0 - 1	m	23,375
0 - 2	w	21,235



$\lambda$   
N<sub>2</sub> Second Positive

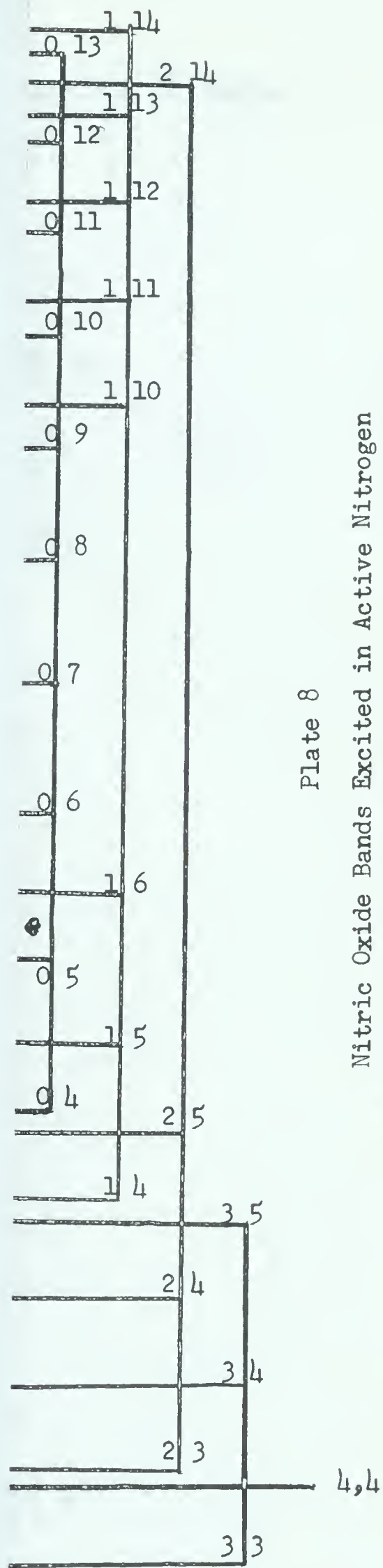
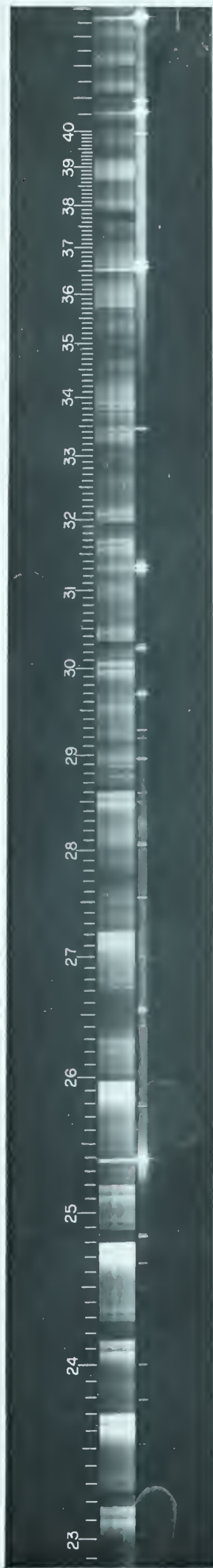
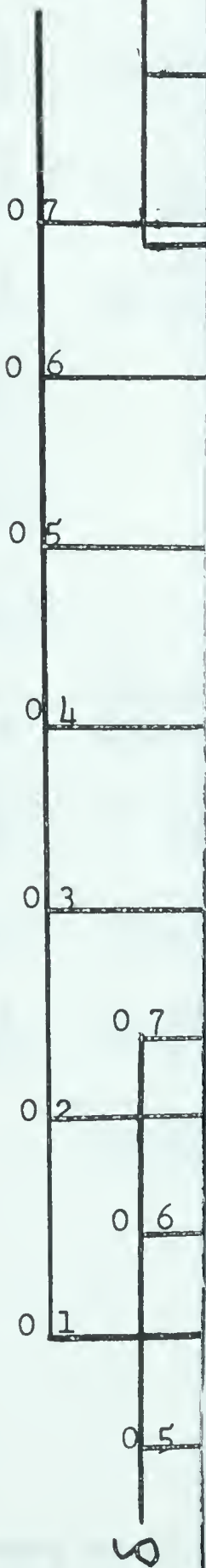


Plate 8

Nitric Oxide Bands Excited in Active Nitrogen

Medium Hilger Prism Spectrograph

Slit Width 100

Kodak Type 103a-0 Spectroscopic Plates

Exposure Time 30 minutes





TABLE 17

Nitric Oxide  $\beta$  Bands Excited in Active NitrogenNO ( B  $2\Pi \rightarrow$  X  $2\Pi$  )

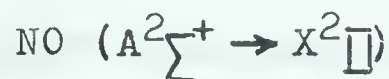
$v''$	$v'$	0	1	2	3	4
2				43 $\frac{714}{---}$ vw	44 $\frac{721}{803}$ w	
3				41 $\frac{904}{990}$ vw	42 $\frac{893}{981}$ vw	
4	38	$\frac{072}{161}$ m	39 $\frac{095}{185}$ w	40 $\frac{106}{196}$ w	41 $\frac{102}{190}$ w	42 $\frac{084}{166}$ vw
5	36	$\frac{307}{395}$ w	37 $\frac{332}{422}$ m	38 $\frac{339}{431}$ w	39 $\frac{335}{428}$ vw	
6	34	$\frac{571}{660}$ m	35 $\frac{595}{681}$ w			
7	32	$\frac{862}{950}$ m				
8	31	$\frac{183}{270}$ m				
9	29	$\frac{530}{617}$ m				
10	27	$\frac{906}{992}$ m	28, $\frac{928}{019}$ vw			
11	26	$\frac{310}{396}$ m	27 $\frac{334}{418}$ w			
12	24	$\frac{741}{827}$ w	25 $\frac{769}{851}$ m			
13	23	$\frac{203}{290}$ w	24 $\frac{225}{310}$ m			
14			22 $\frac{720}{801}$ w	23 $\frac{724}{806}$ m		
15			22 $\frac{241}{322}$ w		*	
16			20 $\frac{870}{---}$ vw	21 $\frac{713}{863}$ w		
17				20 $\frac{441}{---}$ vw		

vw = very weak

\* = overlapped

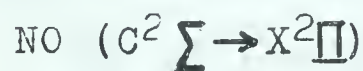


TABLE 18

Nitric Oxide  $\gamma$  Bands Excited in Active Nitrogen

Transition $v' - v''$	Relative Intensity	$\nu_{\text{cm}^{-1}}$	
0 - 0	w	44,065	44,193
0 - 1	m	42,191	42,314
0 - 2	s	40,344	40,468
0 - 3	s	38,525	38,647
0 - 4	m	36,735	36,875
0 - 5	m	34,971	35,090
0 - 6	w	33,236	33,360
0 - 7	vw	31,539	31,665

TABLE 19

Nitric Oxide  $\delta$  Bands Excited in Active Nitrogen

Transition $v' - v''$	Relative Intensity	$\nu_{\text{cm}^{-1}}$	
0 - 3	w	46,701	46,821
0 - 4	m	44,907	45,029
0 - 5	m	43,146	43,264
0 - 6	m	41,415	41,535
0 - 7	w	39,825	39,698





of ordinary Kodak Type "O" spectroscopic plates.

The nitric oxide bands were not present in the unpoisoned system even with considerable increases in exposure times to allow for lowered intensity. The most intense heads of the  $\gamma$  bands were sometimes faintly visible on the first exposure taken after the system had been "un-poisoned" by rinsing. Subsequent exposures usually did not show these  $\gamma$  heads at all.

In the late stages of the experimental work a small trace of carbon containing impurity found its way into the reaction system and showed its presence by the emission of two series of bands from the cyanogen violet system (Table 20). The nature of such cyanogen emissions in active nitrogen systems containing carbon has been discussed by Bayes.<sup>42</sup>

TABLE 20

Cyanogen Violet Bands Excited in Active Nitrogen

CN ( $B^2\Sigma \rightarrow X^2\Sigma$ )

	Transition $v' - v''$	Relative Intensity	$\nu$ cm <sup>-1</sup>
$\Delta v = 0$	0 - 0	s	25,751
	1 - 1	s	25,830
	2 - 2	m	25,894
	3 - 3	w	25,942
	4 - 4	w	25,968
$\Delta v = 1$	0 - 1	s	23,719
	1 - 2	m	23,825
	2 - 3	s	23,918
	3 - 4	m	23,993



## DISCUSSION

ON THE NATURE OF NBr

If it is assumed that the reactive species in active nitrogen with bromine is ground state nitrogen atoms, then it is possible to form NBr from two ground state atoms. The quantum numbers of the ground state atoms are as follows:<sup>13</sup>

	L	S	J	State
N	0	3/2	(3/2)	4s
Br	1	1/2	3/2	<sup>2</sup> P <sub>3/2</sub>

Using the Wigner-Witmer correlation rules, the recombination of these atomic states will give rise to a molecule in either a  $\Sigma$  or a  $\Pi$  state. The atomic spins can produce either a triplet state (corresponding to the pairing of one electron from each atom), or a quintet state (no-pair formation).<sup>12\*</sup>

Since nitrogen belongs to group 5a of the periodic table and bromine to group 7a, a diatomic molecule forming from these two atoms is isoelectronic to S<sub>2</sub>, a group 6a molecule. Atomic sulfur has the configuration



Using the notation of Lennard-Jones, the corresponding diatomic sulfur molecule is<sup>85</sup>



Thus, diatomic sulfur has four bonding pairs of electrons and four antibonding electrons (one pair and two equivalent unpaired electrons) giving a molecular configuration designated as  $\pi^2$ .

Such a configuration can give rise to  $^3\Sigma$ ,  $^1\Sigma^+$ , and  $^1\Delta$  molecular

\* In general Chapter VI of this reference has been utilized for background theory in this section.





states.<sup>86</sup> It would be expected from the Hund multiplicity rule that  $3\Sigma^-$  would have the lowest energy of these three states. Indeed,  $3\Sigma^-$  is found to be the ground state in diatomic sulfur, as it is also in molecular oxygen. Thus we might expect that in NBr  $3\Sigma^-$  could also be the ground state of the molecule.

In the case of NBr we are not forming our molecular orbitals from two equivalent sets of 3s and 3p electrons as in sulfur (nor from 2s and 2p as in oxygen), but from 2s, 2p electrons from nitrogen and 4s, 4p electrons from bromine. To describe the molecular orbitals formed from these atomic orbitals it is convenient to utilize the abbreviated nomenclature proposed by Mulliken.<sup>87</sup> Using this nomenclature 2s and 4s atomic orbitals combine to form a  $\sigma$  bonding orbital and a  $\sigma^*$  antibonding orbital, while 2p and 4p form  $\pi$  and  $\pi^*$  bonding, and  $\pi$  and  $\pi^*$  antibonding orbitals in the molecule formed. NBr can be formed from recombining ground state atoms in the manner shown in Figure 19. The only difference in structure from that of diatomic sulfur is the origin of the two unpaired  $\pi$  antibonding electrons, in sulfur one comes from each atom while in NBr both come from the bromine atom; but since after molecule formation has occurred the source of the electrons is indistinguishable, the two configurations are identical ( $\pi^2$ ). Thus it is likely that NBr will assume the same ground state configuration as diatomic sulfur. This  $\pi^2$  configuration is compatible with the spectroscopic interpretation of the observed emission bands since it would allow a  $3\Sigma^-$  ground state for NBr.



To obtain the observed transition with Q and S branches we require a forbidden  $1\Sigma^+ \rightarrow 3\Sigma^-$  transition. Such a transition is observed in oxygen near 7600 Å, the atmospheric absorption bands. However, in homonuclear oxygen the electric dipole transition is highly forbidden. The transition can, nevertheless, occur through magnetic dipole radiation. In heteronuclear NBr, the transition seems to be much less forbidden and can occur through electric dipole radiation. Normally a  $1\Sigma^+ \rightarrow 3\Sigma^-$  transition would be expected to show five branches (Figure 21) one from  $F_2$ ,  $Q_Q$  ( $Q_{Form} Q$ ),







and two each from  $F_1$  and  $F_3$ , the observed  $Q_P$ ,  $S_R$  and the missing  $Q_P$ ,  $Q_R$ .

The explanation for the appearance of only two of the five possible branches in NBr is not clear, but it is probably related to the type of coupling between the electrons spins and the inter-nuclear axis of the NBr molecule in the  $3\Sigma^-$  state.

Both oxygen and sulfur molecules can be treated as intermediate between two extreme coupling cases, denoted by Hund as case "b" and case "c". Case "b" molecules have strong coupling of the electron orbital angular momentum ( $\Lambda$ ) to the inter-nuclear axis but only weak coupling of the electron spin (S) to this molecular axis (Figure 20i). Light molecules generally approach this coupling case. On the other extreme, case "c", a strong interaction occurs between the orbital angular moments of the electrons (L) and electron spin (S). Their resultant is the total (atomic) angular momentum ( $J_a$ ) which is coupled to the inter-nuclear

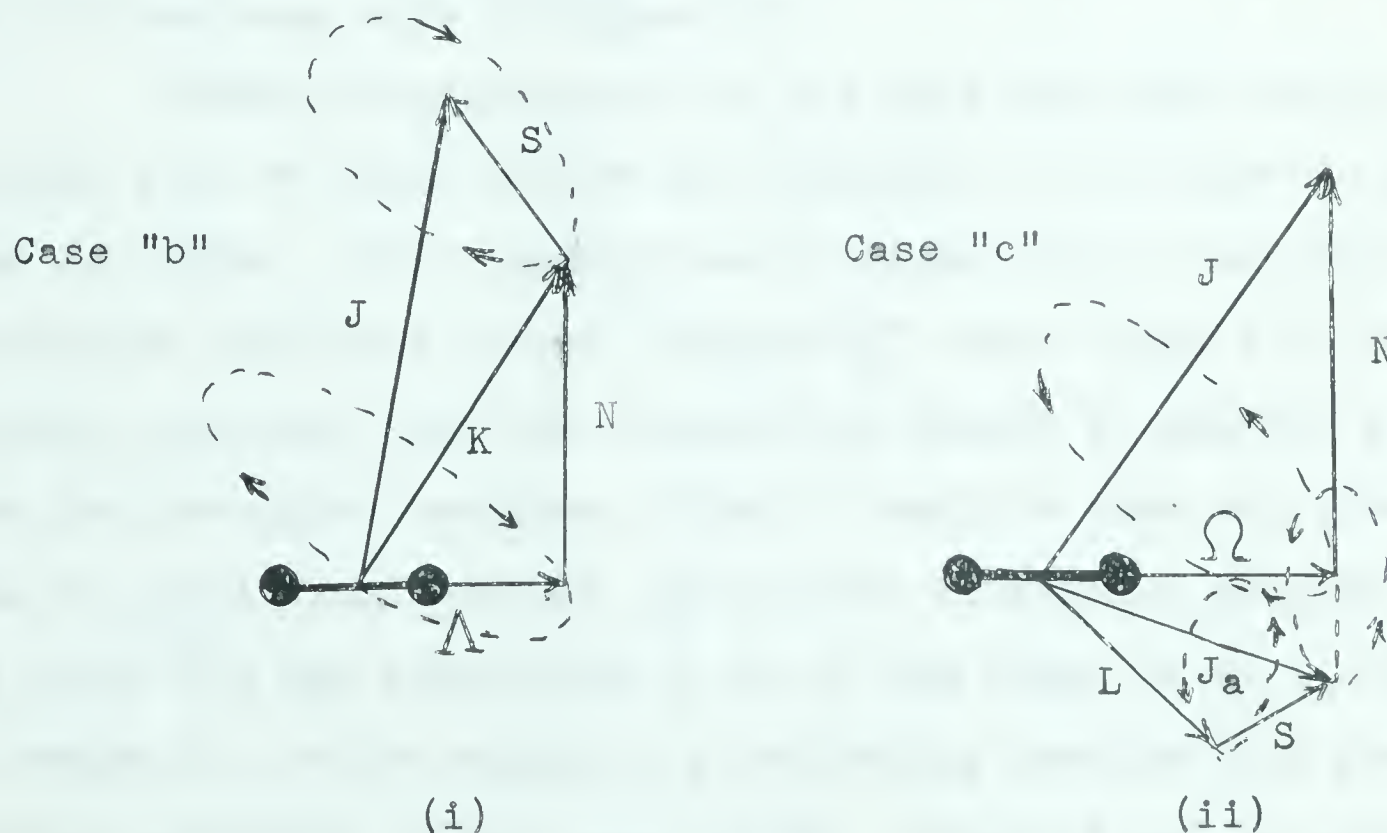
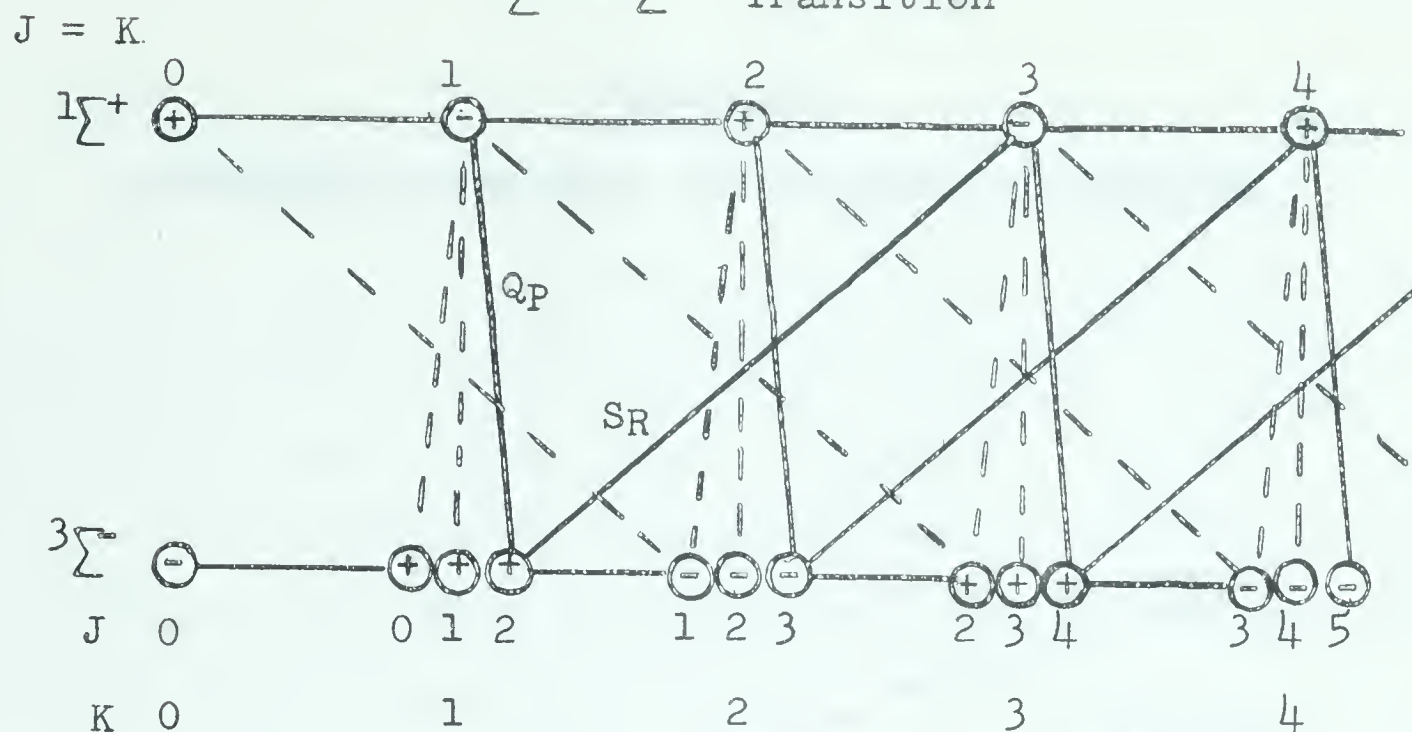


Figure 20

Hund's "b" and "c" Coupling Cases



$1\Sigma^+ \rightarrow 3\Sigma^-$  Transition


axis of the molecule forming a quantized component ( $\Omega$ ) along this axis.  $\Omega$  contributes to the total angular momentum of the molecule ( $J$ ) (see Figure 20ii).<sup>86,88</sup> Such coupling resembles that presented by an atom in a weak electrical field in the absence of Paschen-Back effect. It is characteristic of halogen molecules. The effect of transition between the two extreme coupling cases "b" and "c" has been shown in Figure 22.

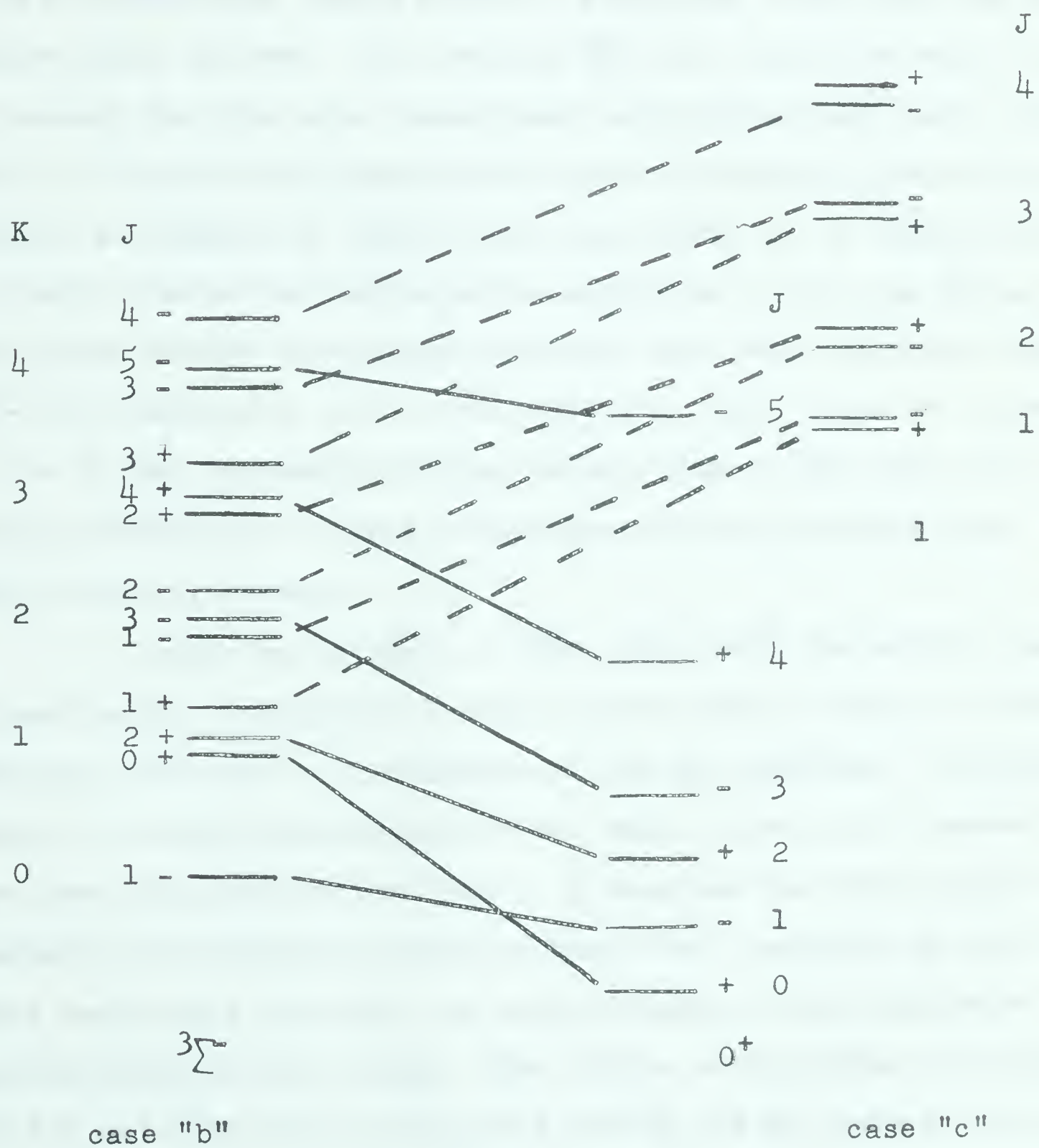
From a consideration of the fact that NBr contains one halogen atom we might expect the molecule to be closer to case "c" than is oxygen. This supposition is borne out by the shape of the calculated splitting curves for the  $3\Sigma^-$  state (Figure 18) which clearly indicates that the observed  $F_1$  branch is greatly separated from the two other branches, which is not the case in oxygen.<sup>89</sup> From the splitting constant ( $\lambda$ ) and the rotational constant ( $B$ ), the ratio  $\lambda/B$  was calculated to be of the order of 25 in NBr while in oxygen the ratio equals 1.4 indicating considerably greater triplet splitting in the case of NBr. Thus, it may be quite reasonable to assume that the  $3\Sigma^-$  ground state of NBr has progressed





Figure 22

Transition from Case "b" to Case "c" Coupling





well towards a case "c" configuration in which the  $F_1$  levels have taken the characteristics of a  $0^+$  state and the  $F_2$  and  $F_3$  levels have formed a 1 state (which resembles case "b"  $\Pi$  state). The observed transition should now be more properly classified as a  $1\Sigma^+ \rightarrow 0^+$  transition, which is not a forbidden transition but is rather quite allowed. The related  $1\Sigma^+ \rightarrow 1$  transition may be able to account for the faint unassigned bands which have been noted in the  $9^1-7^1$  and  $8^1-6^1$  bands (yet with the present intensities certain assignment of these lines has proven to be impossible). No simple theoretical explanation exists as to why the  $1\Sigma^+ \rightarrow 1$  transition should be any less probable than the intensely observed  $1\Sigma^+ \rightarrow 0^+$  transition, but if the observed faint lines do correspond to the  $F_2$  and  $F_3$  levels of the ground state of NBr then the transition probability to these levels must be considerably lower than that to the  $F_1$  levels.

In his early study of NBr, Elliott<sup>76</sup> had noted a number of weak bands, one group of which appears about midway between members of the  $\Delta v = 2$  sequence of the NBr spectrum. Elliott was unable to assign these bands to the main sequence and assumed that some were connected to the  $\Delta v = 2$  sequence and that others were fragments of different sequences from those assigned in the study. These bands have not shown up on the weaker, high resolution spectra taken in this study. The choice of splitting constants  $\lambda = 8.7$  and  $\gamma = -0.7$  do not place the  $F_2$  and  $F_3$  heads at the unassigned wavelengths of Elliott's study but they do place these unobserved heads close to a number of very diffuse unassigned lines located amidst the region where the  $N^{79}\text{Br}$  and  $N^{81}\text{Br}$  tail



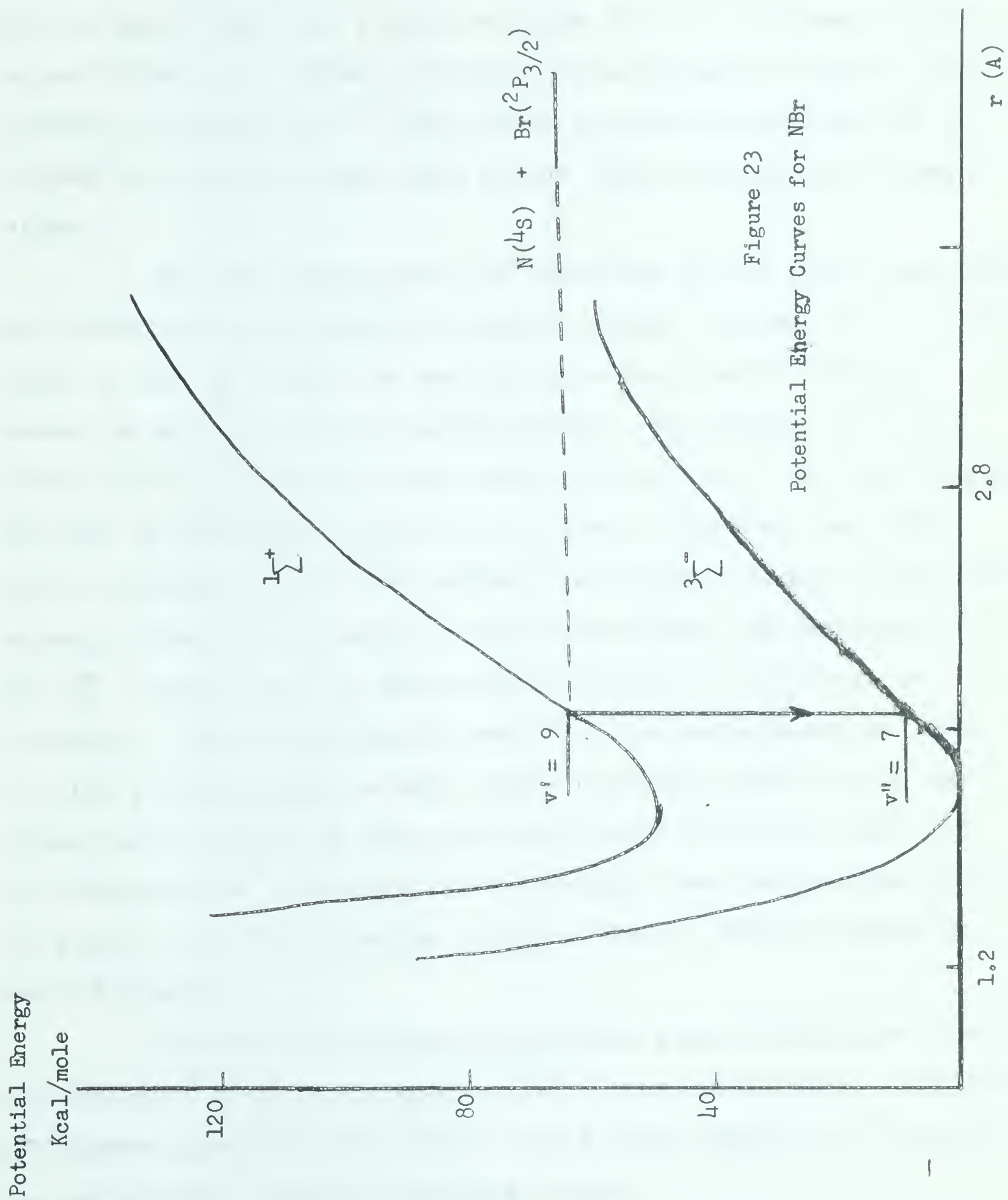


branches overlap and cross each other (around  $16,867\text{ cm}^{-1}$  in the  $8'-6''$  band). Several sequences of lines have been followed from these "heads" but the certainty of the position of the faint lines, especially when close to the brighter  $F_1$  lines, frustrates positive assignment. On the other hand, it would not be inconsistent with the observed  $F_1$  bands to choose a value of  $\lambda$  which would allow the  $F_2$  and  $F_3$  components to account for a number of Elliott's weaker bands. However, in the  $8'-6''$  band at least, Elliott's weak band occurs at  $16,888\text{ cm}^{-1}$  which is in the region of the intensity maxima shown by the two isotopic tail branches of the main bands, and almost midway between two very intense tail lines at  $16,874$  and  $16,900\text{ cm}^{-1}$ .

The observed NBr spectrum can be fully accounted for by a  $1\Sigma^+ \rightarrow 0^+(3\Sigma^-)$  transition. Theory corroborated observation in the fact that in the spectrum  $J'' = 2$  is the lowest level observed in the tail branch, which is indeed the lowest  $J''$  level to which a  $F_1$  transition can occur. However, no simple direct proof exists that the same bands cannot be explained by a  $1\Sigma^- \rightarrow 3\Sigma^+$  transition or some other type of transition.

On the assumption that the proposed assignment of the molecular states is correct we must explain how the observed bands could be excited in active nitrogen. From the Wigner-Witmer correlation rules it follows that a  $1\Sigma^+$  state cannot arise directly from ground state nitrogen and bromine atoms. Thus we are forced to conclude that the  $1\Sigma^+$  state correlates with some higher states of the separated atoms, probably N ( $^2D$ ) and ground state bromine ( $^2P$ ). From this we conclude that the potential energy curves for NBr must be of the form shown in Figure 23.









A prominent feature of the spectrum is that the vibrational levels of the upper state are populated up to the  $v' = 10$  level but not beyond (Plate 9). Kinetic evidence in a companion study to the present investigation <sup>90</sup> leads us to the conclusion that NBr is formed in active nitrogen from ground state nitrogen and bromine atoms.

At room temperature the combining ground state atoms can only have one or two kcal. of kinetic energy and thus the  $v' = 10$  level of the  $1\Sigma^+$  state can not lie more than one or two kcal. above the energy of the separated atoms. The energy of  $v' = 10$  above the  $v'' = 0$  ground state level is 63.4 kcal. The very sharp cut-off of the bands at the  $v' = 10$  level indicates that this level is quite close to the actual dissociation energy of the NBr molecule itself. By making a long Birge-Sponer extrapolation of the  $3\Sigma^-$  ground state, a dissociation energy of 71.5 kcal. is obtained. Since the inherent error in such extrapolations tend to give a dissociation energy higher than the actual value, the dissociation energy of NBr agrees well with the lower limit for the dissociation energy obtained directly from the spectrum (about 62 kcal.). The dissociation energy of NBr is thus estimated to be  $67 \pm 5$  kcal.

It is obvious from the observed flame intensities that the emission is favoured when the NBr forms on (or near) the walls. It appears plausible that ground state atoms combine to form NBr in one of three allowable excited states



Of these three states only the  ${}^3\Pi$  could correspond to a bonding



5881.84 Å

5944.83 Å

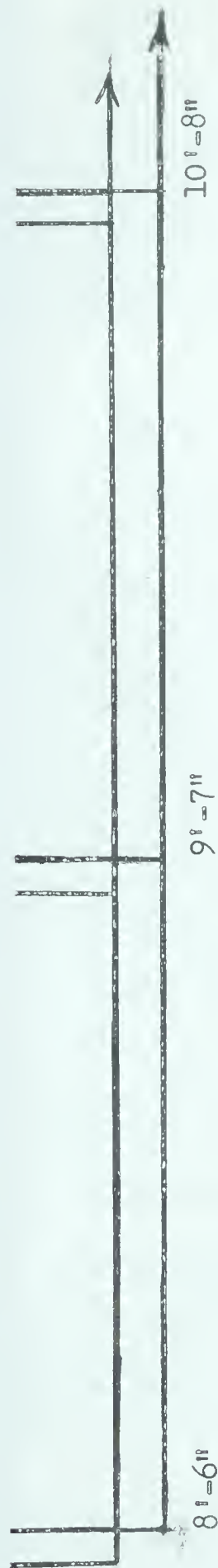


## Plate 9

Break-off of the NBr Bands at  $\nu^i = 10$ 

N.R.C., 10 m.,  $f/100$  grating spectrograph      Slit Width  $60\mu$   
 Kodak Type 103a-F Spectroscopic Plates      Exposure Time 8 hours



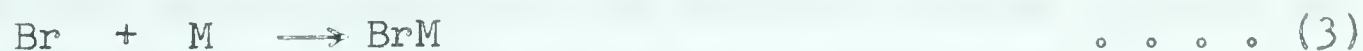


configuration, but no evidence exists to prove whether or not it should be a stable state. The two quintet states would dissociate in a single vibration since they involve no bonding electrons. To explain the observations, the excited NBr molecule (NBr\*) must upon formation undergo a radiationless transition into an excited state.



As a result of such a process the observed emission could arise.

The mechanism of radiationless transitions is well known in the recombination of nitrogen atoms in active nitrogen<sup>9,41</sup> and the combination of nitrogen with oxygen to form nitric oxide (NO),<sup>91</sup> and has been proposed more recently for the formation of excited NH in active nitrogen.<sup>92-3</sup> The reverse process to such transitions has been proposed for predissociation phenomena in nitrogen.<sup>21</sup> The enhancement of radiationless transition by external perturbations has been treated theoretically by Zener<sup>94</sup> and Landau<sup>95</sup> and recently re-examined by Bates.<sup>96</sup> Experiments have been performed examining the effect of collisions upon dissociation and recombination spectra of both nitrogen and the halogens.<sup>97-9</sup> In a study of the recombination of bromine, Strong, Chien Graf, and Willard<sup>100</sup> proposed the following mechanism for the process



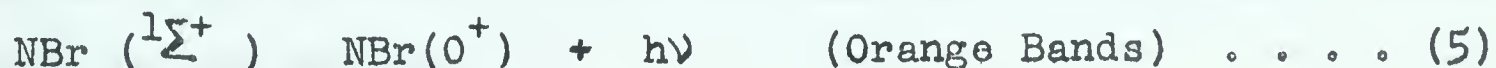
which employs a "sticky" bimolecular collision in the primary process preceeding an encounter with the third body. Such a mechanism is not incompatible with the desired mode of the NBr formation sequence. In fact, if reaction 1 was to be considered



as a "sticky" collision, followed immediately by a collisionally-induced radiationless transition into the  $^1\Sigma^+$  excited state upon encounter with a third body (which can, in our case, it seems be either another gas phase molecule or the walls of the vessel) then we can account for the observed emission from ground state atoms.

The only unusual factor in the presently postulated mechanism is, for the nature of the emission to be explained, that we require either the original NBr formation process (in reaction 1) or the radiationless crossover into the  $^1\Sigma^+$  excited state (in reaction 2) to occur preferentially at, or near, the wall. We thus have to assume that either reaction 1 or reaction 2 is catalytically assisted by the walls. There is no evidence that reaction 2 requires the wall to occur. The adsorption of bromine atoms upon a wall is well known. The dependence of the emission upon the condition of the wall may indicate that adsorbed bromine atoms may be participating in reaction 1.

Following the radiationless transition process into the  $^1\Sigma^+$  excited state the NBr radiates to the ground state, emitting the observed bands



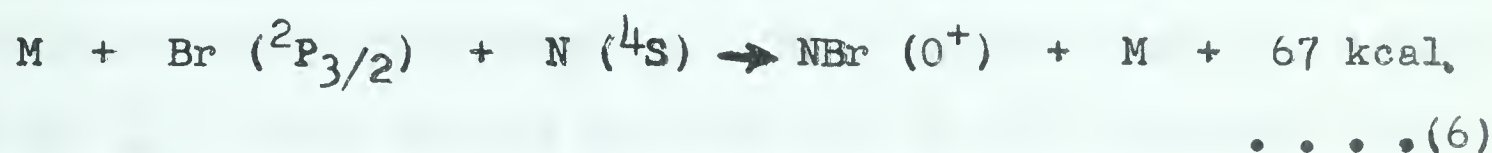
The ultimate fate of NBr, no matter how it forms is to return to the original  $\text{Br}_2$  (in the process forming  $\text{N}_2$  from two nitrogen atoms). We thus recover the original reactants as products of the reaction, with no other stable chemical products being formed. In order to provide a mechanism for the entire process which is compatible with the chemical kinetic schemes proposed for similar active nitrogen reactions where definite stable products do result from the reaction, we require that only a small percentage of the NBr originally formed radiates.<sup>90</sup> A recent study of the atom



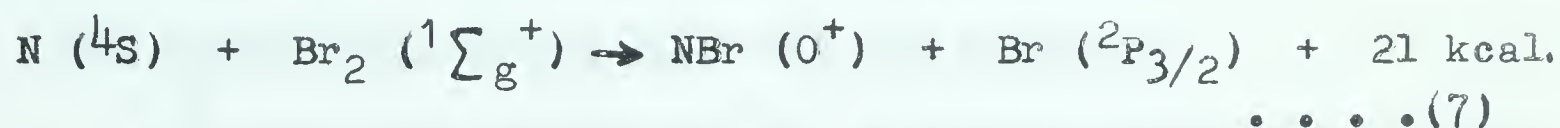




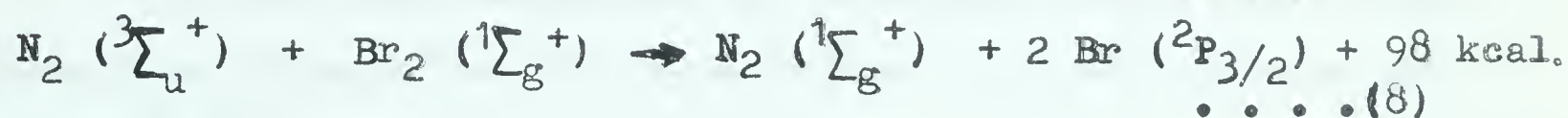
recombination indicates that almost all diatomic molecules formed by a combination of atoms, catalyzed by a third body, are in the ground state; substantially fewer molecules end up in excited states than is predicted by the statistical weights of the states arising out of the Wigner-Witmer correlation rules (rigidly applicable to two-body recombination).<sup>101</sup> In essence, this means that the majority of the NBr should be formed directly in the ground state by a gas phase reaction.



The source of ground state bromine atoms might be from either of two reactions

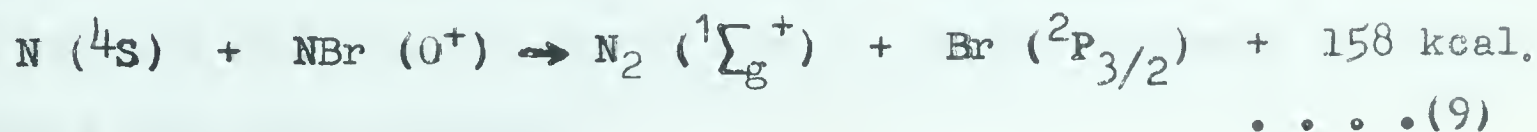


or



depending upon whether nitrogen atoms or excited nitrogen molecules initiate the dissociation of the bromine molecules. The present study has provided no evidence capable of separating these two possible modes of initiation; both reactive nitrogen species are present in the system.

Once atomic bromine has been formed, reaction 6 can occur in the gas phase producing ground state NBr, while reaction 1 can occur at the walls producing excited NBr and the observed emission. Both processes will ultimately supply ground state NBr molecules which will be attacked by active nitrogen



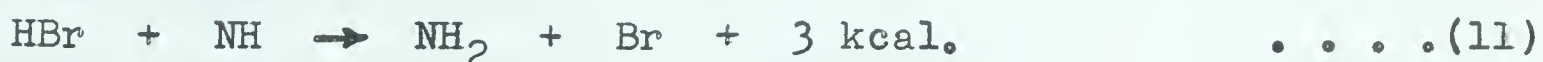
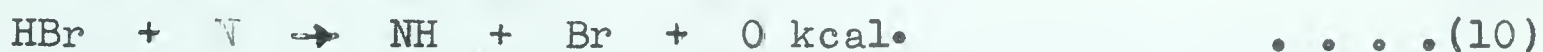
effecting the recombination of two nitrogen atoms and replenishing the supply of ground state bromine atoms. In the process NBr has



acted as the intermediate in the catalytic recombination of nitrogen atoms using bromine as the third body. Several reactant molecules introduced into active nitrogen have been noted to serve as a catalyst for the recombination of nitrogen atoms.<sup>90,102</sup> It has been noted in the present study that bromine is very efficient as a quenching agent for the nitrogen afterglow. The above reaction sequence can probably remove the nitrogen atoms quickly enough to markedly deplete the number of atoms left free in the gas phase and thus explain the quenching. But a direct attack by bromine on the  $N_2 \text{ } ^5\Sigma_g^+$  state can not be ruled out as the quenching mode, especially if it can be shown that excited molecular nitrogen is responsible for the induction reaction.

#### THE CORRELATION OF NBr WITH THE HBr KINETICS

In previous studies of the reaction of hydrogen bromide with active nitrogen the following series of reactions have been proposed.<sup>3,78,90</sup>



From the stoichiometry of the system and the kinetic data obtained in the previous studies, it was apparent that at 80°C about 90% of the active nitrogen was being destroyed by the catalytic recombination of nitrogen atoms on hydrogen bromide.



The initial reaction was postulated to proceed through an intermediate collision complex,<sup>3</sup>

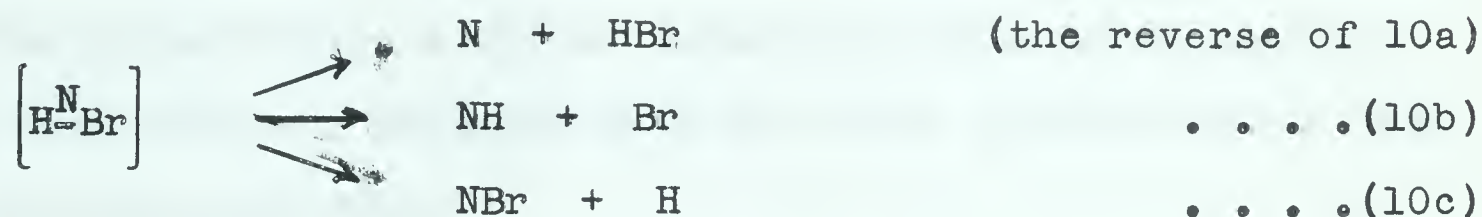








which might be considered as a "sticky" collision (analogous to that proposed for bromine recombination<sup>100</sup>). The fate of this complex might be reconsidered in terms of a possible NBr intermediate being formed. The complex might decompose spontaneously in three ways.



Of these reactions, the one liberating NBr (10c) is not likely to occur to any extent since the reaction



is not energetically favoured, and atomic hydrogen has not been detected in the system.<sup>3</sup> Should the complex survive long enough to collide with a second nitrogen atom the following reactions are possible.



Here, both modes of decay are possible from energy considerations. The former results in the catalytic recombination of nitrogen on hydrogen bromide and would effect the greatest release of energy (reaction 14). The latter reaction could provide a source of NBr in the HBr decomposition mechanism and may be written as



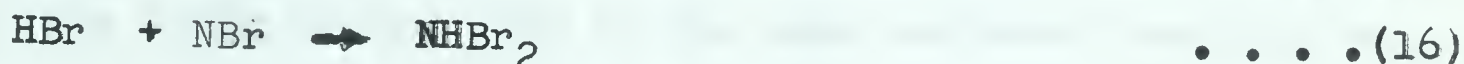
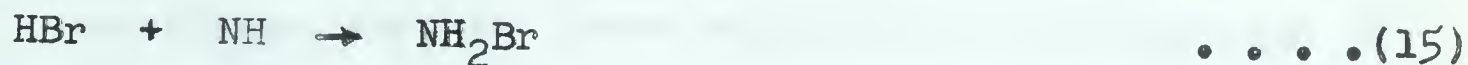
It is possible that this reaction occurs to some extent in the system despite the fact that it would release less energy than reaction 14. Should NBr be produced in this way, most of the NBr liberated would be in the ground state and would be used up in reaction 9, while the NH formed would be consumed by reaction 11.

Since traces of compounds believed to be bromamine and bromimine have been mentioned to have been found in the reaction

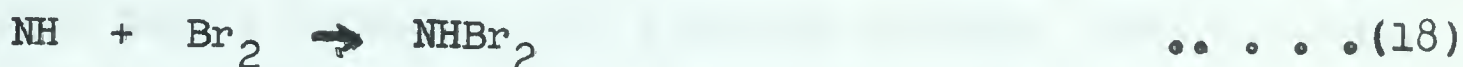
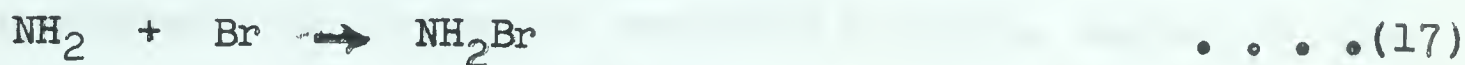




products, it would be desirable to explain their formation. These trace products could possibly arise from the reaction of hydrogen bromide with the products of reaction 14b.



Both reactions require a rather severe molecular rearrangement and it might be more probable that the trace products arise from the following reactions.



Bromimine could even be formed through the attack of a bromine atom upon the collision complex.



The postulation that the reaction of hydrogen bromide with active nitrogen occurs via a "sticky" collision is quite compatible with the observed temperature effects upon the amounts of product formed by the reaction. The lifetime of the collision complex should determine the relative occurrences of decomposition to products (reactions 10a-10c) and catalytic recombination of nitrogen atoms on hydrogen bromide (reaction 14). At elevated temperatures the lifetime of the collision complex would be diminished favouring decomposition of the hydrogen bromide to products. A simpler alternative explanation for the observed temperature effect has been presented previously;<sup>3</sup> the competition of reactions 10 and 14. Higher temperatures would favour the bimolecular process (reaction 10) over the trimolecular process (reaction 14). Because fewer three body encounters should occur at elevated temperatures, the increased decomposition of hydrogen bromide<sup>3</sup> would be expected.





At lower temperatures the kinetics indicate that reaction 14 is the predominant one, denotative of more three body collisions.

The liberation of ground state bromine atoms in the kinetic sequences proposed above would allow the formation of NBr at the walls giving rise to the same emission spectrum as has been observed with bromine in active nitrogen.

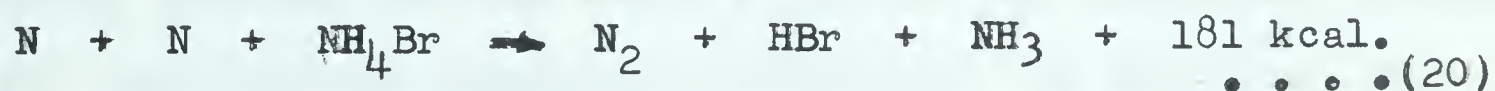
#### THE AMMONIUM BROMIDE REACTION

A previous study has reported<sup>3</sup> that when active nitrogen is reacted with traces of ammonium bromide, deposited upon the walls during reaction with hydrogen bromide, that all but traces of the ammonium bromide are consumed by the ensuing reaction. The products of the reaction have been reported as bromine, hydrogen bromide, and bromimine.

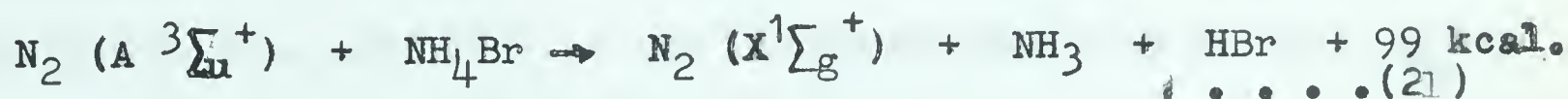
For the reaction to occur we must somehow supply sufficient energy to enable the active nitrogen to sublime the ammonium bromide off the wall;  $\Delta H_{\text{sublimation}}$  for  $\text{NH}_4\text{Br}$  is 44 kcal.<sup>3</sup> It is doubtful if the reaction



could provide sufficient energy to effect the sublimation. However, the recombination of two nitrogen atoms upon ammonium bromide at the wall might liberate the salt.



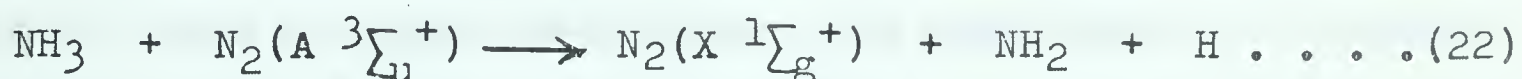
Or, the salt could be attacked by metastable nitrogen molecules.



Once the ammonium bromide has been decomposed into ammonia and hydrogen bromide, then the entire hydrogen bromide reaction scheme could be re-initiated in the ammonium bromide-active nitrogen system.



After being liberated into the gas phase, the ammonia and hydrogen bromide could migrate back to the walls and recombine (by reaction 13), or they could react with other species present. The hydrogen bromide can be consumed by at least three reactive species, probably nitrogen atoms (reaction 10), NH (reaction 11), and NH<sub>2</sub> (reaction 12). Ammonia, on the other hand, will only be consumed by molecular nitrogen. A reaction with metastable A  $^3\Sigma_u^+$  nitrogen has been proposed as the primary process for the ammonia decomposition in active nitrogen.<sup>4,6</sup>



At room temperature, the primary reaction is followed by an attack on the NH<sub>2</sub> radicals by active nitrogen to produce molecular nitrogen and hydrogen. Evidence supporting reaction 22 is that traces of hydrazine have been recovered from recombination of two NH<sub>2</sub> radicals. When the reaction is carried out at liquid nitrogen temperatures hydrazine is the main product of the decomposition process.<sup>5,103</sup> Such a primary process for the decomposition of ammonia in active nitrogen would be entirely compatible with the partial quenching of an afterglow precursor.<sup>41</sup>

The formation of free bromine atoms from the reactions consuming hydrogen bromide would allow for NBr formation, accounting for the observed orange wall emissions. In addition, the liberation of free bromine atoms and ammonia by the reactions would aid in the quenching of the nitrogen afterglow in the region of the wall reaction with the salt.

A reaction mechanism initiated by the sublimation of ammonium bromide by active nitrogen, followed by attack on the liberated ammonia and ammonium bromide by the active nitrogen would







explain how the reaction zone moves down the reaction tube from the nitrogen inlet towards the cold trap. It would allow a portion of the products from the reactions to be re-deposited upon the walls of the vessel downstream from the reaction zone as a fresh supply of ammonium bromide. The products recovered can be explained by the mechanism.

#### THE BLUE BROMINE AFTERGLOW

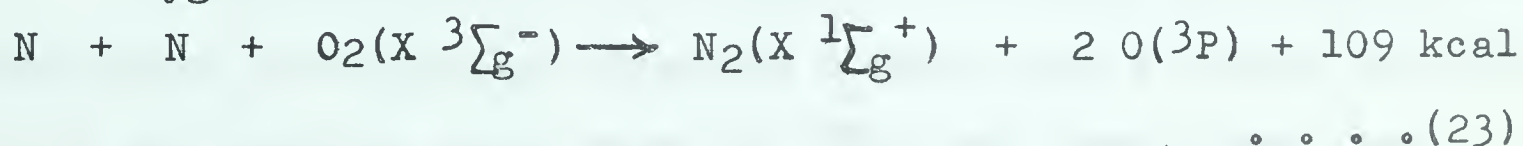
The spectrum of the blue bromine afterglow appeared to be identical whether hydrogen bromide or bromine was used. The dominant feature of the spectrum was the appearance of sequences belonging to the  $\beta$  bands of nitric oxide. All of the bands observed originated from levels below  $v' = 6$  of the  $B^2\Pi$  upper state. The intensity distribution of the bands observed during the blue afterglow differed from those noted in active nitrogen alone; the system extended further into the red and was more intense. In active nitrogen, the  $\beta$  bands were observed to extend much further into the violet than they did when bromine was present. At the same time, members of the  $v' = 0$  progressions of the  $\gamma$  and  $\delta$  bands of nitric oxide were always present when the nitric oxide bands were excited in active nitrogen, but were completely absent in the presence of bromine.

In both the hydrogen bromide and bromine experiments the wall condition seemed to be important for the production of the blue afterglow. The blue glow could be produced by keeping the bromine or hydrogen bromide flow rates very low, but a marked deterioration of the intensity of the blue afterglow occurred with time. After three-quarters of an hour of reaction, the blue afterglow rapidly diminished in intensity and could not be restored to

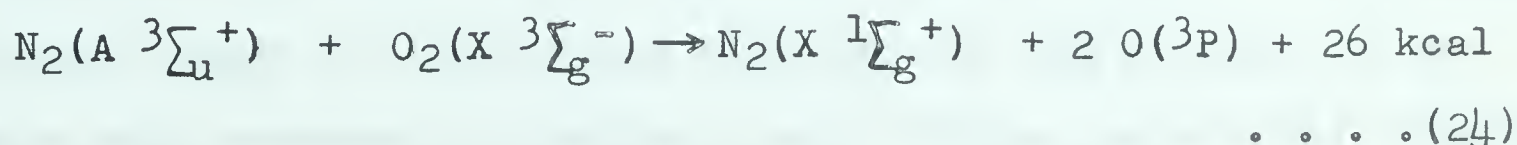


its original brilliance unless air was admitted to the system. Even when small quantities of air were admitted to the apparatus the blue afterglow was enhanced. The diminution of the blue afterglow was especially pronounced when bromine was the reactant. If the bromine flow was allowed to become too great, even for a short period of time, the blue afterglow disappeared and could not be regenerated without the admission of air. The other criterion required for the production of the blue afterglow was the presence of a weak nitrogen afterglow, without which no emission was noted.

When the bromine or hydrogen bromide flow was stopped a sufficient concentration of nitrogen atoms could build up to allow a faint Lewis-Rayleigh afterglow to appear, since the concentration of bromine present was no longer large enough to remove the nitrogen atoms before they could recombine. Under these conditions we would have a small transition zone of increasing nitrogen atom concentration between the orange NBr emission and the yellow nitrogen afterglow. In this transition region, the blue afterglow could be produced from the liberation of oxygen atoms from the wall. The liberation could be achieved by the recombination of two nitrogen atoms on oxygen at the wall.



Or, by the dissociation of molecular oxygen by metastable nitrogen molecules





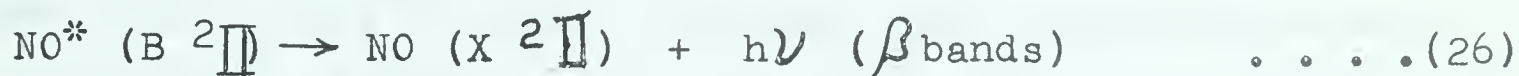




Once produced, the atomic oxygen would react with nitrogen atoms at, or near, the wall.



This reaction is well known in active nitrogen and has no activation energy.<sup>10</sup> Some of the nitric oxide produced appears in an excited state and produces the nitric oxide bands,<sup>104</sup> which were observed in our experiments.



Ground state nitric oxide is rapidly consumed by nitrogen atoms regenerating atomic oxygen.<sup>104</sup>



This reaction occurs over a very small zone of mixing, while the slower recombination of nitrogen and oxygen atoms (reaction 25) will occur over a considerable volume.<sup>105</sup>

The disappearance of the blue glow in the presence of higher concentrations of nitrogen atoms (indicated by a more intense Lewis-Rayleigh afterglow) probably occurs because the nitrogen atoms are flushing the oxygen atoms out of the system quite rapidly depleting the source of the emission.

The fact that in the presence of bromine the bands show a vibrational distribution favouring higher levels during the formation of the excited upper state ( $\text{B } ^2\Pi$  of NO) from atoms, can probably be accounted for by considering the action of bromine as a third body for reaction 25. However, the reason for the markedly different number of transitions observed for the  $\beta$  bands in the absence and presence of bromine is not obvious, especially considering that except for transitions from  $v' = 5$  (which is not present in active nitrogen alone) the upper state vibrational levels in the



blue afterglow are identical with those observed in active nitrogen alone. The absence of both the  $\gamma$  and  $\delta$  band systems of nitric oxide in the presence of bromine may indicate that bromine is capable of quenching the states ( $A \ ^2\Sigma^+$  and  $C \ ^2\Sigma^+$ ) giving rise to these emissions. Any further comment upon the absence of these two band systems is necessarily speculative, yet the phenomena observed here might be similar to the selective enhancement observed for radiationless transitions in active nitrogen when foreign gases are present.<sup>41,59,60</sup> Tanaka and co-workers<sup>106</sup> were able to selectively enhance the cross-over from  $N_2 \ ^5\Sigma_g^+$  into the  $Y \ ^3\Sigma_u^-$  state (emitting the Y bands) simultaneously suppressing the cross-over into the  $B \ ^3\Pi_g$  state (first positive bands) by choice of appropriate third body and pressure.

The blue glow noted at the interface between the orange NBr glow and the yellow nitrogen afterglow, when the nitrogen afterglow was quite intense, appeared as a fluorescence on the pyrex walls. Kenty has noted a similar fluorescence in a nitrogen system containing metastable krypton atoms which radiate at 1750 Å.<sup>17,107</sup> The energy of the former fluorescence is almost equal to the recombination energy of ground state nitrogen and oxygen atoms (6.487 e.v.), and might possibly arise from a direct recombination of the two atoms, involving bromine, on the wall.

The mechanism proposed for the emission of the  $\beta$  bands of nitric oxide in the presence of bromine could also explain the appearance of the blue glow in portions of the apparatus where very low concentrations of nitrogen atoms occur during the course of the reaction itself, namely downstream from the reaction zone in dead-end portions of the apparatus (out of the direct line of flow







to the pumps) and above the cold point in the cold trap.

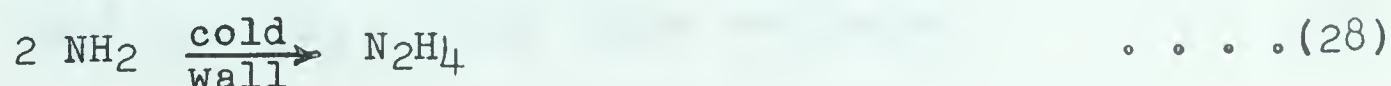
The apparent continuum noted by Dunford<sup>3</sup> was not observed in the present study. In view of the fact that both Dunford's continuum and our observation of the bands of nitric oxide had long wavelength edges near  $5100 \text{ \AA}$ , it might be that with the poorer resolution of his small, hand spectroscope that the nitric oxide bands noted in this work were mistaken for a continuum.

In their early study of NBr, Strutt and Fowler reported a broad symmetrical band with ill-defined edges at  $2930$  and  $2890 \text{ \AA}$ .<sup>75</sup> Cameron and Elliott<sup>108</sup> attributed this band to a continuum associated with a  $^1\Sigma^+$  state of bromine with  $\omega_e = 147 \text{ cm}^{-1}$ . In the quest to collect information about the blue afterglow associated with the bromine and hydrogen bromide reactions, attention was directed towards photographing this ultraviolet band but no success was had in obtaining any spectrum in this region.

#### THE AMMONIA TRAP GLOW

The blue trap reaction observed during the reaction of ammonia with active nitrogen at  $-196^\circ\text{C}$  was shown to be a continuum with no underlying structure in the blue region. The continuum appeared between  $3150 \text{ \AA}$  and the red limit of our photographic emulsion ( $6800 \text{ \AA}$ ).

The primary reaction is the decomposition of ammonia in active nitrogen, probably leading to the formation of  $\text{NH}_2$  radicals and hydrogen atoms (reaction 22). Zabolotny and Gesser<sup>5</sup> have shown that the primary product of the reaction at  $-196^\circ\text{C}$  is hydrazine. The reaction, occurring at the wall accounts for the yield of



and it is not at all clear that the Commission will

be able to do so.

It is not clear that the Commission will be able to do so.

It is not clear that the Commission will be able to do so.

It is not clear that the Commission will be able to do so.

It is not clear that the Commission will be able to do so.

It is not clear that the Commission will be able to do so.

It is not clear that the Commission will be able to do so.

It is not clear that the Commission will be able to do so.

It is not clear that the Commission will be able to do so.

It is not clear that the Commission will be able to do so.

It is not clear that the Commission will be able to do so.

It is not clear that the Commission will be able to do so.

It is not clear that the Commission will be able to do so.

It is not clear that the Commission will be able to do so.

It is not clear that the Commission will be able to do so.

It is not clear that the Commission will be able to do so.

It is not clear that the Commission will be able to do so.

It is not clear that the Commission will be able to do so.

It is not clear that the Commission will be able to do so.

It is not clear that the Commission will be able to do so.

It is not clear that the Commission will be able to do so.

It is not clear that the Commission will be able to do so.

It is not clear that the Commission will be able to do so.

It is not clear that the Commission will be able to do so.

hydrazine. In the present study, the blue continuum might arise from recombination of the products, from the primary decomposition of ammonia, on the wall at the cold point.



This is followed by emission.



A green fluorescence has been noted from ammonia during photolysis.<sup>109</sup> Should the observed continuum be due to excited ammonia, formed in reaction 29, then the effect of oxygen and mercury upon the emission might be explained as follows. Either oxygen or mercury would be readily attacked by the reactant species ( $\text{NH}_2$  and  $\text{H}$ ) postulated to give rise to the ammonia emitting the blue continuum. Thus, the blue continuum should be quenched in the presence of either oxygen or mercury. The yellow-green ammonia  $\alpha$  bands (which are emitted by ammonia burning in oxygen) could explain the change in shade of the emission from blue to green in the presence of traces of oxygen or air. These ammonia  $\alpha$  bands are believed to arise from  $\text{NH}_2$  rather than from ammonia itself.<sup>110</sup> The black deposits left when mercury is present could be nitrides of mercury. The ready solubility of these black deposits in water or dilute acid solutions would then be explained.

An alternative source for the continuum might be from recombination of two nitrogen atoms upon ammonia at the walls.



The energetics of this reaction could give rise to an excited  $\text{NH}_2$  radical, which could provide the observed emission by







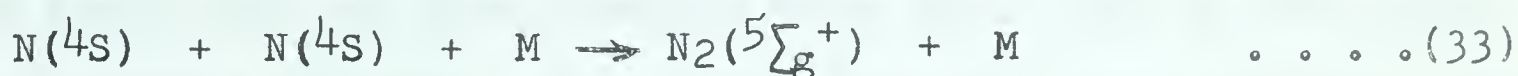


or, the  $\text{NH}_2^*$  could recombine with a hydrogen atom and give rise to excited ammonia which emits (as above in reactions 29 and 30).

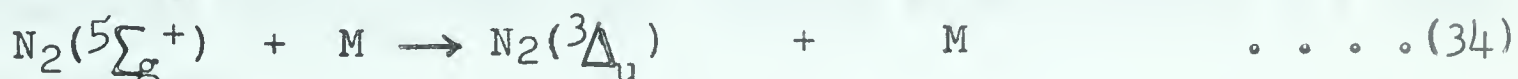
Since only a continuum has been observed we can only speculate as to its source. The observation of some banded structure in the infra-red (associated with the continuum) would provide a better means of determining the source of the emission.

### ON THE ACTIVE NITROGEN EMISSIONS

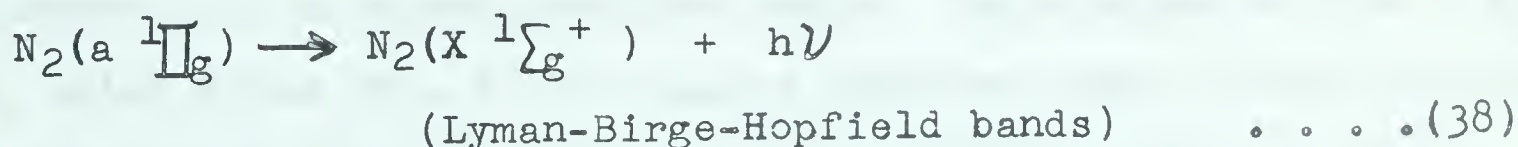
The Lewis-Rayleigh Afterglow: The yellow nitrogen afterglow has been explained by the recombination of ground state nitrogen atoms.<sup>9</sup> The mechanism involves the recombination of the nitrogen atoms into a shallow molecular state of nitrogen,  $^5\Sigma_g^+$ , for which no direct spectroscopic evidence exists.<sup>111</sup>



Several collisionally-induced, radiationless transitions can occur from this  $^5\Sigma_g^+$  state into other excited states of nitrogen.<sup>41</sup>



Transition is allowed from all of these states. The  $\text{a } ^1\Pi_g$ <sup>29</sup> and  $\text{Y } ^3\Sigma_u^-$ <sup>39,45</sup> states have been observed in emission.



While transition has been postulated from the  $^3\Delta_u$  state.<sup>41</sup>





The most prominent feature of the Lewis-Rayleigh afterglow is the emission bands belonging to the first positive band system of nitrogen. These bands occur from the products of reactions 36, 39, and 40, summarized in reaction 41.



Bands from  $v' = 12, 11$  and  $10$  arise by reaction 36, from  $v' = 4, 3$ , and  $2$  by reaction 39, and from  $v' = 7, 6$ , and  $5$  by reaction 40. Bayes and Kistiakowsky<sup>41</sup> have stated that bands from  $v' = 0, 1$ , and  $2$  of the  $\text{B } ^3\Pi_g$  state might arise from a radiationless transition from levels  $v'' = 7, 8$ , and  $9$  of the  $\text{A } ^3\Sigma_u^+$  state. The  $\text{A } ^3\Sigma_u^+$  state has been shown to be long-lived,<sup>4,6</sup> explaining why the Vegard-Kaplan bands have not been observed from this state to the ground state in active nitrogen. Only bands from the first positive system were observed in the Lewis-Rayleigh afterglow during the present investigation since spectra were limited to the visible and ultraviolet regions.

Other Nitrogen Emissions: Band members belonging to the second positive and first negative systems of nitrogen appear to originate directly from a pink discharge occurring in the reaction tube. A similar discharge has been noted by Kaplan<sup>57</sup> to produce enhancement of the second positive bands. The minimum of the  $\text{C } ^3\Pi_u$  state, which gives rise to the second positive bands, lies  $11.1 \text{ e.v.}$  above the ground state of nitrogen. This state should be crossed by both the repulsive  $^7\Sigma_u^+$  state arising from ground state nitrogen atoms, as well as by molecular states arising from recombining  $^4\text{S}$  and  $^2\text{D}$  nitrogen atoms. The  $\text{C } ^3\Pi_u$  state has been shown to predissociate at  $97,944 \text{ cm}^{-1}$  ( $v' = 1, 2, 3$ , and  $4$  at  $K = 65, 55, 43$ ,







and 28 respectively)<sup>19</sup> as well as at  $v' = 2$  and  $3$ ,  $K = 80$  and  $67$ .<sup>112</sup> Several intensity perturbations have been noted.<sup>12</sup> It is known that the former predissociation is associated with  $4S$  and  $2D$  nitrogen atoms; the latter might be coincident with a predissociation into ground state nitrogen atoms. Since bands arising from  $v' = 0$ ,  $1$ , and  $2$  have been observed in our spectra, the lower cross-over is favoured. However, the excitation required to reach the cross-over point is prohibitive (55kcal). Since there is no obvious source of metastable nitrogen atoms in sufficient quantities to produce the observed intensities shown by the second positive bands in our spectra, we must find another mode of excitation for these bands.

It is possible that the simplest explanation for the observed second positive bands is for their excitation to arise by electron impact in the pink discharge. Lichten<sup>18</sup> has produced all of the singly excited states of molecular nitrogen using a molecular beam bombarded by energetic electrons. Such excitation requires transitions, obeying the Franck-Condon principle, from the ground state to the excited states (Figure 24). The excitation of the second positive bands by energetic electrons corresponds to the observed levels in this study.

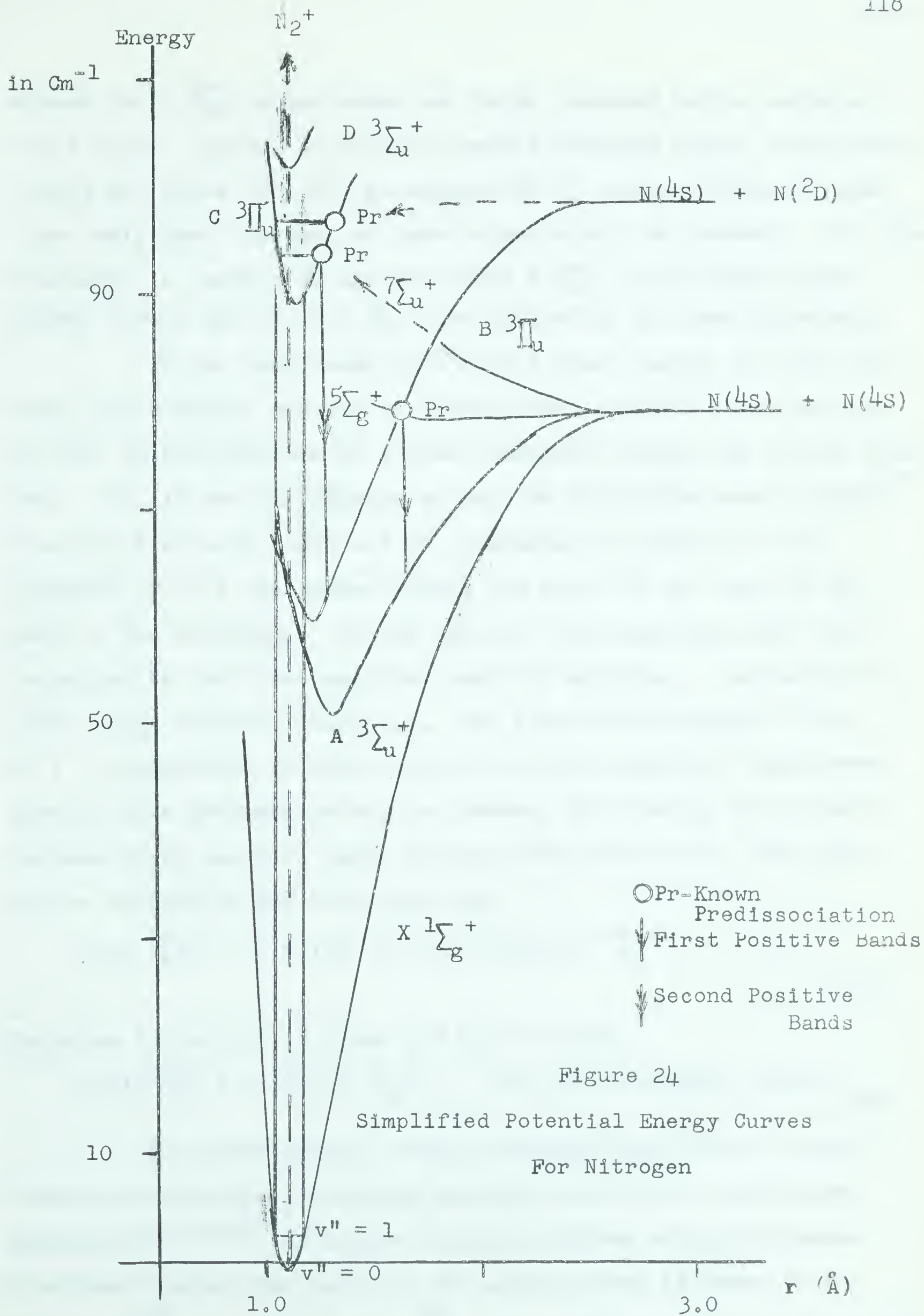


Transition accompanied by emission of the second positive bands would follow such electronic excitation.



The absence of members of the fourth positive bands, noted by other observers, could conceivably indicate that in our



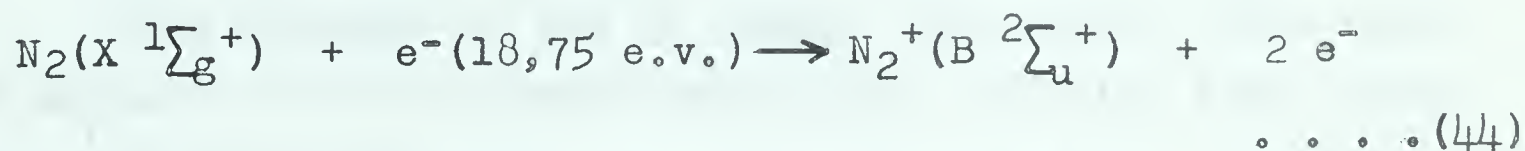




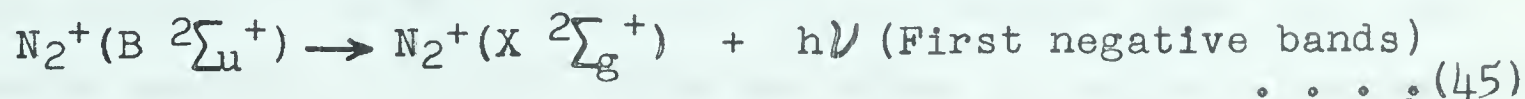


system the  $D \ ^3\Sigma_u^+$  upper state was being quenched before emission could occur. Again, as with the second positive bands, these bands should not arise from the recombination of excited nitrogen atoms since only small amounts of these atoms should be present. The pink discharge is capable of exciting this  $D \ ^3\Sigma_g^+$  state since higher energy levels above the  $D \ ^3\Sigma_g^+$  are excited in the same discharge.

It has been shown that only a small number of free electrons are normally present in active nitrogen.<sup>63-65</sup> This may not be true in the presence of a pink discharge through the active nitrogen. Yet, in our experiments as well as in another recent study,<sup>73</sup> the pink discharge could not be eliminated completely by the presence of foil electrodes around the walls of the tube in the path of the discharge. In our system, weak emissions were noted belonging to the first negative bands of nitrogen. Excitation of these bands requires 18.75 e.v. The first three members of the  $v' = 0$  progression of these bands have been observed; higher members of this progression may be present, but overlap by the more intense first positive bands obscures their detection. The bands may be excited in the following way.



Emission to the ground state (of  $N_2^+$ ) follows.



In recent years, several observers have noted a short-lived pink afterglow in active nitrogen excited by a microwave generator.<sup>45,71-73</sup> In active nitrogen excited using microwaves the first vibrational level of the ground state is known to be populated.<sup>47</sup> Levels of the  $B \ ^3\Pi_g$  state (emitting the first positive



bands) could be populated up to  $v' = 20$ , the second positive bands could be excited up to  $v' = 4$  (of the upper  $C\ ^3\Pi_u$  state), and the  $N_2^+B\ ^2\Sigma_u^+$  state could be populated to levels 5 e.v. above the ground state if both  $v'' = 0$  and  $v'' = 1$  (of the  $X\ ^1\Sigma_g^+$  ground state of nitrogen) were being excited by the bombarding electrons. Thus, it is not unreasonable to conclude that the pink discharge observed in the present study is the condensed discharge counterpart to the short-lived pink afterglow observed when active nitrogen is produced with a microwave generator. Carrying the comparison even further, the vibrational distribution noted in the second positive bands while cooling the pink discharge<sup>113</sup> can be explained by utilizing bombarding electrons as the mode of excitation. Excitation of  $v'' = 1$  of the ground state by the bombarding electrons would especially favour the excitation of  $v' = 4$  of the  $C\ ^3\Pi_u$  upper state, while  $v'' = 0$  would populate the  $v' = 0$  level. Since the lowered temperature would substantially lower the number of ground state molecules with  $v'' = 1$  the relative populations of  $v' = 0$  and 4 could be explained without involving metastable nitrogen atoms.

The presence of the NO Bands: The nitric oxide bands which appeared in the poisoned system seem to arise from direct reaction of active nitrogen with the poisoned wall. The  $\beta$ ,  $\gamma$ , and  $\delta$  band systems of nitric oxide have been observed when less than equimolar amounts of nitric oxide are added to active nitrogen.<sup>103,105</sup> It has been shown<sup>104</sup> that nitric oxide undergoes a fast reaction with active nitrogen releasing atomic oxygen (reaction 27). This oxygen slowly recombines with nitrogen atoms by a third body process producing the emissions (reactions 25 and 26).







Reaction producing free oxygen probably occurs at the walls involving direct nitrogen recombination upon the occluded oxygen (as in reaction 23) or by metastable nitrogen dissociating the oxygen (as in reaction 24). The liberated oxygen is then able to migrate away from the walls and react with a nitrogen atom (reaction 25) to form nitric oxide. Most of the nitric oxide will be formed in the ground state,<sup>101</sup> but a small percentage of the molecules should form in excited states and so be capable of radiating (by reaction 26).

The observed  $\beta$  bands are compatible with the formation of nitric oxide in vibrational levels of the B  $^2\Pi$  state lower than  $v' = 7$  (Figure 25). The B  $^2\Pi$  state does not correlate with ground state atoms, so that excitation of the state must occur via a radiationless transition (in a similar manner to that proposed in  $N_2$  and NBr).<sup>91</sup>

The  $\delta$  bands have been observed for only the  $v' = 0$  level of the C  $^2\Sigma^+$  state. This lends evidence to the postulate that the  $\delta$  bands are excited, as was the B  $^2\Pi$  state, by a radiationless cross-over. The  $v' = 0$  level of the C  $^2\Sigma^+$  state lies just 0.01 e.v. above the  $v' = 7$  level of the B  $^2\Pi$  state, which has the same energy as the combining atoms.<sup>113</sup>

The  $\gamma$  bands can arise from a cross-over of the combining atoms into  $v' = 3$  of the A  $^2\Sigma^+$  state, which has about the same energy as  $v' = 6$  of the B  $^2\Pi$  state. Unlike Tanaka,<sup>113</sup> who observed  $\gamma$  bands from  $v' = 0, 1$ , and  $2$ , only a very intense  $v' = 0$  progression was observed in the present study. The absence of bands from  $v' = 1, 2$ , and  $3$  seems to indicate that rapid collisional deactivation of the upper levels to  $v' = 0$  can occur before radiation of



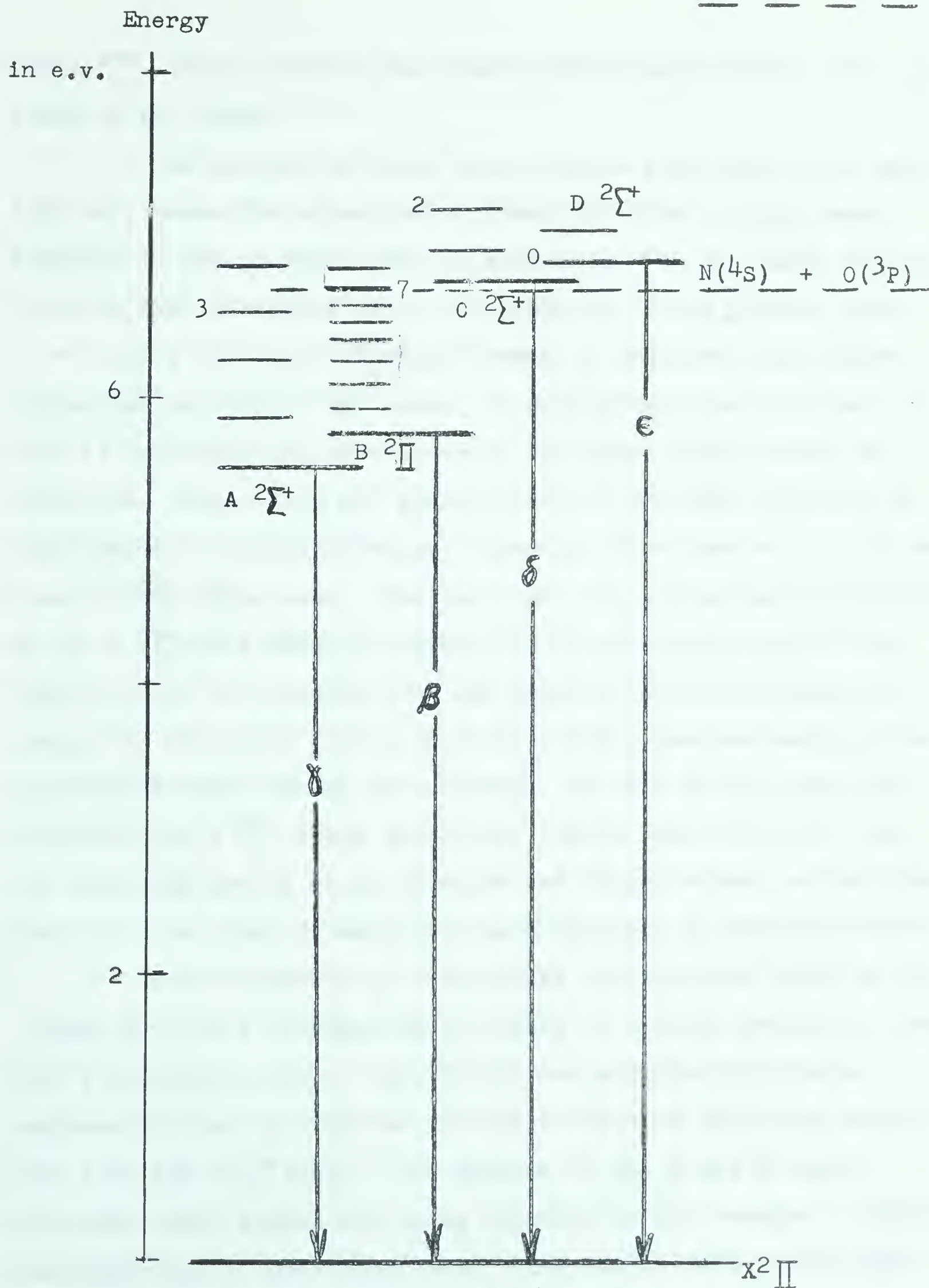


Figure 25

Energy Levels in Nitric Oxide





the  $A \ ^2\Sigma^+$  state, possibly the deactivation occurs during the formation of the state.

The absence of the  $\epsilon$  bands, whose zero level lies just 0.12 e.v. above the dissociation energy of nitric oxide lends evidence to the proposed mode of excitation for the bands observed. The fact that no transitions were observed in the  $\beta$  bands from  $v' = 7$  and 6 (of the  $B \ ^2\Pi$  state) tends to indicate that either cross-over into the  $A \ ^2\Sigma^+$  state, or collisional deactivation, or both is depleting the population of the upper levels prior to radiation. Bands from all levels below  $v' = 6$  were observed in the  $\beta$  bands in active nitrogen, although those from  $v' = 3, 4,$  and 5 were often quite weak. The fact that the vibrational distribution of the  $B \ ^2\Pi$  state seems to favour the lower energy levels, may indicate that the formation of the state in active nitrogen is being induced by collision with a third body which removes energy from the excited state during the process. If this is so, then population of the  $A \ ^2\Sigma^+$  state would more likely occur directly from the combining ground state nitrogen and oxygen atoms, rather than from the  $v' = 6$  and 7 levels of the  $B \ ^2\Pi$  state as mentioned above.

The difference in vibrational distribution shown by the bands in active nitrogen when bromine is present probably arises from a differing rate of collisional deactivation by bromine compared to that by nitrogen or nitric oxide in effecting cross-over into the  $B \ ^2\Pi$  state. The absence of the  $\gamma$  and  $\delta$  bands indicates these states are being quenched by the bromine. Similar quenching effects and vibrational distribution differences have been noted in active nitrogen when other foreign gases have been added. 41,59,60,106



The possibility of oxygen entering the system from sources other than with the wall poison was carefully investigated and eliminated in our experiments. Because the nitric oxide bands were entirely absent in the unpoisoned experiments, the only conclusion was that either the wall poison itself or oxygen (or water vapour) occluded on the wall by the wall poison could be responsible for the emission. Since the system was very carefully dried under vacuum after poisoning (in order to produce strong afterglows) it was tentatively concluded that the wall poison itself was responsible for retaining the source of oxygen from which the nitric oxide bands were produced.

#### CONCLUSIONS

The molecule NBr presents an interesting study in molecular coupling. Its constituent atoms each belong to a series in the periodic system showing markedly different characteristic types of molecular coupling. Nitrogen and the other molecules in the group 5a series exhibit Russell-Saunders coupling, while bromine and the other halogens form J-J coupled molecules. The hybrid molecule NBr is closer to a group 7a halogen molecule than it is to being a member of the nitrogen group. The NBr molecule lies much closer to case "c" coupling than do members of the oxygen series, which lie quite close to case "b" coupling only exhibiting a small amount of transition towards case "c". NBr is unique, in that it is the only molecule known exhibiting so much transition from case "b" towards case "c". The dissociation energy of the ground state of NBr seems to lie midway between the dissociation energies shown by the halogen molecules and those shown by the oxygen type molecules.







The process of molecule formation from atoms in which a "sticky" collision is followed by a collisionally-induced, radiationless transition into an excited state may not be as unique a process as once was thought. Already three molecules,  $N_2$ , NO and NBr are known to form in such a manner, and it may be that NH also forms in this way. A reconsideration of the recombination processes for other molecules may show such a process to be occurring for many of them.

The formation of excited NBr on the wall is similar to results obtained from recent studies of recombination on metal surfaces.<sup>114</sup> The result implies that collision with, or formation of molecules upon, the wall of a reaction vessel does not necessarily result in deactivation of an excited state and can result in transition into an excited state. Thus, the a priori assumption that all unreacted excited species will be deactivated on the wall, so eliminating them from the system, can no longer be made unless evidence is given to its support.

Bromine is a very efficient quenching agent for the afterglow, presumably due to its reaction with nitrogen atoms. The admission of very low flow rates of bromine into active nitrogen results in complete quenching of the yellow afterglow. Ammonia, on the other hand, even when allowed to flow in excessive amounts into active nitrogen can only quench the afterglow slightly more than by dilution; it can never completely quench the nitrogen molecular precursor state.

Active nitrogen when produced in a condensed discharge not only consists of ground state nitrogen atoms (some of which recombine in the reaction vessel producing the characteristic



yellow afterglow), but, in addition, it contains several excited molecular species. The metastable  $A\ ^3\Sigma_u^+$  nitrogen molecules are probably formed in the main condensed discharge and migrate into the reaction region, but other excited molecular species seem to originate from a pink discharge passing through the reaction region itself. The source of the pink discharge seems to be the main discharge; it flows from the discharge tube through the active nitrogen to the pump. Grounded electrodes, both within the stream of flowing nitrogen gas and wrapped around the outside of the reaction tube, can not completely quench this pink discharge. The spectrum of the pink discharge seems to be the condensed discharge counterpart of a short-lived pink discharge observed when a microwave exciter is used to generate active nitrogen.

Poisoning of the reaction vessel wall to prevent atom recombination seems to have produced conditions favourable to the formation of nitric oxide in active nitrogen. Several band spectra attributable to nitric oxide have been observed strongly in emission in poisoned active nitrogen systems. The implication is that some sort of wall reaction is occurring between nitrogen and oxygen (or water vapour) occluded on the wall by the wall poison.

#### SUGGESTIONS FOR FURTHER WORK

Further interesting information about the NBr molecule could be obtained by resolving the two other forms of the triplet ground state. The key to this problem may already be present in the faint unassigned lines observed in the stronger bands of the  $\Delta v = 2$  sequence of the NBr spectrum.







A study might be made with active nitrogen in which ammonia has been added upstream from the bromine inlet to see if the NBr flame can be eliminated in nitrogen in which triplet state molecules are absent. Also, a microwave exciter could be used to generate active nitrogen free of metastable  $A^3\Sigma_u^+$  molecules. This would enable the initiation reaction for bromine addition to be studied. If nitrogen atoms are liberating the atomic bromine required for NBr formation, no diminution of the flame intensity should occur in active nitrogen free from excited molecules. If the afterglow precursor state,  $5\Sigma_g^+$ , is responsible for the initiation reaction it might be difficult to separate the molecular initiation reaction from the atomic mode of initiation.

The chemical reactivity of pink active nitrogen must be considered in the light of recent findings concerning the reaction of ammonia, and some of the lighter saturated hydrocarbon molecules, in active nitrogen. Since these molecules react with molecular nitrogen species, little can be learned about their exact reaction mechanisms until the effects of the various reactive species present is ascertained. A possibility exists that the pink discharge itself might initiate reaction in some of these molecules by direct electron bombardment.

It would prove interesting if the extent of reaction of active nitrogen with wall species could be studied more closely. Possibly a series of different concentrations of ortho-phosphoric acid wall poisons could be studied in active nitrogen, as well as the effects of a number of other known wall poisons. Differences in the spectra produced could be studied, as well as attempts made to detect the reaction by chemical means. If occluded oxygen is the actual source of the nitric oxide produced, then a long time-study might show a decrease in the nitric oxide emissions even though the wall poison still remains effective in producing a strong yellow afterglow.



## BIBLIOGRAPHY

- 1-G.R. Freeman and C.A. Winkler, J. Phys. Chem.  
59 371 (1955).
- 2-G.B. Kistiakowsky and G.G. Volpi, J. Chem. Phys.  
28 665 (1958).
- 3-H.B. Dunford and B.E. Melanson, Can. J. Chem.  
37 641 (1959).
- 4-A.N. Wright and C.A. Winkler, Can. J. Chem.  
40 5 (1962).
- 5-E.R. Zabolotny and H. Gesser, J. Phys. Chem.  
66 408 (1962).
- 6-H.B. Dunford, "On the Half-Life of  $A^3\Sigma_u^+ N_2$ , Using  $NH_3$   
Titration" to be published in J. Phys. Chem.
- 7-E.P. Lewis, Astrophys. J. 12 8 (1900)
- 8-R.J. Strutt, Proc. Royal Soc.(London) A85 219 (1911).
- 9-J. Berkowitz, W.A. Chupka, and G.B. Kistiakowsky,  
J. Chem. Phys. 25 457 (1956).
- 10-G.B. Kistiakowsky and G.G. Volpi, J. Chem Phys.  
27 1141 (1957).
- 11-M.A.A. Clyne and B.A. Thrush, Proc. Royal Soc. (London)  
A261 259 (1961)
- 12-G. Herzberg, Spectra of Diatomic Molecules, D. Van  
Nostrand Co. Inc, (New York, 1957).
- 13-A.G. Gaydon, Dissociation Energies, Chapman and Hall Ltd.,  
(London, 1953)
- 14-A. Loftus and R.S. Mulliken, J. Chem Phys.  
26 1010 (1957)
- 15-P.G. Wilkinson, J. Chem. Phys. 32 1061 (1960).
- 16-K.D. Bayes and G.B. Kistiakowsky, J.Chem. Phys.  
29 949 (1958).
- 17-C. Kenty, J. Chem. Phys. 35 2267 (1961).
- 18-W. Lichten, J. Chem. Phys. 26 306 (1957).
- 19-G. Bittenbender and G. Herzberg, Ann. Physick  
21 577 (1935).
- 20-J. Kaplan, Phys. Rev. 38 373, 1079 (1931).





- 21-A.E. Douglas and G. Herzberg, Can. J. Phys. 29 294 (1951).
- 22-A. van der Zeil, Physica 1 353 (1934), 4 373 (1937).
- 23-A.G. Gaydon, Nature (London) 153 407 (1944).
- 24-E. Wrede, Z. Physik 54 53 (1929).
- 25-D.S. Jackson and H.I. Schiff, J. Chem. Phys.  
21 2233 (1953), 23 2333 (1955).
- 26-J.T. Herron and V.H. Diebler, J. Chem. Phys.  
31 1662 (1959).
- 27-M.A. Heald and R. Beringer, Phys. Rev. 96 645 (1954).
- 28-Y. Tanaka, Proc. Aeronomy Conf., Cambridge Mass.,  
Pergamon Press (1956).
- 29-G.R. Freeman and C.A. Winkler, J. Phys. Chem.  
59 780 (1955).
- 30-D.R. Bates, Ann. Geophys 8 194 (1952).
- 31-P.A. Gartaganis and C.A. Winkler, Can. J. Chem.  
34 1457 (1956).
- 32-A.N. Wright and C.A. Winkler, Can. J. Chem.  
40 1291 (1962).
- 33-J.T. Herron, J.C. Franklin, P. Bradt, and V.H. Diebler,  
J. Chem. Phys. 30 879 (1959)
- 34-A.N. Wright, R.L. Nelson, and C.A. Winkler, Can. J. Chem.  
40 1082 (1962).
- 35-D.A. Armstrong and C.A. Winkler, J. Phys. Chem.  
60 1100 (1956).
- 36-R. Kelly and C.A. Winkler, Can. J. Chem. 37 62 (1959).
- 37-A. Fowler and R.J. Strutt, Proc. Royal Soc. (London)  
A85 377 (1911).
- 38-A.E. Ruark, P.D. Foote, P. Rudnick, and R.L. Chenault,  
J. Opt. Soc. Am. 14 17 (1927).
- 39-G.B. Kistiakowsky and P. Warneck, J. Chem. Phys.  
27 1417 (1957).
- 40-N.P. Carleton and O. Oldenberg, Results, Fourth European  
Conf. on Molecular spectra, Bologna (1959).



- 41-K.D. Bayes and G.B. Kistiakowsky, J. Chem. Phys.  
32 992 (1960).
- 42-K.D. Bayes, Can. J. Chem. 39 1074 (1961).
- 43-J. Noxon, J. Chem. Phys. 36 926 (1962).
- 44-D.T. Stewart, Proc. Phys. Soc. (London) B69 956 (1956).
- 45-Y. Tanaka, F. LeBlanc, and A. Jursa, J. Chem. Phys.  
30 1624 (1959).
- 46-J.M. Benson, J. Appl. Phys. 23 757 (1952).
- 47-F. Kaufman and J.R. Kelso, J. Chem. Phys. 28 510 (1958).
- 48-H.B. Dunford, unpublished results.
- 49-K. Dressler, J. Chem. Phys. 30 1621 (1959).
- 50-S.J. Lukasik and J. E. Young, J. Chem. Phys.  
27 1149 (1957).
- 51-J.T. Vanderslice, E.A. Mason, and E.R. Lippincott,  
J. Chem. Phys. 30 129 (1959)
- 52-E.P. Lewis, Astrophys. J. 20 49 (1904).
- 53-R.J. Strutt, Proc. Royal Soc. (London) A86 56 (1911),  
A91 303 (1915); Lord Rayleigh, *ibid*,  
A151 567 (1935), A176 1 (1940),  
A180 123, 140 (1942).
- 54-A. Fowler and R.J. Strutt, Proc. Royal Soc. (London)  
A85 377 (1911).
- 55-H. Sponer, Z. Physik 34 622 (1925).
- 56-R.S. Mulliken, Phys. Rev. 23 767 (1924).
- 57-J. Kaplan, Phys. Rev. 33 189 (1929).
- 58-J. Okubo and H. Hamada, Phil. Mag. 15 103 (1933).
- 59-Lord Rayleigh, Proc. Royal Soc. (London) A102 453 (1922).
- 60-J.C. McLennan, R. Ruedy, and J.M. Anderson,  
Trans. Royal Soc. (Canada) III 22 303 (1928).





- 61-T. Wentink, Jr., J.O. Sullivan, and K.L. Wray,  
J. Chem. Phys. 29 231 (1958).
- 62-L.H. Reinecks, Z. Physik 135 361 (1953).
- 63-K.T. Chao and H.P. Chang, Phys. Rev. 76 970 (1949).
- 64-C. Kenty, J. Chem. Phys. 23 1556 (1955).
- 65-H.H. Bromer and U. Stille, Optik 15 382 (1958).
- 66-E.P. Lewis, Nature (London) 111 599 (1923).
- 67-S.K. Mitra, Phys. Rev. 90 516 (1953).
- 68-J. Kaplan, Phys. Rev. 42 807 (1932), 45 671 (1934),  
48 800 (1935), 54 176 (1938).
- 69-A.L. Gardner, Phys. Rev. 98 263(A) (1955).
- 70-H.B. Kinkel and A.L. Gardner, Phys. Rev. 98 558 (1955).
- 71-G.E. Beale and H.P. Broida, J. Chem. Phys.  
31 1030 (1959).
- 72-H.P. Broida and I. Tanaka, J. Chem. Phys. 36 236 (1962)
- 73-R.A. Young, J. Chem. Phys. 36 2854 (1962).
- 74-W. Kasner, W. Rogers, and M. Biondi, Phys. Rev. Letters  
7 321 (1961).
- 75-R.J. Strutt and A. Fowler, Proc. Royal Soc. (London)  
A86 105 (1912).
- 76-A. Elliott, Proc. Royal Soc. (London), A169 469 (1938).
- 77-P.W. Schenk and H. Jablonowski, Z. Anorg. Allgen. Chem.  
244 387 (1940).
- 78-R.H. Ewart and W.R. Rodebush, J. Am. Chem. Soc.  
56 97 (1934).
- 79-R.T. Sanderson, Vacuum Manipulation of Volatile Compounds,  
John Wiley and Sons, Inc., (New York, 1948).
- 80-N.R.C., Iron Hollow-Cathode Wavelength Tables;  
Wavelengths of Emission Spectra, Handbook  
of Chemistry and Physics, Chemical Rubber  
Publishing Co., (Cleveland, 1954).



- 81-F.S. Tompkins and M. Fred, J. Opt. Soc. Am. 41 641 (1951).
- 82-J.H. van Vleck, Phys. Rev. 33 467 (1929).
- 83-H.A. Kramers, Z. Physik 53 422 (1929).
- 84-R. Schlapp, Phys. Rev. 51 342 (1937).
- 85-J.E. Lennard-Jones, Trans. Faraday Soc. 25 668 (1929).
- 86-R.S. Mulliken, Revs. Modern Phys. 3 89 (1931).
- 87-R.S. Mulliken, Revs. Modern Phys. 4 1 (1932).
- 88-R.S. Mulliken, Phys. Rev. 57 500 (1940).
- 89-H.D. Babcock and L. Herzberg, Astrophys J. 108 167 (1948).
- 90-E.R.V. Milton and H.B. Dunford, J. Chem Phys.  
34 51 (1961).
- 91-C.A. Barth, W.J. Shade, and J. Kaplan, J. Chem. Phys.  
30 347 (1959).
- 92-H. Guenebault, G. Pannetier, and P. Goudmand,  
Compt. rend. 251 1480 (1960).
- 93-G. Mannella, J. Chem. Phys. 36 1079 (1962).
- 94-C. Zener, Proc. Royal Soc. (London), A140 660 (1933).
- 95-L. Landau, Z. Phys. Sowjet 2 46 (1932).
- 96-D.R. Bates, Proc. Royal Soc. (London), A257 22 (1960).
- 97-J. Kaplan, Phys. Rev. 38 373, 1079 (1931).
- 98-L.A. Turner, Phys. Rev. 38 574 (1931), 41 627 (1933).
- 99-L. Avramenko and V. Kondratjew, Physik Z. Sowjetunion  
10 741 (1936).
- 100-R.L. Strong, J.C.W. Chien, P.E. Graf, and J.E. Willard,  
J. Chem. Phys. 26 1287 (1957).
- 101-S.W. Benson and T. Fueno, J. Chem. Phys. 36 1597 (1962).
- 102-W. Forst, H.G.V. Evans, and C.A. Winkler, J. Phys. Chem.  
61 320 (1957).





- 103-P. Harteck, R.R. Reeves, and G. Mannella,  
J. Chem. Phys. 29 608 (1958).
- 104-F. Kaufman and J.R. Kelso, J. Chem. Phys. 27 1209 (1957),  
Seventh International Symposium, London(1958) p 53.
- 105-F. Kaufman, J. Chem. Phys. 28 992 (1958).
- 106-C. Kenty, J. Opt. Soc. Am. 93 651 (1954).
- 107-W.H.B. Cameron and A. Elliott, Proc. Royal Soc. (London)  
A169 463 (1938).
- 108-R.G.Dickenson and A.C.G. Mitchel, Proc. Natl. Acad. Sci.  
12 692 (1926).
- 109-A.G. Gaydon, Proc. Royal Soc. (London) A181 197 (1942).
- 110-M. Peyron and H.P. Broida, J. Chem. Phys. 30 139 (1959).
- 111-T. Hori and Y. Endo, Proc. Phys. Math. Soc. Japan  
23 834 (1941).
- 112-Y.Tanaka, F. LeBlanc, and A. Jursa, J. Chem. Phys.  
30 1624 (1959).
- 113-Y. Tanaka, J. Chem. Phys. 22 2045 (1954).
- 114-R.R. Reeves, G. Mannella, and P. Harteck,  
J. Chem. Phys. 32 946 (1960).



## APPENDIX I CALIBRATION OF FLOW JETS

The flow meter was attached to a calibrated gas volume to which was connected a mercury manometer for measuring the pressure of the gas in the volume. Assuming the ideal gas law to apply, the number of moles of gas in the volume could be found directly at constant temperature from the pressure

$$n = \frac{V}{R T} P \quad . . . . (1)$$

The rate of flow of gas through any jet was found by measuring the pressure drop (dP) over a time interval (dT).

$$f = dP / dT \quad . . . . (2)$$

A typical calibration is shown in Table 21.

TABLE 21

Rate of Evacuation of Nitrogen Flow Jet

P <sub>mm</sub>	t <sub>sec</sub>	moles in bulb	moles removed	flow rate
698	0	4.0 x 10 <sup>-2</sup>		
661	300	3.8 x 10 <sup>-2</sup>	2.0 x 10 <sup>-3</sup>	
627	600	3.6 x 10 <sup>-2</sup>	2.0 x 10 <sup>-3</sup>	6.7 x 10 <sup>-6</sup>

Each reactant, excepting bromine, was used to calibrate the rate of flow through the flow jet through which it was used. (Table 22). In addition all flow jets were calibrated with a

TABLE 22

Flow Rates Through Reactant Flow Jets

Jet Designation	Gas	Pressure Head	Rate of Flow	N <sub>2</sub> Pressure	Rate of N <sub>2</sub> Flow
40	HBr	60 mm.	6.7 x 10 <sup>-7</sup>	700	2.2 x 10 <sup>-6</sup>
56	N <sub>2</sub>	700 mm.	6.7 x 10 <sup>-6</sup>		
68	NH <sub>3</sub>	700 mm.	5.1 x 10 <sup>-5</sup>	700	2.7 x 10 <sup>-5</sup>





pressure head of 700 mm of nitrogen. It was found that the relative rate of flow through the jets was directly related to the equilibrium pressure produced in the vacuum flow system gives a convenient means of comparing the flow jets with one another (Figure 26).

The following flow jet combinations were employed in the bromine study where no direct pressure readings could be taken with the reactant (Table 23).

TABLE 23

Bromine--Active Nitrogen Flow Jet Combinations

N <sub>2</sub> jet	Br <sub>2</sub> jet	Observations of Reaction Flame
p <sub>0</sub> =700mm	**	
60	27	Active Nitrogen just quenched, gas phase flame mixed yellow nitrogen afterglow and orange NBr.
60	30	Flame entirely on wall. Blue wall glow can be made to persist under suitable wall conditions.
55	30	Flame less intense, higher flash rate required to maintain reaction.
60	35	Excellent for bright wall flame.
60	40	Wall flame brighter, less localized Active nitrogen afterglow completely quenched.
60	45	Larger fainter flame, beginning to show more in gas phase
60	50	Small faint gas phase flame
60	55	Smallest flame, entirely in gas phase

\*\* - p<sub>0</sub> = Bromine vapour in equilibrium with liquid bromine at room temperature.



Log equilibrium  
pressure (mm)

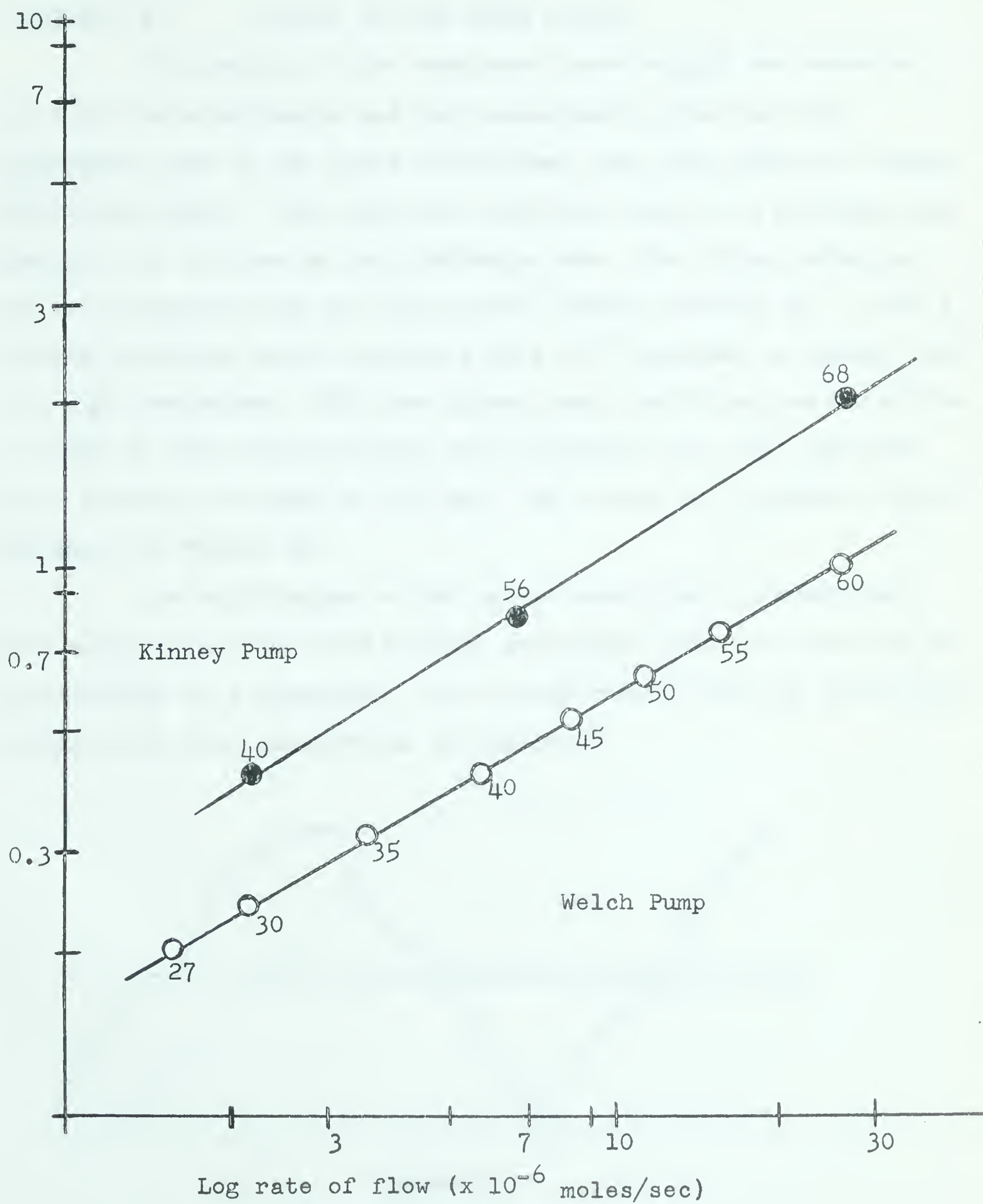


Figure 26

Rate of Evacuation of Flow Jets





## APPENDIX II      OUTPUT OF THE POWER SUPPLY

The output of the condensed power supply was measured. In both the experiments and the measurements, the two 2410 secondary taps on the plate transformer were used (with no center tap connection). When used with the Welch pump at a nitrogen gas pressure of 0.62 mm in the discharge tube, the firing potential of the discharge tube was 3225 volts (Variac setting 55). Such a firing potential would provide  $1.29 \times 10^{-2}$  coulombs of energy from the  $4 \mu\text{f}$  condenser. With the Kinney pump the firing potential was lowered to 1600 volts (Variac 30) providing  $6.4 \times 10^{-3}$  coulombs at a nitrogen pressure of 0.8 mm. The output of the power supply is shown in Figure 28.

An oscillogram of the output wave from the condensed discharge showed the form usually associated with the charging and discharging of a condenser. At a flash rate of ten per second the output wave form appeared as in figure 27.

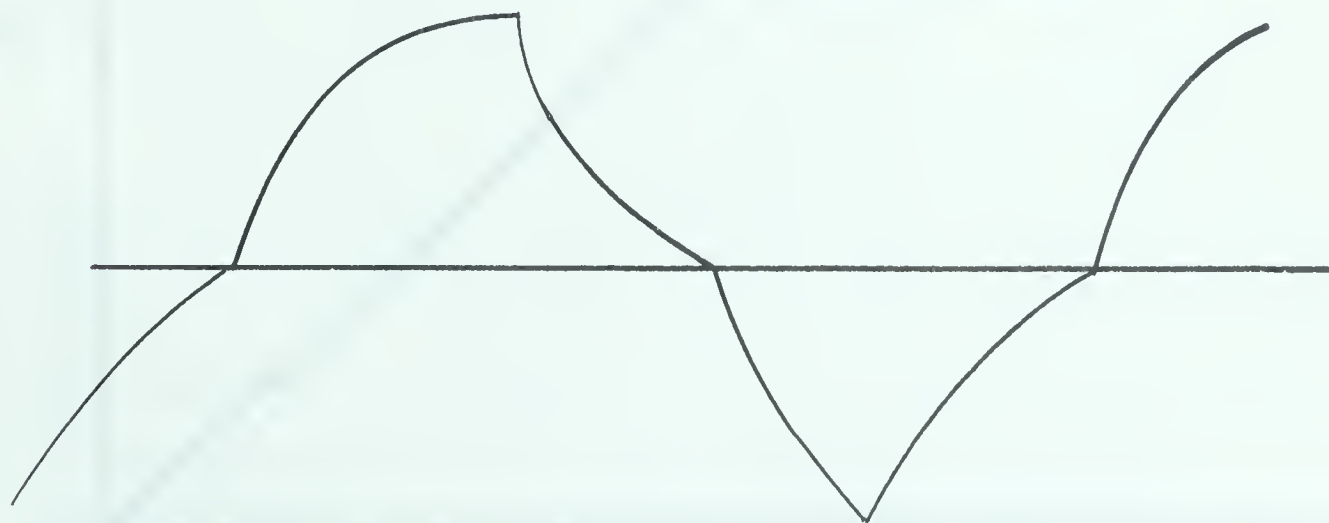


Figure 27

Oscillogram of the Discharge



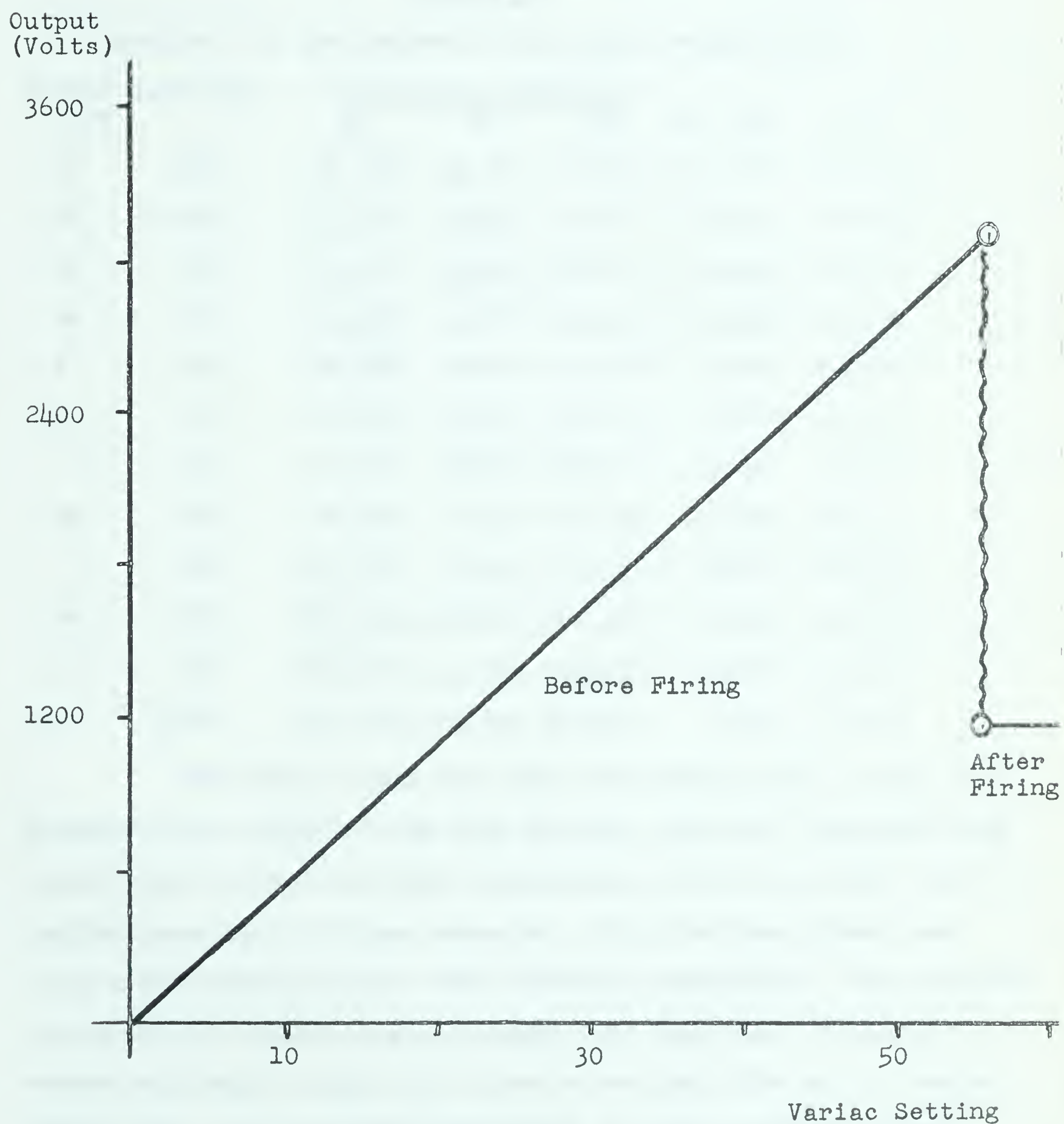


Figure 28  
Output of the Power Supply





## APPENDIX III

## ANALYSIS OF THE SPECTRUM

The reference spectrum was analysed using the manual comparator producing the following data (Table 24).

TABLE 24

Analysis of the Reference Spectrum for NBr 8'-6"

Atomic Line	Intensity	Comparator Readings			$s_0 - s\sum$	$\Delta\lambda$
		S1	S2	$\sum S$		
Fe	300	44.228	43.759	87.987	181.073	64.600
Ne	1000	46.522	46.045	92.567	176.493	62.966
Fe	100	53.016	52.514	105.530	163.530	58.341
Fe	400	62.028	61.507	123.535	145.525	51.917
Fe	150	88.782	88.316	177.098	91.962	52.808
Ne	75	90.322	89.852	180.174	88.886	31.711
?	75	93.356	92.904	186.260	82.800	29.540
Fe	300	98.364	97.912	196.276	72.784	25.966
?	150	100.438	99.950	200.388	68.672	24.499
Ne	500	105.946	105.492	211.438	57.622	20.577
Fe	400	115.375	114.913	230.288	38.772	13.832
Ne	1000	134.755	134.305	269.060	0.000	0.000

The atomic lines were then identified from a table of standard wave lengths. The iron spectrum used was obtained using second order dispersion from the grating and so the actual wave-lengths were half of those observed, while the neon lines were first order dispersion and thus directly comparable. The standard wavelength (or double the wavelength for iron) was corrected to vacuum wavelength using the vacuum correction from air to vacuum (Figure 29). The observed wavelength and the standard vacuum wavelengths were compared to obtain the correction graph for deviation from linear dispersion over the 8-6 NBr band (Table 25, Figure 8).



TABLE 25

Calculation of the Correction Graph

Atomic Line	Intensity	$\lambda_{\text{calc.}}$	$\lambda_{\text{Fe}}$	$\lambda$ Standard	Vacuum Correction	$\lambda_{\text{vac}}$	$\lambda_{\text{cor}}$
Fe	300	5948.11	2973.2356	5946.47	1.64	5948.11	0.00
Ne	1000	5946.48		5944.83		5946.48	0.00
Fe	100	5941.85	2970.106	5940.21		5941.85	0.00
Fe	400	5935.43	2966.8982	5933.80		5935.44	0.01
Fe=	150	5916.32	2957.3646	5914.73	1.63	5916.36	0.04
Ne	75	5915.22		5913.63		5915.26	0.04
	75	5913.05					
Fe	300	5909.48	2953.9400	5907.88		5909.51	0.03
	150	5908.01					
Ne	500	5904.07		5902.46		5904.10	0.03
Fe	400	5897.34	2947.8758	5895.75		5897.38	0.04
Ne	1000	5883.51		5881.89	1.62	5883.51	0.00

The lines of the 8'-6" NBr band were analysed using the comparator in a similar manner to that used for the reference lines (Table 26). The calculated wavelengths were then converted to vacuum wavelengths using the correction for deviations from linear dispersion. All wavelengths were then converted to wavenumbers by taking reciprocals (Table 27).





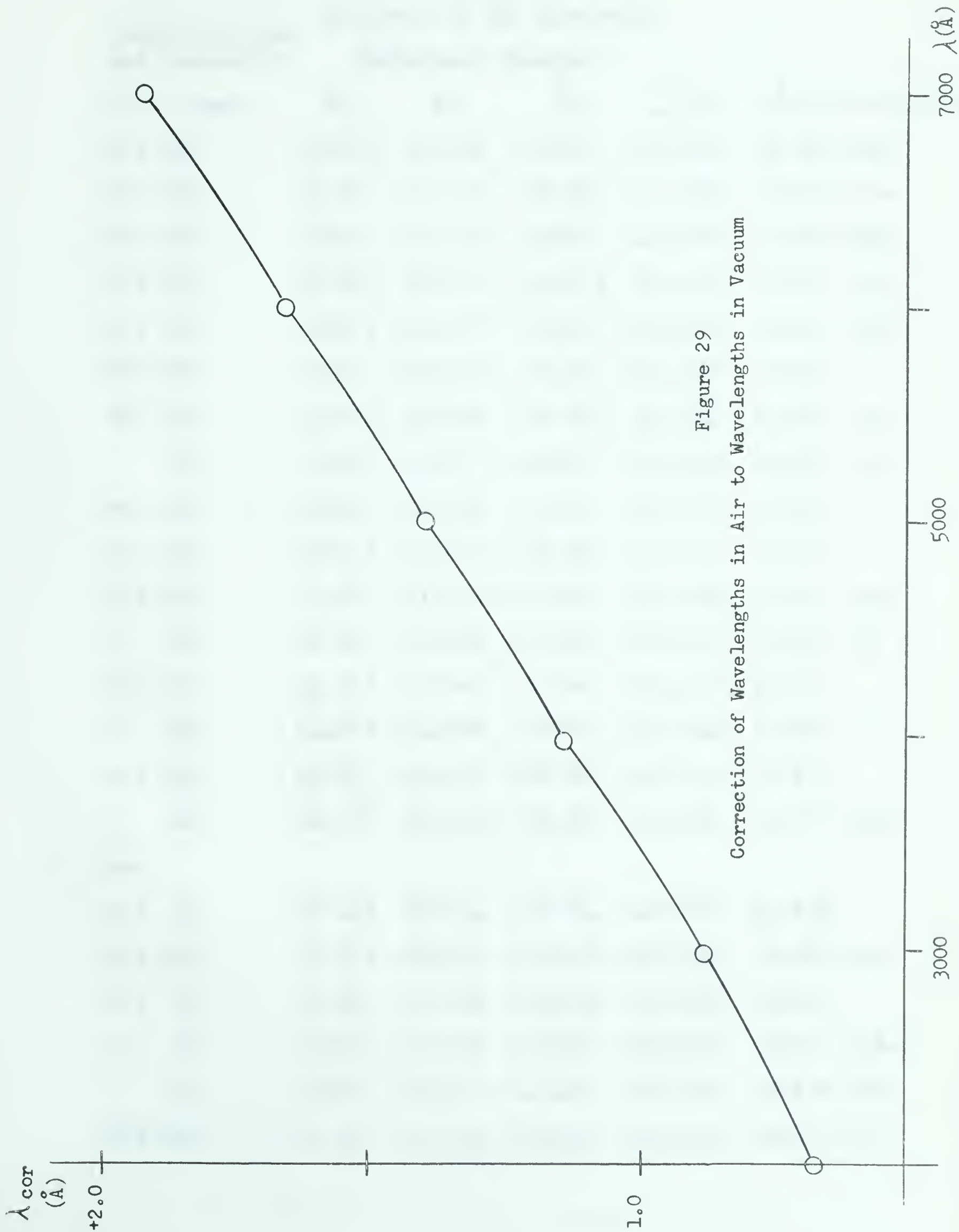


Figure 29  
Correction of Wavelengths in Air to Wavelengths in Vacuum



TABLE 26

Identification and Intensity		Analysis of NBr Spectrum				$\Delta\lambda$	Description
		Comparator Readings					
8'-6" Band		S1	S2	$\Sigma S$	$\Sigma_0 - \Sigma S$		
P81 400		62.129	61.648	123.777	145.283	51.831	Head
P81 200		62.291	61.774	124.065	144.995	51.728	s1bd
P81 300		62.361	61.890	124.251	144.809	51.662	s1bd
P81 300		62.542	62.077	124.619	144.441	51.531	bd-v
P81 200		62.723	62.277	125.000	144.060	51.395	vbd-v
P81 200		62.927	62.456	125.383	143.677	51.258	
P81 100		63.195	62.684	125.879	143.181	51.081	df
50		63.325	62.833	126.158	142.902	50.982	vdf
P81 100		63.438	62.952	126.390	142.670	50.899	
P81 250		63.719	63.237	126.950	142.110	50.699	
P79 400		63.887	63.414	127.301	141.759	50.574	Head
P 300		64.029	63.554	127.583	141.477	50.473	bd
P79 250		64.167	63.694	127.861	141.199	50.374	
P 400		64.358	63.858	128.216	140.844	50.248	
P79 200		64.542	64.055	128.597	140.463	50.112	
P 300		64.728	64.246=	128.974	140.086	49.977	df-r
***							
P79 50		70.167	69.674	139.841	129.219	46.100	
R81 100		70.339	69.881	140.220	128.840	45.965	df-r
R79 75		70.457	69.985	140.442	128.618	45.886	
(P) 25		70.687	70.189	140.876	128.184	45.731	vbd-r
25		70.995	70.531	141.526	127.534	45.499	vdf
R,P 400		71.257	70.793	142.050	127.010	45.312	bd





TABLE 26 (Page 2)

Identification and Intensity		Analysis of NBr Spectrum				
		Comparator Readings				
8'-6"		S1	S2	$\Sigma S$	$\Sigma_0 - \Sigma_s$	$\Delta\lambda$ Description
P81	50	71.858	71.388	143.246	125.814	44.885 dg-v
R	300	72.161	71.687	143.848	125.212	44.671
P	40	72.461	72.019	144.480	124.580	44.445 dg-v
R,P	350	73.084	72.629	145.713	123.347	44.005 vdf bd
	25	73.302	72.787	146.089	122.971	43.871 bd-r
P79	50	73.767	73.291	147.058	122.002	43.525 dg-r
R79	100	73.976	73.522	147.488	121.562	43.368
R81	100	74.110	73.620	147.730	121.330	43.286
	20	74.459	73.953	148.412	120.648	43.042 dg-v
	10	74.733	74.267	149.000	120.060	42.833
R79	100	74.947	74.493	149.440	119.620	42.676
R81	200	75.118	74.643	149.761	119.299	42.561 dg-r
***						
R79	100	86.020	85.521	171.541	97.519	34.791 dg-r
	10	86.251	85.771	172.022	97.038	34.619
	10	86.389	85.900	172.289	96.771	34.524
R81	100	86.661	86.182	172.843	96.217	34.326 dg-v
	20	86.745	86.312	173.057	96.003	34.250
	20	87.159	86.699	173.858	95.202	33.946
R79	100	87.300	86.815	174.115	94.945	33.873 dg-r
	20	87.617	87.159	174.776	94.284	33.637
R81	150	87.930	87.467	175.397	93.663	33.415 dg-v

Key to Symbols:

bd — broad      df — diffuse      dg — degraded  
 v — very      sl — slightly  
 -v to violet    -r to red

81,79 refer to isotopes      P,R refer to branches



TABLE 27

## Calculation of NBr Wavelengths

Id.	In.	$\Delta\lambda$	$\lambda_{\text{obs}}$	$\lambda_{\text{cor}}$	$\lambda_{\text{vac}}$	$\nu_{\text{vac}} (\text{cm}^{-1})$
P81	400	51.831	5935.34	0.02	5935.36	16,848.17
P81	200	51.728	5935.24		5935.26	16,848.46
P81	300	51.662	5935.17		5935.19	16,848.66
P81	300	51.531	5935.04		5935.06	16,849.02
P81	200	51.395	5934.91		5934.93	16,849.39
P81	200	51.258	5934.77		5934.79	16,849.79
P81	100	51.081	5934.59		5934.61	16,850.30
	50	50.982	5934.49		5934.51	16,850.59
P81	100	50.899	5934.41		5934.43	16,850.81
P81	250	50.699	5934.21		5934.23	16,851.38
P79	400	50.574	5934.08		5934.10	16,851.75
P	300	50.473	5933.98		5934.00	16,852.03
P79	250	50.374	5933.88		5933.90	16,852.32
P	400	50.248	5933.76		5933.78	16,852.66
P79	200	50.112	5933.62		5933.64	16,853.06
P	300	49.977	5933.49		5933.51	16,853.43
***						
P79	50	46.100	5929.61	0.03	5929.61	16,864.43
R81	100	45.840	5929.48		5929.51	16,864.79
R79	75	45.886	5929.40		5929.43	16,865.02
P	25	45.731	5929.27		5929.27	16,865.48
	25	45.499	5929.01		5929.04	16,866.13
R, P	400	45.312	5928.82		5928.85	16,866.67
P81	50	44.885	5928.40	0.03	5928.43	16,867.87





TABLE 27 (Page 2)

Id.	In.	$\Delta\lambda$	$\lambda_{\text{obs.}}$	$\lambda_{\text{cor}}$	$\lambda_{\text{vac}}$	$\nu_{\text{vac}} (\text{cm}^{-1})$
R	300	44.671	5928.18		5928.21	16,868.49
P	40	44.445	5927.96		5927.99	16,869.12
R,P	350	44.005	5927.52		5927.55	16,870.37
	25	43.871	5927.38		5927.41	16,870.77
P79	50	43.525	5927.04		5927.07	16,871.74
R79	100	43.368	5926.88		5926.91	16,872.19
R81	100	43.286	5926.80		5926.83	16,872.42
	20	43.042	5926.55		5926.58	16,873.13
	10	42.833	5926.34		5926.37	16,873.73
R79	100	42.676	5926.19		5926.22	16,874.16
R81	200	42.561	5926.07		5926.10	16,874.50
***						
R79	100	34.791	5918.30	0.03	5918.33	16,896.65
	10	34.619	5918.13		5918.16	16,897.14
	10	34.524	5918.03		5918.06	16,897.42
R81	100	34.326	5917.84		5917.87	16,897.97
	20	34.250	5917.76		5917.79	16,898.20
	20	33.964	5917.47		5917.50	16,899.02
R79	100	33.873	5917.38	0.04	5917.42	16,899.25
	20	33.637	5917.15		5917.19	16,899.91
R81	150	33.415	5916.93		5916.97	16,900.54



## APPENDIX IV

## THE 8'—6" BAND

Analysis of the NBr 8'—6" band was made on the manual comparator from the most intense plate. The band system so obtained showed extensions over that procured on the semi-automatic comparator, which provided the more accurate wavelength readings used in the main text. In general the manual comparator readings agreed with those taken on the semi-automatic comparator within  $0.1 \text{ cm}^{-1}$ , however the scatter shown in the assignments was considerable and variable.

For comparison purposes the main  $F_1$  sequences of the 8'—6" band have been listed in Table 28.

TABLE 28

$F_1$  Lines of the NBr 8-6 Band (Manual Comparator)

$J''$	$N^{79}\text{Br}$	S(R)	Q(P)	$N^{81}\text{Br}$	S(R)	Q(P)
2		16,858.06			16,854.45	
3		59.28			55.64	
4		60.61			57.01	
5		61.98			58.34	
6		63.52			59.79	
7		65.02			61.41	
8		66.67			63.03	
9		68.49			64.79	
10		70.37			66.67	
11		72.19	16,851.75		68.49	16,848.17
12		74.16	52.03		70.37	48.46
13		76.21	52.32		72.42	48.66
14		78.26	52.66		74.50	49.02
15		80.40	53.06		76.69	49.39
16		82.56	53.43		78.83	49.79
17		84.81	53.97		81.08	50.30
18		87.09	54.45		83.33	50.81
19		89.43	55.02		85.67	51.38
20	16,891.83		16,855.64	16,888.06		16,852.03

(continued)





TABLE 28 (Page 2)

J"	N <sup>79</sup> Br	S(R)	Q(P)	N <sup>81</sup> Br	S(R)	Q(P)
21		16,894.23	16,856.35		16,890.40	16,852.66
22		96.65	57.01		92.91	53.43
23		99.25	57.80		95.40	54.16
24		901.77	58.65		97.97	55.02
25		04.37	59.48		900.54	55.81
26		07.05	60.42		03.22	56.72
27		09.71	61.41		05.91	57.69
28		12.48	62.32		08.60	58.65
29		15.26	63.32		11.37	59.68
30		18.09	16,864.43		14.23	16,860.73
31		20.98			17.09	
32		23.88			19.90	
33		16,926.77			22.93	
34					25.77	
35					16,928.80	

In addition to the  $F_1$  lines which have been assigned a goodly number of fainter lines were recorded which have not been suitably assigned to any definite sequences. These fainter lines are listed in Table 29 with their relative intensities.

TABLE 29

Listing of Faint Unassigned Lines in 8-6 Band

$\nu$ cm <sup>-1</sup>	Int.	Description	$\nu$ cm <sup>-1</sup>	Int.	Description
16,850.00	20	vft	16,873.13	20	
50.59	50	vdf	73.73	10	
53.55	20		75.24	10	
55.30	25		75.98	10	
56.05	15	vft	77.29	10	
57.26	10		77.52	15	
57.35	10		79.60	10	
58.85	10	vft (lines <sup>2</sup> )	80.17	20	df
60.15	10	vft	81.59	10	df
61.04	25		82.16	10	
61.81	15		83.85	5	vft
63.76	10		85.27	30	vbd
64.20	25		86.30	10	
65.48	25	vbd-r	86.60	5	
66.13	25		88.63	20	bd
67.87	50	dg-v	89.03	20	bd
69.12	40	vdf-v	16,889.83	10	
70.77	25	bd-r			
16,871.74	50	dg-r			



TABLE 29 (Page 2)

$\nu$ cm <sup>-1</sup>	Int.	Description	$\nu$ cm <sup>-1</sup>	Int.	Description
16,890.20	10		16,899.91	20	
90.69	10	bd, df	902.71	40	dg=v
91.46	20		03.37	5	
92.12	10		03.62	10	
92.63	10		04.68	10	
93.20	10		05.11	20	
93.74	20		07.57	20	bd
94.83	10	bd	10.14	10	
95.08	20		12.60	20	bd
95.83	10		13.29	20	
96.23	20		23.48	25	
97.14	5		24.31	20	df
97.42	5		25.05	25	
98.20	20		27.63	75	
99.02	20		16,929.18	20	

Numerous attempts have been made to assign these faint lines to some definite sequence which would have significance in resolving the two other forms of the  $3\Sigma^-$  ground state of NBr. The splitting constants obtained from Schlapp's equations were used to predict possible wavelengths for the other forms of the spectrum and the magnitude of the first differences that would be expected from these sequences, but no successful application of the predictions could be made to the observed faint lines.













**B29804**